PhD degree in Molecular Medicine
(curriculum molecular oncology)

European School of Molecular Medicine (SEMM)
University of Milan and University of Naples "Federico II"

Identification of neoantigens released by *Salmonella*-infected tumor cells for a novel approach to cancer immunotherapy

Alessia Melacarne

European Institute of Oncology (IEO), Milan
Matricola: R10722

Supervisor: Maria Rescigno, PhD
European Institute of Oncology, Milan, Italy

Internal Supervisor: Angela Bachi, PhD
IFOM - FIRC Institute of Molecular Oncology Foundation, Milan, Italy

External Supervisor: Prof Pedro Romero, PhD
UNIL- Ludwig Center for Cancer Research, Lausanne, Switzerland

Academic year: 2016/2017

Table of content

Index of figures and tables

Abbreviation

ACT	Adoptive T-cell transfer
APC	Antigen presenting cells
ATP	Adenosine 5'- triphosphate
BSA	Bovine serum albumin
CTL	Cyotoxic T-lymphocytes
CTLA4	Cytotoxic T-lymphocyte antigen 4
CTA	Cancer testis antigen
Cx	Connexin
CX3CR1	Chemokine (C-X3-C motif) receptor 1
DC	Dendritic cell
DDA	Data dependent analysis
DNA	Deoxyribonucleic acid
ESI	Elettro-spray ionization
FACS	Fluorescence-activated cell sorting
FASP	Filter aid separation protein
FBS	Fetal bovine serum
FCS	Fetal calf serum
FDC	Follicular dendritic cell
GJ	Gap junctions
GO	Gene ontology
FASP	Filter aided sample preparation
HLA	Human Leucocyte Antigens
IF	Interferon
IL	Interleukin
LPS	Lipopolysaccharide
LOH	Loss of heterozygosity

MHCI/II	Major histocompatibility complex class I/II
MS	Mass spectrometry
nLC	Nano liquid chromatography
OSA	Osteosarcoma
PBS	Phosphate buffered saline
PBMC	Peripheral blood mononuclear cells
PMA	Phorbol myristic acid
PSM	Peptides sequence match
PTM	Post translational modified
RNA	Ribonucleic acid
ROS	Reactive oxygen species
SLP	Synthetic long peptides
STS	Soft tissue sarcoma
TAA	Tumor associated antigens
TAP	ATP-dependent peptides transporter
TCR	T cell receptor
TDA	Target data acquisition
TEIPP	T-cell epitopes associated with impaired peptides processing
TGF-β	Transforming growth factor β
Th	T helper
TLR	Toll-like receptor
TNF-α	Tumor necrosis factor α
Tregs	T regulatory cells
UTR	Untranslated region
WT	Wild type

Abstract

Advancements in cancer immunotherapy have revealed the importance of targeting neoantigens. Neoantigens are tumor specific antigens that prompt a strong antitumor response escaping from the central T tolerance. Our laboratory has previously shown that infection of murine tumor cell lines with *Salmonella* elicits the transfer of antigens between adjacent cells through hemichannels (Saccheri et al. 2010). Now we demonstrate that *Salmonella* not only leads to the transfer of immunogenic antigens between adjacent cells, but also to the release of peptides in the extracellular milieu. A first ATP assay showed that infection of murine cell lines with *Salmonella* induces ATP release, and its accumulation is hemichannel dependent, thus proving that *Salmonella* induces hemichannel opening. We also demonstrate that dendritic cells loaded with peptides derived from *Salmonella*-infected murine melanoma B16-OVA cells, induced the activation of OT1-CD8a^{+} cells. Moreover, mass spectrometry (MS) analysis of B16 OVA-derived peptides revealed the presence of the ovalbumin-derived peptide (SIINFEKL). These peptides when tested as components of a vaccine formulation to prevent tumor progression in a murine model of melanoma, shown to be immunogenic.

Furthermore, we also attested that human melanoma cell lines release peptides upon *Salmonella* infection. T2 binding assays performed on two different human melanoma cell lines suggested that also in this case, the high peptide release is mediated by hemichannels. Specifically, we demonstrated that peptides released by a human melanoma cell line induced the expansion of anti-tumor CD8-T cells from healthy-donor peripheral blood mononuclear cells. An MS analysis of proteins and peptides released by infected murine and human melanoma cells revealed that among them there are novel tumor epitopes. Through an innovative MS-approach, that combined the analysis of classical database searching engine with the analysis of the features at MS1-level, we gained knowledge of peptides that otherwise would not be accessible (neoantigens, spliced tumor antigens, post

translational modified peptides). De novo sequencing procedures will allow us to identify their sequence in the future. Encouraging preliminary results, that also proved the feasibility and safety of the approach have been shown in the treatment of both canine osteosarcoma and canine high grade sarcoma. Specifically, the therapeutic vaccine treatment of animals using peptides derived from their own *Salmonella*-infected tumor cells appeared to be extremely successful.

Hence, we propose to treat patients-derived tumor cells with *Salmonella* in order to obtain neoantigens that could be applied in clinical studies as a vaccine formulation.

1. INTRODUCTION

1.1 Cancer immunosurveillance and cancer immunoediting

The role played by the immune system in body-surveillance against cancer progression was first hypothesized in 1943 by Gross and colleagues. They reported that mice undergoing a primary tumor resection were protected by a subsequent re-exposure. Furthermore, they observed that tumor development was also avoided by a preventive exposure of mice to lethally irradiated tumor cells (Gross 1943). Since then, the development of mouse tumor models with defined immune-deficiencies and the production of highly specific blocking monoclonal antibodies able to target particular immune cells led to the description and immune characterization of the so called "cancer immunosurveillance" hypothesis. In the late 1980 Boon and colleagues were the first ones to describe that the antitumor immune surveillance was due to lymphocytes recognition of aberrant derived by tumor-derived peptides, later defined tumor antigens (De Plaen et al. 1988). The hypothesis of the immune surveillance cannot explain why cancers can evolve in the presence of a competent immune system. Increasing knowledge about the contribution of the immune system to cancer development has led to describe immune system as a dynamic process that can protect the host against tumor development but also promote tumor growth by selecting for more aggressive tumors (Dunn et al. 2004a).

This process referred as "cancer immunoediting" comprises of three phases: elimination, equilibrium and escape (Dunn et al. 2004b). During the elimination phase the activation of the innate and adaptive immune system leads to an efficacious cancer immune surveillance preventing tumor development. In order to elicit an effective antitumor immune response a number of stepwise events must be initiated. First, tumor antigens need to be taken up by dendritic cells (DCs) at the tumor site and presented to their MHC class I and II. Then, pro-inflammatory signals have to enable DCs to properly mature and migrate to the lymph

nodes to prime and activate T cells. At this point T cell expansion occurs if the DC-presented antigen has broken both central and peripheral immunological tolerance whose aim is to prevent autoimmunity (Träger et al. 2012). The antigen needs to be different from all the self-antigens presented at thymus level during T cell development thus avoiding the negative selection of antigen-specific-T cell. Moreover, at lymph nodes level, DC-presented antigens need to be recognized with high affinity by the TCR of antigen-specific T cell (Redmond & Sherman 2005). As last step, activated T lymphocytes infiltrate the tumor site and kill their target cells upon tumor antigen recognition. However, some tumor cells may avoid the elimination phase and keep coexisting with immune cells transitioning to a period of latency called equilibrium phase. During this phase, tumor cells with reduced immunogenicity are selected and these cells are more capable of surviving in an immunocompetent host. The ability of cancer to evade the specifically activated antitumor response became eventually recognized as cancer hallmark: "Immune destruction evasion" (Hanahan & Weinberg 2011). This property that was only ultimately described as cancer hallmark is possibly the most critical aspect of cancer. There are many mechanisms through which tumor cells can evade the immune system. Tumor cells can acquire lesions in antigen processing and presentation pathway (Seliger et al. 2001) that facilitate evasion from adaptive immune recognition; or they can express ligands for inhibitory receptors, such as, the programmed cell death protein ligand 1 (PDL1) leading PD-1-expressing tumor-specific lymphocytes to anergy (Taube et al. 2012). Tumor cells can also promote the escape phase by directly acting on the tumor microenvironment through the secretion of cytokines and chemokines that inhibit the protective functions of the immune system, such as the transforming growth factor β (TGF-β) or the interleukin-10 (IL-10). Recent studies have documented that tumors may also facilitate the generation, activation, or function of immunosuppressive T cell populations such as interleukin-13 (IL-13)-producing NKT cells (Terabe et al. 2000) or $CD4^{+}CD25^{+}$ regulatory T cells (T reg)

(Shimizu et al. 1999). The latter play an important role in inhibiting naturally occurring and therapeutically induced protective immune responses against tumors (Shimizu et al. 1999).

1.2 Tumor antigens

Nucleated cells have the capacity to present peptides derived from endogenous proteins on their MHC class I molecules. This property is needed for the activation of $CD8^+$ cytotoxic T lymphocytes (CTLs) that are able to recognize only the antigenic peptides associated with MHC class I molecules (Leone et al. 2013). Four different classes of tumor antigens have been described until now: tumor associated antigens (TAA), that are peptides encoded by the normal genome but aberrantly expressed by tumor cells (i.e. overexpressed, (Menard et al. 2000)); cancer testis antigens (CTAs), that are peptides belonging to developmental protein (hence not present during adulthood) whose expression is re-stored by cancer cells (van der Bruggen et al. 1991); neoantigens, that are mutated peptides generated by non-synonymous mutation or other genetic alteration (Heemskerk et al. 2012); and the recently identified spliced antigens that arise from post translational splicing (Vigneron 2004; Vigneron & Van den Eynde 2014; Liepe et al. 2016). The stronger and more efficient immune response is directed against antigens that are highly tumor specific. First, T cell responses that are elicited against such antigens in cancer patients ought to leave normal tissues completely unharmed. Second, our natural tolerance mechanisms should not prevent or repress these responses (Coulie et al. 2014). Neoantigens and spliced tumor antigens, having a different sequence from all the self-peptides, can be considered as the best-choice target for an effective antitumor response.

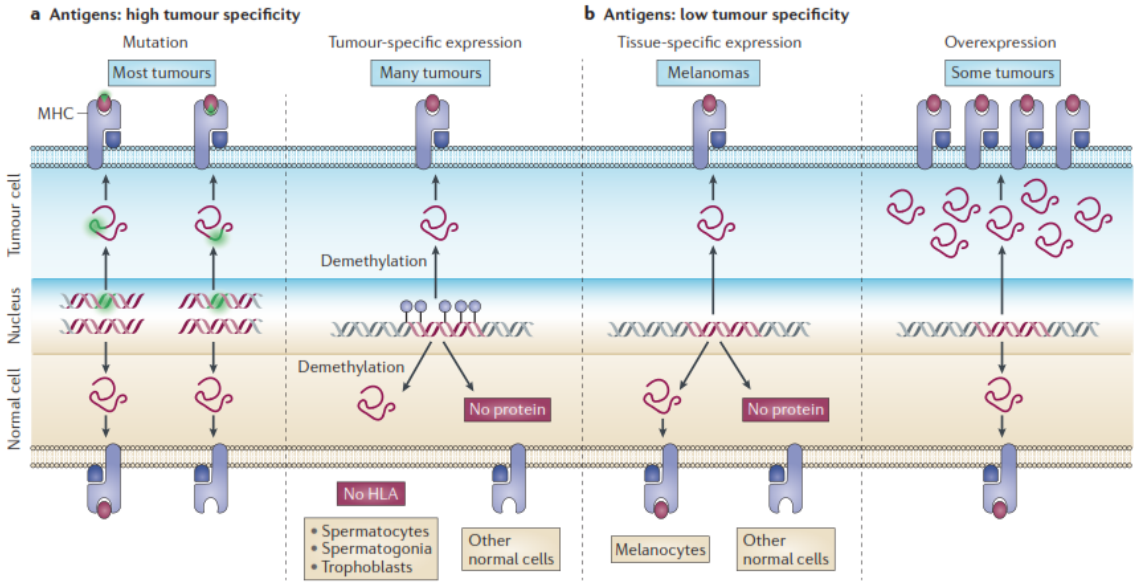

Figure 1-1. Tumor antigens specificity. *A* High specific tumor antigens arise from single non synonymous mutation: an epitope different in sequence from the parental peptide is associates to the MHC molecules (neoantigens), or the presentation of a peptide that normally do not bind MHC molecule is promoted (germ-line tumor antigens). *B* Low tumor specificity antigens are instead antigens that usually have a tissue-specific expression (like melanoma associated antigens, gp100) but also antigens that are recognized because overexpressed. Adapted from *Boon et al Nature 2014*

1.2.1 Antigen presentation and immunoediting

Endogenous proteins are processed in an ubiquitin-proteasome-dependent manner at the level of the cytosol; proteasome-derived peptides, either spliced peptides or conventional peptides, are translocated into the endoplasmic reticulum by TAP (ATP-dependent peptide transporter associated with antigen processing) where can be further trimmed by ER-amino-terminal peptidases (ERAP) to properly fit into the groove of the MHC class I molecule. Peptide binding on class I heavy chain and ß2-microglobulin and the stabilization of the trimeric complex occurs by the assistance of four chaperones: calreticulin, calnexin, ERp57 and tapasin. Then the complex is transported via the trans-Golgi apparatus to the cell surface.

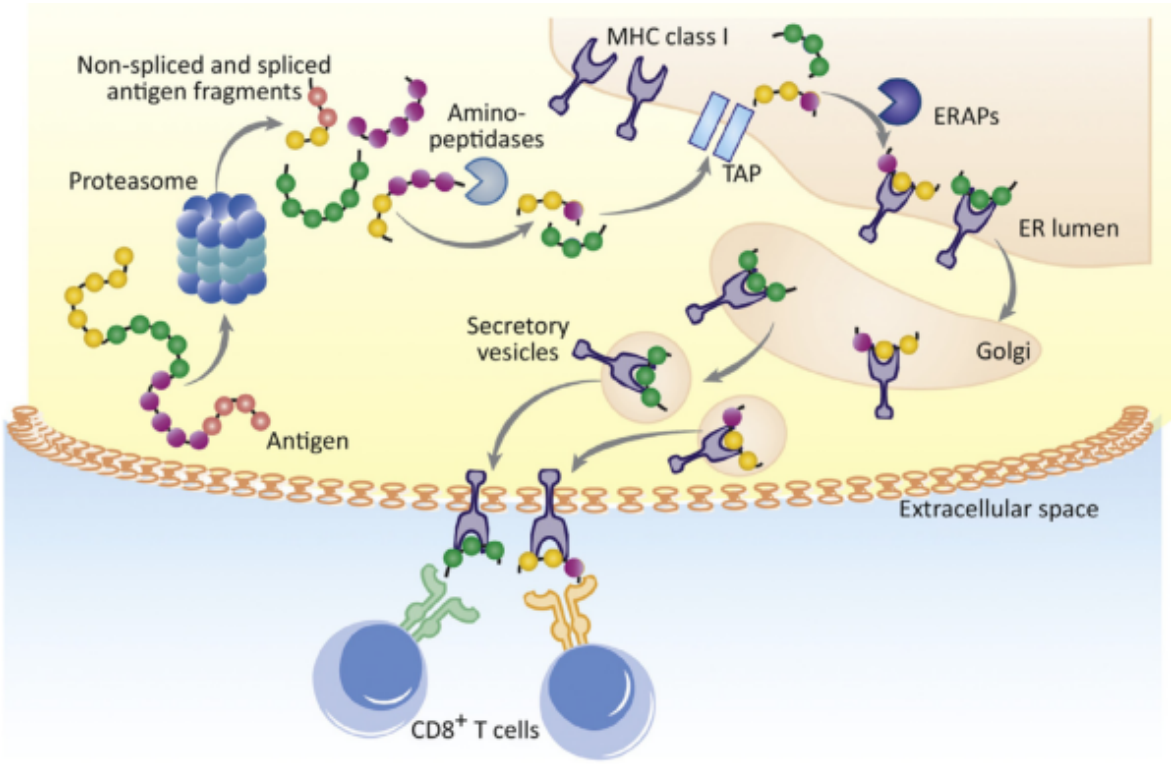

Figure 1-2. Class I antigens presentation. Endogenous proteins are processed in an ubiquitin-proteasome-dependent manner at the level of the cytosol; proteasome-derived peptides, either spliced peptides or conventional peptides, are translocated into the endoplasmic reticulum by TAP where can be further trimmed by ERAP to properly fit into the groove of the MHC class I molecule Adapted from *Mishto M and Liepe J. Trends in Immunology 2017*

Immunoediting pressure can lead tumor cells to accumulate defects in MHC class I proteins expression (Ferrone & Marincola 1995) or other components of the antigen processing machinery (APM) (Restifo et al. 1993), leading to a reduced MHC molecules expression (Durgeau et al. 2011). By these alterations tumors lower the chance to be recognized by immune cells avoiding their activation. Aberrations in MHC class I expression can be sometimes reversed targeting gene expression regulators; for example treatment with IFN-γ agonist or with histone deacetylase inhibitors enable to re-establish a correct MHC class I expression (Khan et al. 2008). In most of the cases APM-defective tumors are not responsive to any treatment that targets gene expression. Strategy to counteract these tumors have been recently proposed thanks to the discovery that APM-

defective tumor cells express on the residual MHC class I molecules a unique class of $CD8^+$ T cell epitopes that is associated with impaired peptides processing (TEIPP)(Seidel et al. 2012). TEIPP are mainly derived by non-mutated sequences of housekeeping genes (Lampen et al. 2010) but, since they fail to be presented by cells that have a functional APM, central tolerance is not a concern thus becoming an attractive target for tumor specific-CTL (van Hall et al. 2006). In a preclinical study, therapeutic vaccination with TAP-inhibited DCs induced TEIPPs-specific CTLs that successfully avoided APM-defective tumor growth (Chambers et al. 2007).

1.2.2 Antigen presentation by antigen presenting cells: cross-presentation and immunoproteasome

Antigen presenting cells (APC) are responsible for the activation of naïve $CD8^+$ T cells toward effector antigen-specific CTL, enabling them to recognize and kill infected cells and tumor cells. If the APCs are not directly infected (hence they cannot process pathogen antigens by the standard ubiquitin proteasome pathway), they need to acquire exogenous antigens from the infectious agent (or from cancer cells) and present them on MHC class I molecules, by a mechanism known as cross-presentation (Joffre et al. 2012). This property is uniquely shared by APC cells. Exogenous proteins are taken up by endocytosis or by autophagy and delivered to the endosomes. From here proteins can follow two different pathways, either a vesicular pathway or a cytosolic pathway (Joffre et al. 2012). By the former pathway, endosomes can fuse with lysosomes where lysosomal peptidases process the exogenous protein and the derived peptides are loaded on MHC class I molecules. Proteasome and TAP are not involved in antigen loading, in this pathway. Alternatively, following the cytosolic pathway, proteins can be exported from the endosomes to the cytosol and being processed into peptides at this level in a proteasome-dependent manner or by proteases like insulin-degrading enzyme, nardilysin and thimet oligopeptidase. Cytosol-generated peptides are then loaded on MHC class I molecules

following the classical MHC class I-mediated antigen presentation pathway, in a TAP-dependent manner. MHC class I molecules loaded with the antigens are eventually transported via the trans-Golgi apparatus to the cell surface for presentation to CTLs (Joffre et al. 2012).

It is known that mature APCs express almost a uniquely variant of proteasome, the immunoproteasome (Vigneron & Van den Eynde 2014), that differs in structure and for cleavage quality from the standard proteasome expressed by all body cells. Both *in vitro* (Toes et al. 2001) and *in vivo* (Kincaid et al. 2012) studies have shown that immunoproteasome and standard proteasome give rise to antigens that only partially overlap; hence DCs could prime T cells towards antigens that eventually are not exposed by tumor cells (Morel et al. 2000).

1.2.3 Gap junction

Exogenous peptides can enter the cross-presentation pathway also via gap junctions (GJ) (Saccheri et al. 2010; Neijssen et al. 2005). GJ are formed by the docking of the plasma-membrane hemichannels of two adjacent cells that create an overall 3D structure that resembles a channel through which substances with a molecular weight up to 1KDa are transferred. Small peptides up to 2KDa (or about 16 amino acids) can also diffuse over gap junctions (Neijssen et al. 2005); indeed the lack of secondary structure of such small peptides enable them to be transferred through adjacent cells (Neijssen et al. 2005). A single functional hemichannel is composed by six connexin molecules (Unger et al. 1999) and every connexin molecule is formed by four membrane spanning domains, two extracellular domains and a large cytoplasmic C-terminal tail, which is important in the gating of the channel. Connexin isoforms are expressed in a strictly tissue-specific manner with the exception of Cx43 isotype that is expressed ubiquitously (Oyamada et al. 2005). Connexons formed by different connexin isotypes can still combine to form a gap junction.

Two adjacent cells have an homotypic interaction if both cells express the same connexons, heterotypic interaction if cells express different connexons (Weber et al. 2004).

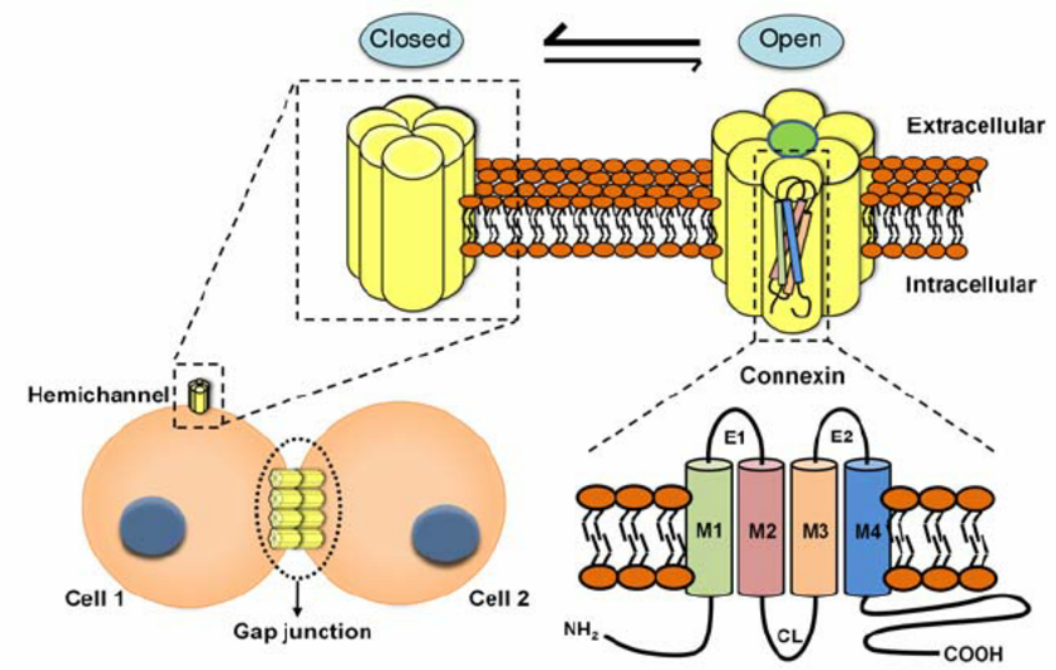

Figure 1-3. **Hemichannels and gap junction**. A single functional plasma membrane hemichannel is composed by six connexin molecules (Unger et al. 1999) and every connexin molecule is formed by four membrane spanning domains, two extracellular domains and a large cytoplasmic C-terminal tail which is important to regulate the opening of the channel. The hemichannels of two adjacent cells can either combine to form gap junctions or simply stand as unopposed hemichannels. Adapted from *Orellana et al Journal of Neuroscienc 2011.*

In the skin, GJ-mediated intercellular communication is likely to be involved in the regulation of keratinocyte growth, differentiation, migration and in keratinocyte-melanocyte interaction. Alterations of the physiological GJ-mediated communication also play a role both in carcinogenesis and in cancer progression of different tumors (Mesnil et al. 2005). GJ downregulation or their complete loss, allows tumor cells to be isolated from the surrounding cells prompting their expansion. Several factors, such as tumor-promoting agents, oncogenes, and growth factors, can be responsible for the reduced GJ level. Among the genetic alteration that have been identified, some involve the connexin genes and are

responsible for their low transcription; others instead induce an aberrant trafficking thus avoiding a proper connexin proteins transport to the membrane (Oyamada et al. 2005). Several different connexin isoforms are expressed in skin, including Cx26, Cx30, Cx31, and Cx43. Both mouse skin carcinomas and human skin cancer cell lines have shown to express low levels of these connexins (Mesnil et al. 2005).

Cx proteins are also expressed by cells of the immune system and GJ are commonly used by immune cells to receive and send biochemical information with the surrounding cells. Multiple studies have demonstrated that GJ-intercellular communication contributes to the activation of a functional antitumor response, and that a GJ-mediated communication between DCs is required for their own effective maturation and activation (Matsue et al. 2005). At the level of lymphoid germinal center, Cx43-GJ functionally couples follicular DCs to each other and to B lymphocytes allowing delivering of signals (Krenacs T et al. 1997). Moreover, in the intestine the transfer of fed antigens via GJ from $CX3CR1^{+}$ macrophages to $CD103^{+}$ DCs has been shown to enable the establishment of oral tolerance (Mazzini et al. 2014). Connexin proteins are also recruited to the immunological synapse during T cell priming as both GJs and stand-alone hemichannels (Mendoza-Naranjo et al. 2011); intercellular communication between DCs and T cells is bidirectional and the silencing of Cx43 impairs the crosstalk necessary for T cells activation (Elgueta et al. 2009). In addition, GJs allow melanoma antigen transfer between tumor and DCs that can activate melanoma-specific CTLs (Mendoza-Naranjo et al. 2007). The involvement of GJs and particularly Cx43 in this process was demonstrated by the inhibition of Ag acquisition after the addition of either a Cx-mimetic peptide or GJ blockers (Mendoza-Naranjo et al. 2007). Accordingly, cross-presentation via GJs from tumor cells to immune cells can be targeted to improve immunotherapy protocols. By GJs-mediated antigen transfer, DCs can present not only tumor antigens that have been processed by DC-immunoproteasome, but also by tumor antigens that have been pre-processed by tumor-proteasome (Matsue et al.

2005). GJs-mediated intercellular methods of communication have been largely exploited by our laboratory identifying a promising immunotherapy approach based on the peptides that are specifically transferred through GJs, following *Salmonella* infection (Saccheri et al. 2010). We have shown that infection of human and mouse melanoma cells with *Salmonella* induces the up-regulation of connexin 43, the most abundant and ubiquitous component of hemichannels. Furthermore, we have demonstrated that bacteria-treated melanoma cells establish GJs with DCs, thus allowing the transfer of pre-processed antigens from the tumor cells to the DCs (bypassing the DC-immuneproteasome function), ultimately leading to the activation of potent antitumor cytotoxic responses (Saccheri et al. 2010). The possibility that *Salmonella* could also induce immunogenic peptides release through the unopposed connexin hemichannels is still to be elucidated

1.2.4 Mass spectrometry approaches to detect tumor antigens

Identification of tumor antigens is pivotal to design efficient immunotherapy strategies. The first and successful approach was based on DNA-cloning technology and was proposed by Boon and colleagues (Van der Bruggen et al. 1991). They created a genomic library of a patient's derived tumor, and targeted each library component with patients PBMCs sensitized to tumor cells *in vitro*. The DNA clones form the genomic libraries responsible for lymphocyte stimulation were then identified. The discovery that tumor antigens were expressed on HLA molecules lead to the development of mass spectrometry (MS) strategies to identify the whole collection of antigens presented by tumor cells, the immunopeptidome (Caron et al. 2015). Data obtained by the analysis of immunopeptidome were mainly derived applying an MS data acquisition method called discovery-based method or data dependent analysis (DDA). By this method the most abundant precursor ions detected by the mass spectrometer in a survey scan per millisecond (MS1) are selected for fragmentation (MS2). MS identification was performed after isolation of MHC class I peptides from tumor cells by immunoaffinity columns coupled with antibody against HLA

molecules. Isolated peptides were then identified by MS after liquid chromatography separation (Berlin et al. 2015; Walter et al. 2012; Kumari et al. 2014). The discovery of neoantigens and the compelling evidence that they are the best candidates to induce a clinically efficient antitumor response have boosted the development of new MS approaches for their identification. Neoantigens are mutated peptides generated by non-synonymous mutation or other genetic alteration, hence their identification cannot be achieved without taking into consideration their sequence differences. To overcome this challenge the database search has been performed on customized databases of peptides usually derived by exome sequencing data. The integration of exome sequencing data (followed by a plethora of in silico analysis to prioritize neoantigens list) with MS approaches allowed to unravel neoantigens (Kalaora et al. 2016; Yadav et al. 2014; Castle et al. 2012; Lu et al. 2014) and spliced tumor antigens that could be exploited for immunotherapy purposes (Liepe et al. 2016). Although the important achievements, this approach has some drawbacks; it is time consuming, still costly considering that it should be applied to each single patient.

1.3 Immunotherapy of cancer

Immunotherapy is an anticancer approach aimed at promoting or enhancing antitumor immune responses. This concept dates back to the late nineteenth century, when William B. Coley observed tumor shrinkage and eventually complete regression following injection of bacterial products in and around tumors (Coley 1891). Following this revolutionary approach, several immunotherapeutic strategies were developed, consisting of both passive and active immunotherapy (Salem et al. 2007). Passive strategies include the use of immunomodulators such as cytokines, adoptive cells transfer (ACT) and antibodies. On the contrary, active immunotherapy strategies rely on cancer vaccines and oncolytic viruses, seeking the generation within the patients of long-lasting antitumor responses able to

protect in case of relapse (Mellman et al. 2011). The immunotherapeutic approaches proposed till now aim to promote or enhance the anticancer response at different levels (Chen & Mellman 2013): promoting immunogenic tumor-cell death, instructing immune cells towards tumor antigens and counteracting the immune suppressive mechanisms imposed by the tumor cells. Considering the complexity of tumor development and the negative regulation of the immune responses exerted by tumor cells, the more promising approach to treat cancer is by far the one that combines more immunotherapeutic strategies.

1.3.1 Cytokines

Cytokines are having a limited clinical application due to the opposite effect they can exert on the immune system; they can increase or decrease various aspects of the immune response. The two cytokines whose administration in patients has been exploited are IFN-α and IL-2. Both cytokines often showed low overall response rate, drug's low tolerability and potentially life-threatening side effects (Rosenberg et al. 1985).

1.3.2 Adoptive cell transfer

Adoptive cell transfer (ACT) is the transfer of patient's T lymphocytes that show reactivity toward tumor antigens. They are reintroduced into the patient after *ex vivo* expansion with cytokines and/or transduction with tumor-specific T-cell receptor (TCR) (McGranahan et al. 2016). Lymphocytes can be isolated from peripheral blood (PB) or from tumor specimens (tumor infiltrating lymphocytes, TILs). While TILs isolation is not always feasible for each patient, the use of PB-derived T cells showed encouraging results. Nevertheless, the main drawback of ACT therapy still remains the toxicity due to lymphodepletion induced by high dose chemotherapy or radiotherapy, and by administration of high doses of IL-2. Moreover, the identification of the right antigens to be used for this approach represents a limitation. A recently developed antitumor strategy

relies on T cells genetically engineered to express chimeric antigen receptors, CARs. CARs are synthetic receptors that have an extracellular antigen specific target binding domain (derived from scFv), a hinge and transmembrane segment (derived from CD8α or IgG4) as well as an intracellular domain (Schmitt 2017). The advantages of CAR T cells rely on the capability of these cells to specifically recognize target antigens in an HLA-independent manner, and to exerted T cell cytotoxicity activity, without the need to recruit other effector immune cells. Although CAR T cells can be envisioned as a possible treatment of several cancers, this possibility has thus far been severely limited by the lack of suitable tumor antigens that would avoid toxicity from off-target immune activation (Maude et al. 2014). Advancement in neoantigens identification may pave the path of successful CAR T cells against solid tumor sas it was recently shown in a preclinical model of adenocarcinoma (Posey et al. 2016).

1.3.3 Monoclonal antibodies

Monoclonal antibody (mAb) can be used to harness the host defense mechanisms, either targeting immune cell receptors to boost their activation or by the binding of tumor cell receptors to directly inhibit tumor growth. Several effects can be prompted upon the recognition of the targets on tumor cells. Some antibodies can directly exert an antiproliferative or apoptotic effect, while others can induce complement system activation or an antibody-dependent cellular cytotoxicity. A category of monoclonal antibodies that is providing significant benefits to cancer patients is represented by immunocheckpoint inhibitors. It has been clearly demonstrated that antibodies against either programmed cell death 1 receptor (PD-1) and its ligand (PDL-1), or the CD28/cytotoxic T-lymphocyte antigen 4 (CTLA-4) release the breaks by which antitumor-lymphocytes are constrained by tumor cells.

Although immunocheckpoint inhibitors have different targets, their effect is not tumor-type specific but is exerted on T cells level within the tumor microenviroment, hence their

success relies on the existing T cell repertoire (Gros et al. 2014). This explains why the combinatorial use of anti PD-1 and anti CTLA-4 antibodies showed improvement in clinical response only on a subset of patients (Wolchok et al. 2013; Larkin et al. 2015) with a high mutational burden (Rizvi et al. 2015; Le et al. 2015). Specifically, it was observed that higher mutational load (that correlates with a higher number of neoantigens presented on their HLA) was associated with improved patient survival (Zaretsky et al. 2016) (Hugo et al. 2017). All these observations suggest that immunocheckpoint inhibitors are successful only in those patients that, having tumors with high number of mutations, are prone to induce an antitumor response mediated towards neoantigens. Hence, combining checkpoint blockade with therapies that provide the necessary neoantigen-specificity to the antitumor response could be clinically successful, for patients that have an immunogenic tumor but do not develop a neoantigen antitumor, and for patients suffering of a poorly immunogenic tumor (Ott et al. 2017). Cancer vaccines, discussed below, can be a valuable option for combinatorial strategies.

1.3.4 Oncolytic viruses

Advancement in viral biology, tumor immunology and in molecular genetics techniques allowed researchers to investigate oncolytic viruses as novel anticancer therapeutic agents. Although oncolytic viruses can enter both normal and cancer cells, genetic alteration in cancer cells provides a selective advantage for viral replication. Virus replication within tumor cells eventually provokes cell lysis and the subsequent antigen release causes viral propagation to other tumor cells. Released tumor antigens can be taken up by DCs prompting a systemic anti-tumor response (Kaufman et al. 2015). Once injected at the tumor level, viruses exert an adjuvant function per se, due to their pathogenicity. They provide stimulatory signals both to favor immune cell recruitment at the tumor site and to promote immune cell activation (Kaufman et al. 2015). Another advantage of oncolytic viruses is that their genetic content can be modified to produce cytokines or specific

proteins upon infection that could be subsequently released by tumor cell' lysis. This possibility has been recently exploited to generate the talimogene laherparepvec (T-VEC) oncovirus, a modified herpes simplex virus type 1, encoding granulocyte–macrophage colony-stimulating factor (GM-CSF) (Andtbacka et al. 2015). Nevertheless, oncolytic virus adoption as cancer therapy needs to be accurately evaluated since not every accessible tumor is suitable for oncolytic viruses treatment. Challenges to the development of oncolytic viruses as therapeutic strategies include validated pharmaco-dynamic and pharmacokinetic assays due to the fact that viruses are not eliminated as a result of cell metabolism, but need to be eradicated by patient immune system; biosafety issues need also to be taken into consideration (Chiocca & Rabkin 2015).

1.4 Anti-cancer vaccines

Anti-cancer vaccines can be potentially applied to overcome primary resistance to checkpoint blockade of tumors with low mutational load and increasing response rate of highly mutated tumors (Gross et al. 2017). The challenges that avoid the initiation of the stepwise events necessary to prompt a proper antitumor response need to be taken into account at the moment of designing a novel anti-cancer vaccine; the choice of a tumor-specific antigen able to overcome peripheral tolerance; the choice of an adjuvant capable to properly boost the immune response; and the development of a cancer vaccine that can overcome the immunesuppression of tumor-specific CTL and elicit a long lasting antitumor response.

Anti-cancer vaccines can be divided into two major groups: DC-dependent and DC–independent vaccines. Numerous studies have evaluated the efficacy of DCs pulsed with tumor-derived proteins or peptides in cancer immunotherapy (Nair et al. 1997; P Paglia et al 1996; Fong et al. 2001). From an immunologic standpoint, DCs-based immunotherapy carries the highest potential of inducing effective anticancer immune responses since DCs

are key players in the activation of T cells. In order to induce powerful and specific CTL responses, the best option has been to load DCs with tumor-associated antigens either derived from tumor MHC molecules, (Berlin et al. 2015; Stronen et al. 2016), or newly predicted through exon sequencing data (Kalaora et al. 2016; Lu et al. 2014). Specific tumor antigen prediction was then evaluated on their ability to bind MHC class I by in silico tools or cell-based approaches (Carreno 2015; Bassani-Sternberg & Coukos 2016). When high affinity neoantigens identified by patients-derived melanoma cells were loaded on DCs and used for autologous vaccinations, not only was observed an increased T cell immunity directed at naturally occurring neoantigens, but also an expanded breadth of the antitumor response by revealing subdominal neoantigens (Carreno 2015). Recently, the result of twelve-year survival of non-resectable metastatic melanoma patients vaccinated over two years with monocytes-derived DCs matured *in vitro* was reported to be similar to the one observed in Ipilimumab-treated patients without any major toxicity (>2grade)(Gross et al. 2017) suggesting that the combinatorial treatment with therapies that target the immunesuppression can provide unprecedented benefits to melanoma patients. Unfortunately, one major drawback of DC-based approaches is that they are specific for each patient and require leukapheresis, processing and culturing of PBMCs, therefore allowing a limited number of vaccinations.

Immunization strategies that overcome these limitations are DC-free vaccines. Tumor-specific neoantigens are selected as described above but instead of being loaded on DCs, they are conjugated with adjuvant and used as vaccine formulation (Castle et al. 2012; Yadav et al. 2014). These peptide-based vaccines are well tolerated, are not patient-specific and can potentially induce a multi-target and strong immune response when several antigens are included in the vaccine formulation thus targeting tumor heterogeneity as well as minimizing the chance of tumor escape by loss of antigens. In vaccine formulations, either peptides of the exact length that directly bind to MHC molecules or

15-35 amminoacid-long peptides (synthetic long peptides, SLP) that span the MHC-binding-epitope, can be included. SLPs have been shown to activate a broader and long lasting T cell response than peptides that precisely fit into MHC class I molecule independently from adjuvant choice (Bijker et al. 2007). Moreover dendritic cells process synthetic long peptides better than whole proteins, improving antigen presentation and T-cell activation (Rosalia et al. 2013). SLP constant inclusion in designing novel strategies could prompt the development of high immunogenic and durable cancer vaccines. Recently, the results of a trial involving 6 melanoma patients that were vaccinated with patients-specific neoantigens combined with a TLR3 agonist (poly:IC synthetic analog of double-stranded RNA), showed that four patients had no tumor recurrence at 25 months after vaccination, while 2 patients with recurrent disease were treated with anti PD-1 antibody and had complete tumor regression (Ott et al. 2017). This latter result highlighted the success of multi-targets approaches for cancer treatment. In this setting, patient-specific neoantigens used for the immunization were SLPs and together with the chosen adjuvant not only expanded pre-existing neoantigen-specific T cell populations but also induced a broader repertoire of new T cell-specificities. Compelling evidence demonstrated the feasibility and safety of neoantigens-based cancer vaccines and furthermore their ability to elicit an antitumor T cell response. All together these reports have eventually provided a strong rational for cancer vaccine development either as monotherapy or in combination with other cancer treatments that target tumor-escape strategies.

1.4.1 *Salmonella*'s biology and *Salmonella*-based cancer immunotherapy

Salmonella enterica serovars are Gram-negative facultative intracellular bacteria that, depending on the serovar, can cause local gastroenteritis or systemic disease called typhoid fever through food and water intake. Indeed, human infections by *Salmonella* enterica serovar Typhi (hereafter referred to as *S. typhi*) causes typhoid fever, while *Salmonella* enterica serovar Typhimurium (referred to as *S. typhimurium*) induces only locally

restricted infection. On the contrary, mice are susceptible to oral infection with *S. typhimurium*, but not *S.typhi*, resembling the human systemic disease (Voedisch et al. 2009). Therefore *S. typhimurium* oral infection in mice is widely used as model of human systemic infection.

Salmonella, is able to cross the membranes and get inside the cytosol of infected cells through the expression of effector proteins belonging to the type III secretion system (TTSS) (Sukhan et al. 2001). These translocated effectors, encoded by chromosomal regions are called *Salmonella*'s pathogenicity island 1 and 2 (SP-1, SP-2), and are able to alter host-cell functions such as signal transduction, cytoskeletal architecture, membrane trafficking, and cytokine gene expression. These modifications create an intracellular compartment distinct from a classical phagosome that is permissive for bacterial growth (Sukhan et al. 2001). Genes of the SPI-1 TTSS are activated at the early stage of cell infection and are required for translocating effectors across the host cell plasma membrane (Sukhan et al. 2001). The SPI-2 encoded proteins have been associated to the ability of *Salmonella* to survive in the host cell and to spread systemically (Ochman et al., 1996).

Salmonella, as other bacteria including *Listeria*, *Clostridium*, *Bacillus Calmette-Gu* (BCG) has been extensively studied as anticancer agent, both as immunostimulatory agent and as vaccine vector (Paterson et al. 2015). The advantage of using bacteria instead of viruses is that bacteria can be readily and irreversibly attenuates, their infection can be curtailed by antibiotics and can be produced at lower costs. Pathogens can induce a strong pro-inflammatory innate immune response through the action of pathogen associated molecular pattern (PAMPs) and potently activate DCs mainly through engagement of their toll-like receptors (TLRs) (Van Duin et al. 2006), representing the most powerful natural adjuvants. These properties have been exploited to overcome the tolerance associated with tumors.

Salmonella can infect both phagocytic cells and non-phagocytic cells, via the expression of a type-three secretion system (TTSS); moreover, if systemically injected, *Salmonella* is

also able to colonize preferentially tumor areas. This ability, shared also by the Gram+ bacteria *Listeria*, has been exploited following the development of attenuated and non-pathogenic bacteria strains, and through DNA manipulation tailored to regulate specific gene expression (Vendrell et al. 2011; Sun et al. 2009; Singh et al. 2014). Preclinical studies have shown the feasibility of tumor antigens delivery as well as cytotoxic proteins by *Salmonella* and *Listeria*. Recently a non-virulent *Salmonella* was engineered to secrete heterologous flagellin (TLR5 agonist) which showed the capability to suppress tumor development (Zheng et al. 2017).

Salmonella as an immunotherapy agent that can also be directly injected inside the tumor mass. It has been shown that *Salmonella* injection in melanoma-B16 tumor mass, resulted in the regression of even bulky tumor masses, and had also impacts on the growth of distant untreated lesions (Avogadri et al. 2008). Three main mechanisms are responsible for its antitumor effect. First, infected tumor cells express *Salmonella* antigens on their HLA and become target of *Salmonella*-specific CTLs (Avogadri et al. 2005). Second, both innate and adaptive immune cells are recruited at the infection site, overcoming the tumor suppressive environment (Yoon et al. 2017; Hong et al. 2013). Third, infection with *Salmonella* promotes cross-presentation of tumor antigens and establishment of systemic antitumor response (Saccheri et al. 2010). The transfer of antigens occurs mainly through gap junctions (Mendoza-Naranjo et al. 2007). This last event has been extensively investigated in our laboratory (Saccheri et al. 2010) and is the fundamental basis of the presented study.

1.5 Melanoma

Melanoma is a malignant tumor that arises from melanocytic cells and primarily involves the skin; according to an updated epidemiologic report, in Europe the incidence rate is <10-25 new melanoma cases per 100.000 inhabitants (Whiteman 2016 Jinvet Dermat).

While melanomas are usually heavily pigmented, they can also be amelanotic. Melanoma has the tendency to develop metastasis and become resistant to therapy: these aggressive features make it one of the deadliest forms of cancer. Although it accounts roughly for 4% of all skin cancers, it is responsible for 90% of skin cancer deaths (Dummer et al. 2015).

The anatomical classification of melanoma is based on the thickness of the tumor and whether cancer has spread to lymph nodes or other parts of the body. This classification, reported below in figure 1.4, includes four stages of disease progression and was proposed in 2009 by the American Joint Committee on Cancer; it is still the cornerstone for classifying melanomas (Balch et al. 2009).

Stage	Primary tumour (pT)	Regional lymph node metastases (N)	Distant metastases (M)
0	*In situ* tumour	None	None
IA	≤1.0 mm, no ulceration	None	None
IB	≤1.0 mm with ulceration or mitotic rate ≥1/mm^2	None	None
	1.01–2.0 mm, no ulceration	None	None
IIA	1.01–2.0 mm with ulceration	None	None
	2.01–4.0 mm, no ulceration	None	None
IIB	2.01–4.0 mm with ulceration	None	None
	>4.0 mm, no ulceration	None	None
IIC	>4.0 mm with ulceration	None	None
IIIA	Any tumour thickness, no ulceration	Micrometastases	None
IIIB	Any tumour thickness with ulceration	Micrometastases	None
	Any tumour thickness, no ulceration	Up to three macrometastases	None
	Any tumour thickness ± ulceration	None but satellite and/or in-transit metastases	None
IIIC	Any tumour thickness with ulceration	Up to three macrometastases	None
	Any tumour thickness ± ulceration	Four or more macrometastases, or lymph node involvement extending beyond capsule, or satellite and/or in-transit metastases with lymph node involvement	None
IV			Distant metastases

Figure 1-4. Staging of melanoma. Melanoma includes four stages of disease progression. This classification was proposed in 2009 by the American Joint Committee on Cancer Adapted from *C. Garbe et al., European Journal of Cancer 2016*

Staging of melanoma inversely correlates with survival. Melanoma that are diagnosed as primary tumor without evidence of metastasis are associated with 75-85% of 10-year survival (Stage I and stage II). Stage III melanoma patients have a different life expectancy according to the type of diagnosed metastasis:

- satellite metastases: up to 2 cm distant from primary tumor; the 10-year survival is 30-50%.

- in-transit metastases: located in the skin, distant more than 2 cm from the primary tumor; the 10-year survival is 30-50%
- micrometastases: located in the regional lymph nodes, diagnosed by sentinel lymph node biopsy; the 10-year survival is 30-70%
- macrometastases: located in the regional lymph nodes; palpation or imaging techniques are sufficient for diagnosis; the 10-year survival is 20-40%

Stage IV melanoma patients with distant metastases have a grim prognosis with a median survival in untreated patients being only of 6-9 months, although there is considerable variation depending on aggressiveness of the individual tumor (Garbe et al. 2016).

Although melanoma is a highly heterogeneous disease, deep molecular analyses have revealed consistent genetic patterns among different melanoma subtypes that can be considered 'driver mutations'. The BRAF, NRAS and NF-1 mutations can be considered driver mutations that then lead to the accumulation of several other genetic alterations. The mutational load of melanoma is high; a median of 171 mutations are found in melanoma while an average of 80 mutations are found in colon cancer as well as breast tumor (Greenman et al. 2007). Most of the mutations are not necessary for the survival of the tumor but increase the number of potential neoantigens, thus leading to an increased immunogenicity and a higher opportunity for immune system recognition. Melanoma antigens and neoantigens can be divided in four categories:

1. germ cells/cancer testis antigens, peptides belonging to proteins expressed during the development but not in adult stage: NY-ESO/MAGE/BAGE/GAGE
2. differentiation antigens, peptides belonging to protein expressed only by melanocytes: Tyrp1, gp100, MelanA
3. overexpressed antigens: beta catenin/Cyclin dependent kinase

4. sequestered antigens, peptides usually hidden from immune detection: TEIPP peptides

1.5.1 Melanoma therapies

The first line of melanoma therapy is surgical resection with safety margins. Evaluation of the draining lymph nodes by palpation or by sonography is required and, if metastases are diagnosed, lymph nodes are radically dissected. The surgical removal of metastases detected at skin level is considered a curative practice in stage III patients. In addition to surgery, other conventional therapies can be adopted like laser therapy and cryosurgery; immunotherapy strategies (e.g. IL-2 administration, TLR 9 agonist (imiquimod), and oncolytic viruses-based therapies (as T-VEC). Radiotherapy is indicated in case surgical resection is not complete and when regional lymph nodes are not operable (Garbe et al. 2016).

Mutational test is mandatory for patients with advanced disease (high risk resected melanoma stage IIc, stage III and stage IV) in order to apply a therapy that specifically targets the identified mutation. Vemurafenib and Dabrafenib, drugs that specifically inhibit the kinase activity of mutated BRAF gene, were shown to successful prolong the overall survival of melanoma patients BRAF-mutated (Chapman et al. 2011). The discovery of melanoma antigens and neoantigens has also led to the development of immunotherapy strategies. DC-mediated cancer vaccines, in which monocyte-derived DCs matured *in vitro* and loaded with 4 HLA class I and 6 HLA class II-restricted tumor peptides were used to treat nonresectable metastatic melanoma patients reporting an overall survival of 20% of the patients (Gross et al. 2017). Neoantigens and tumor antigens have also been exploited directly as synthetic peptides in cancer vaccine formulation; successful results of high risk melanoma patients immunization with synthetic long peptides have been recently reported (Ott et al. 2017). Immunotherapies approved for melanoma comprise monoclonal

antibodies against immunocheckpoint, both CTLA-4 (Ipilimumab) (Smith et al. 2011) and PD-1 (Nivolumab and Pembrolizumab) (Postow et al. 2015). It has been shown that melanoma patients treated with the combination of Nivolumab and Ipilimumab had longer overall survival than patients treated with a single antibody (Wolchok et al. 2013; Larkin et al. 2015). Chemotherapy at the moment is considered the second or third line of approach in patients with resistance to immunotherapy and targeted therapy (Garbe et al. 2016).

1.6 Model of human osteo/sarcoma: dog affected by spontaneous osteosarcoma and high-grade sarcoma.

In humans, the most commonly diagnosed primary malignant tumor of the bone is osteosarcoma (OSA). The term OSA is synonymous with osteogenic sarcoma, meaning that these tumors are characterized by the formation of osteoid bone matrix material. It is the third most frequent cause of cancer in adolescents and represents over 56% of all bone tumors (Rowell et al. 2011). Importantly, for OSA-human patients the main cause of death is lung metastasis; only 20% patients survive after 5 years post-diagnosis. To facilitate the introduction of novel therapeutic approaches that had positive results in murine models into human clinical practice, dogs are often considered a testbed. That is because dogs are a valuable model of naturally occurring cancers like osteosarcoma and sarcoma (Rowell et al. 2011). Dogs develop OSA at similar sites as humans and both have similar histology and response to treatment (Rowell et al. 2011). Dogs first participated in clinical trials pioneering limb salvage techniques that are now used in humans.

OSA is the most common primary bone tumor in dogs, comprising 85% of all reported bone neoplasia (Mirabello et al. 2009). On the basis of the quantity of matrix produced and cell arrangement, canine osteosarcoma can be classified as osteoblastic, chondroblastic, fibroblastic, and undifferentiated OSA. Most OSA patients already have microscopic and not visible metastatic disease at the time of diagnosis of the primary tumor (Mirabello et al.

2009). Like in humans, metastases mainly develop at the level of the lung (60%) but also at other bones (5%) or both sites (4,6%) and become the principal cause of death (Spodnick GJ 1992). Median survival times approach 4–5 months with amputation alone (Mirabello et al. 2009), and adjuvant chemotherapy improves median survival times to 8–12 months (Selmic et al. 2014). Recently with the aim to avoid metastasis development, in a multi institutional study conducted in United States, toceranib (multi tyrosin receptor inhibitor) was added to metronomic piroxicam/cyclophosphamide therapy following amputation and carboplatin chemotherapy but the results did not show any improvement of the patients' survival rate (London et al. 2015). Despite the use of various chemotherapy protocols and novel treatment approaches, clinically meaningful improvements in survival have not been achieved, and 90% of dogs die of metastatic disease within 2 years after treatment (Wycislo & Fan 2015).

Soft tissue sarcomas (STSs) are an uncommon and diverse group of malignancies that due to their mesenchymal origin can virtually arise from every tissue of the body; on the basis of their localization 50 different STSs have been described but they are usually classified together because of their similar biological behavior. STSs are more prevalent in childhood and adolescence, where they account for 20% of cancer-related deaths (Young et al. 2014). Most of sarcomas are resistant to both chemotherapy and radiotherapy. Human patients with primary STS, surgery with or without radiotherapy can offer a cure, but nearly half of patients recur and eventually die, with an estimated median survival of 12 to 15 months (Dancsok et al. 2017).

Dogs are an excellent model of STS because they have similar tumor genetic complexity to humans (Rowell et al. 2011). Dog STSs represent between 9 and 15% of all cutaneous or subcutaneous tumors (Liptak & Forrest 2013). There is no apparent breed disposition for STS, but middle to-large dogs are more commonly affected (Mayer & Larue 2005). In dogs, STSs develop most frequently in a subcutaneous location and can arise from several

anatomical sites (e.g. example lymphatic vessels, tendons, joint capsule, ligaments, ascia and nerves) (Liptak & Forrest 2013). Histological criteria are used to define the grade of the tumor. Low (grade I), intermediate (grade II), or high (grade III). For low and intermediate STSs surgery alone remains the most effective strategy in the management of STS (Bray 2016). Local recurrence following surgical resection is the usual reason for treatment failure in the management of STS and may occur in between 7 and 75% of patients, with recurrence consistently associated with reduced overall survival for the dog (Bray et al. 2014). Recurrence is mainly influenced by the size of the excision margins. An inappropriate conservative treatment will adversely affect outcomes for patients with more aggressive disease (Liptak & Forrest 2013). Higher tumor grade is associated with more aggressive biologic behavior and higher rates of local recurrence, distant metastasis and shorter disease free. High grade sarcoma patient's life expectancy is between 3 and 6 months from diagnosis (Frezza et al. 2017).

2. AIM OF THE STUDY

Advancements in cancer immunotherapy have revealed the importance of targeting neoantigens. Neoantigens are tumor specific antigens that prompt a strong antitumor response escaping from the central T tolerance. We have previously shown that infection of mouse melanoma cells with *Salmonella* induces the up-regulation plasma-membrane hemichannels. Furthermore, we have demonstrated that bacteria-treated melanoma cells establish gap junctions with dendritic cells (DCs), thus allowing the transfer of pre-processed antigens from the tumor cells to the DCs, ultimately leading to the activation of potent antitumor cytotoxic responses (Saccheri et al. 2010). We hypothesized that infection of tumor cells with *Salmonella* may also lead to the extracellular release of immunogenic peptides, neoantigens, that could be potentially used as anticancer vaccines. Using both mouse and human melanoma cells, we have addressed the following specific points:

1) Assess if *Salmonella* infection of murine melanoma cells leads to hemichannels opening and to a subsequent release of peptides able to induce an antitumor response as prophylactic vaccine.
2) Assess if human melanoma cells release immunogenic peptides upon *Salmonella* infection able to expand tumor specific T lymphocytes.
3) Address the feasibility and safety of the immunotherapy strategy based on the use of the peptides released from *Salmonella*-infected tumor cells.
4) Investigate whether among the released peptides, known tumor antigen and novel tumor epitopes are found.
5) Optimize a mass spectrometry-based pipeline to identify neoantigens, tumor spliced-peptides and post-translational modified tumor antigens.

3. MATHERIAL AND METHODS

3.1 Mice

6 weeks old WT C57BL/6J mice were purchased from Charles River. For some experiment OTI mice (C57BL/6-Tg(TcraTcrb)1100Mjb/Crl) were also used. These homozygous mice contain transgenic inserts for mouse Tcra-V2 and Tcrb-V5 genes; the transgenic T cell receptor was designed to recognize $OVA_{257-264}$ in the context of $H2K^b$. All experiments were performed in accordance with the guidelines established in the Principles of Laboratory Animal Care (directive 86 /609 /EEC).

3.2 Cell lines and bacterial strain

The murine melanoma B16-F10, B16F10-OVA (called throughout the manuscript B16 and B16-OVA, respectively (Overwijk & Restifo 2001) and T2 cells (HLA-A0201 hybrid human cell line lacking TAP-2 (Hosken & Bevan 1990) were cultured in RPMI 1640 medium supplemented with 10% fetal bovine serum (FBS-South American), 2 mM glutamine, penicillin (100 U/ml), streptomycin (100 mg/ml), and 50 mM β-mercaptoethanol (complete RPMI). Human melanoma cell lines 624.38 (HLA-2A proficient) and 624.28 (HLA-2A deficient) were cultured in RPMI 1640 medium supplemented with 10% of FBS (North American), 2 mM glutamine, penicillin (100 U/ml), streptomycin (100 mg/ml), 1% non-essential amminoacids (NeAA). The immature DC line D1 (Winzler et al. 1997) was cultured in Iscove's modified Dulbecco's medium supplemented with 30% NIH-3T3 supernatant containing 10 to 20 ng/ml mouse granulocyte-macrophage CSF. PBMCs for the expansion of antigen specific $CD8^+$ T cells were cultured in RPMI supplemented with 5% human serum, 2mM L-Glutamine, 100 U/ml penicillin, 100 mg/mL Streptomycin, 10 µg/mL βmercaptoethanol and 1% NeAA.

S. typhimurium SL3261AT is an aroA metabolically defective strain on *SL1344* background and is grown at 37°C in Luria broth (LB).

Vivofit® (Thyphoid vaccine live oral Ty21a) is a vaccine containing the attenuated strain of *Salmonella* enterica serovar Typhi Ty21a and is grown at 37 °C in Luria broth.

3.3 In vitro infection with bacteria

Single bacterial colonies were grown overnight and restarted the next day to reach an absorbance at 600 nm of 0.6 corresponding to 0.6×10^9 colony-forming units (CFUs)/ml. Murine and human melanoma cells were incubated with bacteria for 90 minutes, at a cell-to-bacteria ratio of 1:50, in the appropriate medium added with L-Glutamine without antibiotics. Cells were washed with medium and incubated in medium supplemented with gentamicin (50 mg/ml) for 18 hours to kill extracellular bacteria. At the end of the incubation cells were harvested and then lysed for protein analysis while supernatant was collected and filtered through 0,22µm filter to get rid of potentially still alive bacteria.

3.4 T2 binding assay

To assess peptides enrichment inside tumor cells' supernatant following *Salmonella* treatment T2 cells (Hosken & Bevan 1990) were incubated overnight at 37 °C at $2x10^5$ cells/ well in serum-free RPMI medium either with 100 µL of supernatant or with MART-1 peptide (1 µM and 10 µM) as a positive control. After overnight incubation, cells were blocked with mouse FcR block (1:100 BD), stained with BB7.2, an HLA-A0201 conformation-specific mouse antibody (BD). The cells were washed twice and fixed in paraformaldehyde for later acquisition by Accuri C6 Flow Cytometer (BD).

3.5 Adenosine5'-triphosfate bioluminescent assay

Adenosine 5'- triphosphate (ATP) Biolumescent Assay (Cell-Titer-Glo Luminescent cell viability Assay, Promega) allows to measure the quantity of ATP inside a sample. Firefly luciferase catalyzes the oxidation of D-luciferin giving rise to a colorimetric reaction; light emission is proportional to ATP content thus it can be quantified. Briefly, 100 µL aliquots of each supernatant to include in the test were distributed in a 96-well plates; they were then rapidly mixed with an equivalent volume of MIX-assay solution. Light emission was detected and quantified by a luminometer. ATP standard curve was included every test; higher concentration: 1 µM ATP.

3.6 OTI-CD8a$^+$ activation assay

With the purpose to assess the presence of OVA (SIINFEKL) peptide inside the medium of B16 OVA cells infected with *Salmonella* (as described in **Chapter 3.2**)), OTI-CD8a$^+$ activation assay was performed. ***Samples were prepared as follow.*** Supernatants were enriched of peptides by a TCA-protein precipitation; TCA was added at final concentration 13% and samples were incubated overnight at 4°C. Following high speed centrifugation the supernatant was loaded on chromabond SPE C18 devices (Macherey-Nagel) and peptides were eluted with different percentages of Acetonitrile solution. Fractions were dried with a speed vacuum and peptides were directly solved in IMDM. ***The assay was performed as follow.*** Murine dendritic cells (D1), were incubated for 4 hours at $2x10^4$ cells/well in a 96wells/plate with fractions of supernatants derived by *Salmonella*-treated B16/B16-OVA cells. Cells were then washed twice and incubated for 72 hours with $2x10^5$ CD8a$^+$ cells isolated from the spleen of OTI mice. CD8a$^+$ cells were obtained owing to magnetic column separator device (MACS). IFN-γ production was assessed by ELISA (BD).

3.7 Bone marrow derived dendritic cells derivation

To obtain bone marrow derived dendritic cells (BMDCs), total bone marrow cells derived by C57BL/6 mice were plated in RPMI1640 containing 10% FCS, 0,5mM 2-ßmercaptoethanol, 2mM glutamine, 0,1mM NEAA, 20 µg/ml gentamycin, 30% murine GM-CSF. $2x10^6$cells in $10cm^2$ Petri dish (Corning) with 10ml of medium. After 3 days, 10 ml of fresh complete medium was added to the plates and on day 6, all the medium was replaced with a fresh one. At day 10 non-adherent and loosely adherent cells were harvested and DC markers expression ($CD11c^+$ CD11b GR1 I-A I-E CD86) was assessed by FACS before using BMDCs for in vitro experiments.

3.8 iNKTactivation assay

In order to assess whether supernatant derived from B16 cells upon *Salmonella* infection contained lipids that activate iNKT cells in vitro, BMDCs were plated in a flat bottom 96wells plate ($5x10^4$ per well) in ratio 1:1 with mouse hybridoma Vα14i NKT, FF13 (Schümann et al. 2007). Cells were stimulated either with B16 supernatant or with increasing concentration of sonicated α-Galactosylceramide (Cd1-ligand, Alexis Corporation, Lausen, Switzerland) (higher concentration= 200 ng/ml) or left untreated (BMDc+FF13) up to a final volume of 200ul per well. The co-culture lasted for 48 hours, then ELISA for IL-2 production was performed.

3.9 PBMCs isolation

Peripheral blood was obtained from HLA-$A2^+$ normal donors, and PBMC were obtained by Ficoll (Ficoll/Hypaque density of 1,077 ± 0001) density gradient centrifugation. The blood was layered over the ficoll (**Figure 3-1**), substance which creates a density gradient if subjected to a centrifugation of 300g for 30 minutes at room temperature without brake. The blood cells are stratified according to different densities: the erythrocytes with higher

density than Ficoll settle on the bottom, granulocytes are layered to form a thin whitish above the red blood cells, while PBMC that are less dense than Ficoll are collected at the interface between Ficoll and plasma. To optimize this procedure buffy coats were diluted with PBS to a total volume of 35 mL (to prevent sedimentation of groups of cells) and 15 mL of Ficoll were added, slowly and at the same speed, under diluted buffy coat.

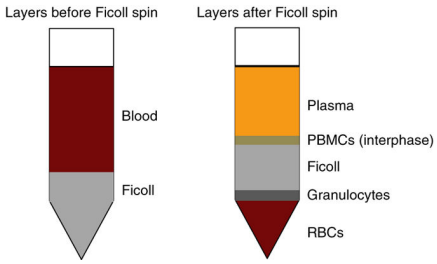

Figure 3-1. PBMCs isolation. PBMC were obtained by Ficoll density gradient centrifugation. The erythrocytes with higher density than Ficoll settle on the bottom, granulocytes are layered to form a thin whitish above the red blood cells, while PBMC that are less dense than Ficoll are collected at the interface between Ficoll and plasma. Adapted from *Zhonghua Lin Nature Protocols 2014*

Samples were centrifuged at 300 g for 30 minutes at room temperature (set up acceler on slow and deceler on off). The PBMC ring was recovered with a pasteur pipette and was transferred to a 50 mL tube PBMC were washed (at 4°C) once with PBS by centrifugation at 300 g for 10 minutes and twice by centrifugation at 160 g for 10 minutes to remove any platelets. PMBC were resuspended in isolation buffer (MACS buffer: PBS, 2mM EDTA, 0,5 % BSA) in case of a subsequent immunomagnetic separation.

3.10 Antigen specific-CD8$^+$ T cells expansion from healthy donor PBMCs

Total PBMCs isolated by healthy HLA-A2$^+$ donor were plated in 24-well plates (2 x 10^6 cells per well) and incubated either with supernatant derived by 2x10^6 62438 cells treated with *Salmonella* or 30uM Mart-1 in a final volume of 2 ml. From day 3 the recombinant

IL-2 (proleukin, Novartis) was added at the final concentration of 20 U/mL. Cells were fed every 2-3 days with 20 U/mL IL-2 and restimulated every 10 day. At every restimulation, expanded lymphocytes were enriched in $CD8^+$ T cells by magnetic column separation (Miltenyi). $2x10^6$ of the isolated $CD8^+$ T cells were plated with $4x10^5$ irradiated (10 Gy) $HLA\text{-}A2^+$ PBMCs that were pulsed either with Mart-1 or with supernatant of 62438 cells infected with *Salmonella*. To pulse PBMC they were incubated for 90 minutes at 37°C in RPMI supplemented with the selected stimulus (Mart-1/cells' supernatant). After incubation, cells were washed twice and irradiated (10 Gy) before mixing with the $CD8^+$ T cells.

3.11 moDCs derivation

$CD14^+$ cells were obtained in accord to Miltenyi biotec protocols. PBMC were labeled with anti-CD14 microbeads to isolate monocytes. The cell suspensions were loaded onto a MACS Column, which were placed in the magnetic field of a MACS Separator. The magnetically labelled $CD14^+$ cells were retained within the column from the magnetic field and these positive cells have been eluted as the positively selected cell fraction. Isolated $CD14^+$ cells were used to produce dendritic cells. Monocytes were plated in 6-well plate ($1x10^6$ /mL) in RPMI 1640 medium. After 1 hour of incubation at 37°C the non-adherent cells were removed by washing with medium. The remaining (adherent) cells were incubated in complete medium plus 10 ng/mL of granulocyte macrophage colony-stimulating factor (BD) and 10 ng/mL of IL-4 (BD). At the 6 day of culture monocyte-derived dendritic cells (MoDCs) were used for in vitro tests.

3.12 Mice immunization

For preventive vaccination, C57BL/6J mice were injected at their left flank with supernatant derived from B16 cells that were infected with *Salmonella* or left untreated.

According to the in vivo test, supernatants were differently prepared. The supernatant was either lyophilized or concentrated by chromabond SPE C18 devices (Macherey-Nagel). Preventive vaccination was performed at day 0, 4, 11. 10^5 B16 cells were injected subcutaneously in the right flank of the mice, at day 40. Tumor growth was monitored by measuring the two visible dimensions with a caliper every 2 days. Blood withdraw was performed at different time points: day 0, 18, 35 and at the moment of sacrifice.

Supernatants used for each vaccination were combined with different type of adjuvants. IFA+Aldara: Aldara cream (Imiquimod, MEDA) was applied at the immunization site until dried; supernatant emulsified with Incomplete Freud's Adjuvant (IFA, Sigma) at ratio 1:1, was then injected subcutaneously at final volume of 100 µl.

CpG: 10 µg of ODN1826 (Invivogen) were combined with the supernatant derived by $2x10^6$ cells and inoculated into the flank of mice at final volume of 100 µl.

DCs: D1 cells were incubated for 2 hours with LPS (1µg/ml) at 37°C and then for other 2 hours either with the supernatant derived by $2x10^6$ B16 cells or with a mix of $Trp2_{180-188}$ and $gp100_{25-33}$ (1 mg/ml each). $3.5x10^5$ D1 cells in a final volume of 100 µl were eventually injected subcutaneously at the flank of the mice.

3.13 Immunomonitoring

3.13.1 CD107a mobilization assay

CD107a mobilization assay enable to assess degranulation of effector cells such as $CD8^+$ T cells upon stimulation with a target cells. CD107 (or LAMP-1) is expressed on granules-membrane hence it is a suitable marker of degranulation. Effector and target cells are incubated together in addition with a CD107 antibody and golgi inhibitors that prevent granules release in the extracellular space thus allowing a proper evaluation of cytotoxic response.

Effector cells included in the test were either peripheral blood mononucleated cells (PBMC) of dog patients or ex vivo expanded $CD8^+$ T cells from human healthy donor PBMCs. Target cells were either dog patient's tumor cells or 62438 cells. Effector cells and target cells were incubated in a tube in complete medium in ratio of 1:1 and 2:1. Anti-CD107a monoclonal antibody conjugated with APC (1:100, BD), brefeldin A 10 μg/ml (BD) and GolgiStop containing monensin (1:1000, BD) were added to the culture for a final volume of 500ul and incubated for 5 h at 37 °C. Cells were then blocked with mouse FcR block (1:100, BD), stained with anti-CD3a, anti CD8 anti CD4 (1:200, BD) and then fixed in 4% PFA. Intracellular staining for IFNg (1:100, BD) production was also performed in order to further assess T cell activation. Stained cells were acquired by FACSCantoII (BD Biosciences).

3.13.2 Delfia

Cell-mediated cytotoxicity of effector cells was measured performing Delfia test. Target cells are colored with Delfia-BATDA and killing ability of effector cells is proportional to Delfia-BATDA release. In detail, target cells (tumor cell lines) were collected, washed once and solved at concentration of $1x10^6$ cells/ml. 2ml of cells were loaded with 3μl of Delfia-BATDA (DELFIA, Perkin Elmer) reagent, at 37°C for 30 min. Following 4 washes with PBS and 1 wash with medium w/o serum, 5000 cells were seeded in a v-bottom plate and incubated with effector PBMCs for 90 min in a humidified 5% CO_2 atmosphere at 37°C. The controls included in the experiment were: background (media without cells), spontaneous release (target cells without effector cells) and maximum release (lysed target cells). After incubation cells were centrifuged for 5 minutes at 500 g and 20 μL of the supernatant was transferred to a flat-bottom plate and 180 μL of Europio solution were added. After 15 minutes of incubation at room temperature the fluorescence was measured in the time-resolved fluorometer. The percentage of specific release is calculated as follows:

$$\frac{Experimental\ release - Spontaneous\ release}{Maximum\ release - Spontaneous\ release} \times 100$$

3.13.3 Humoral response assessment

To assess tumor specific antibodies inside patients' blood, tumor cells were lysed by freeze and thaw and the lysate corresponding to 10000 tumor cells was used to coat single wells of PVC microtiter plates (final volume of 50 µl). The coating was an overnight incubation at 37°C. Then, plates were blocked with 100 µl 5% BSA in PBS per well for 1 hr at 37°C. After removing blocking buffer, cells were probed with serum samples. 50 µl of patient's sera diluted in PBS with 1% BSA was added in each well and incubate for 2 hr at 37°C. Typical dilutions used are 1:10, 1:50, 1:250, 1:1250, 1:6250, and 1:31,250. Wells were then washed three times with 1% BSA in PBS at room temperature and the incubation with HRP-conjugated anti-dog antisera (1:4000) in 1% BSA in PBS for 1 hr at 4°C was performed. Following a last wash step of three washes with 1% BSA in PBS signals was developed with OPD (50 µl) as substrate. Reaction was stopped by adding 50 µl 4M H_2SO_4 per well. Plates were read at 492 nm in an ELISA reader.

3.14.1 nLC-ESI-MS for biochemical characterization of cells supernatants

3.14.1.1 Sample preparation

Supernatants derived from 40x106cells (*Salmonella* treated or left untreated) were concentrated through the use of chromabond SPE C18 devices (Macherey-Nagel). Once eluted with 80% CH3CN in 0.1% Formic Acid (FA) solution, samples were dried by speed vacuum, solved in water and sonicated with Bioruptor 30'' ON + 30'' OFF (2 cycles). Low and high molecular weight peptides were separated with a 10KDa centrifugation filter (Filter aided sample preparation, FASP) (Millipore) and differently analysed. Low molecular weight (LMW) fraction was concentrated in a centrifuge vacuum concentrator and soon acquired by nano-scale liquid chromatographic mass spectrometry (nLC-ESI-MS) on a Q-Exactive HF (as described in the following paragraph), while high molecular

weight fraction, containing mainly proteins, underwent enzymatic treatment before acquisition. Proteins were overnight digested by secret 3D method that enables a more efficient protein digestion (Matafora et.al manuscript in preparation) after reduction and alkylation with 10mM TCEP and 55mM Chloroacetamide added simoultanously. Peptides derived by digestion of proteins (HMW) were desalted and dried in a centrifuge vacuum, resuspended in 10 µL of solvent A (2 % ACN, 0.1% formic acid) and quantified with NanoDrop Spectrophotometer (Thermo Scientific).

3.14.1.2 Mass spectrometry

4µl of each sample were loaded at max pressure of 900 bar on a QExactive-HF mass spectrometer (Thermo Fisher Scientific) coupled with an UHPLC Easy-nLC 1000 (Thermo Scientific) with a 25 cm fused-silica emitter of 75 µm inner diameter. Columns were packed in-house with ReproSil-Pur C18-AQ 1.9 µm beads (Dr Maisch Gmbh, Ammerbuch, Germany) using a high-pressure bomb loader (Proxeon, Odense, Denmark). Peptides separation was achieved on a linear gradient from 95% solvent A (2% ACN, 0.1% formic acid) to 50% solvent B (80% acetonitrile, 0.1% formic acid) over 33 min and from 50 to 100% solvent B in 2 min at a constant flow rate of 0.25 µl/min. MS data were acquired using a data-dependent top 15 method for HCD fragmentation. Survey full scan MS spectra (300–1650 Th) were acquired in the Orbitrap with 60000 resolution, AGC target 3e6, IT 20ms. For HCD spectra, resolution was set to 15000 at m/z 200, AGC target 1e5, IT 80ms; Normalized Collision energy 28% and isolation with 1.2 m/z. Technical replicates were conducted on the LC–MS-MS part of the analysis.

3.14.1.3 Database Searching

Data acquisition was controlled by Xcalibur 3.1. Mass spectra were analyzed using MaxQuant software (version 1.5.2.8). Search parameters were set to an initial precursor ion tolerance of 10 ppm and MS/MS tolerance at 20 ppm. For LMW enzyme specificity was

set to unspecific and methionine oxidation was set as variable modification. For HMW enzyme specificity was set to Trypsin, maximum missed cleavage 2, fixed modification carbamidomethylation, variable modification oxidation, and protein N-terminal acetylation. The spectra were searched by the Andromeda search engine in MaxQuant against the Uniprot_CP_Mouse_2016 or the Uniprot_CP_Human_2017 or Uniprot_Canis-lupus-familiaris_CP_2017 sequence database. Label-free analysis was carried out, including a 'match between runs' option imposing the following parameters: quantification based on extracted ion chromatograms with minimum ratio count of 1 for LMW or of 2 for HMW, peptide and protein false discovery rates (FDRs) were set to 0.01 and the minimum required peptide length was set to 7 amino acids for LMW and to 6 ammino acids for HMW. The reversed sequences of the target database were used as decoy database. Comparative analyses were performed using the Perseus software (version 1.5.1.6). Missing values were replaced by random numbers drawn from a normal distribution by the function 'imputation' (width 0.3, down shift 1.8, separately for each column).For all the statistical analysis a t-test analysis was performed imposing a p-value of 0.05.

LMW peptides were also analyzed by Proteome Discover (version 1.4.0.288, Thermo Fisher Scientific). MS2 spectra were searched with Mascot ver. 2.3.02 engine against uniprot_CP_Mouse database or the Uniprot_CP_Human_2017 or Uniprot_Canis-lupus-familiaris_CP_2017 sequence database. Enzyme specificity was set to unspecific and methionine oxidation was set as variable modification. Peptide tolerance 10 ppm, MS/MS tolerance 20 mmu. Peptide Spectral Matches (PSM) were filtered using percolator imposing the following parameters peptide score > 20, peptide length > 7 ammino acids.

3.14.1.4 XCMS

XCMS Online applies a specific algorithm to filter and identify peaks from the MS1 scan and to match peaks across samples then it performs a two-group comparisons to match the independent dataset, "control" versus "disease" experimental design. Data derived by

Orbitrap QExactive-HF mass spectrometer (Thermo Fisher Scientific) were converted into mzXML format and loaded for two group comparison into two data-sets *Salmonella* and untreated. For features detection by CentWave Method, the parameters were set as follow: ppm=10; minimum peak width=5; maximum peak width=20. Retention time correction was performed by obiwarp methodology. Statistics applied was unpaired parametric t-test (Welch t-test) and features were selected imposing the following parameters: pvalue<0.01 fold change>3 Intensity precursor>$2x10^6$.

1.14.2 MALDI-TOF Mass spectrometry

Matrix-assisted laser desorption ionization (MALDI) mass spectra were acquired on 4800 MALDI-TOF/ TOF mass spectrometer (Applied Biosystems, Foster City, CA) equipped with a nitrogen laser operated at 336nm laser, averaging 2500 laser shots in a random, uniform pattern. Ions were accelerated with a 20 kV pulse, with a delayed extraction period of 170 ns. Spectra were generated by averaging between 200 and 400 laser pulses. Laser intensity was set to optimize the signal-to-noise ratio and the resolution of mass peaks of the analyte. Acquisition was in positive reflector mode in the mass range m/z 700-4000 when samples were crystalized on alpha-ciano-hydroxycinnamic acid matrix while it was in the mass range of m/z 2000-21000 when samples were crystalized on sinapinic acid matrix. All spectra were internally calibrated and processed via the Data Explorer (version 4.9) software.

3.14.3 SACI-ESI_MS

A liquid chromatography Surface-Activated Chemical Ionization/Electrospray Ionization (LC-SACI-ESI) was employed to overall characterize the composition of supernatants derived from murine melanoma cells treated with *Salmonella* or left untreated. Instrument analysis was performed using an Orbitrap mass spectrometer (ThermoFisher) coupled with a SACI/ESI source (Albini et al. 2015). Full-scan spectra were acquired in the wide range

of 40–3500 m/z for non-targeted metabolomics to detect all analyte and calibration m/z signals. Ion source parameters used were as follows: ESI capillary voltage 1500 V, SACI surface voltage 47 V, drying gas: 2 L/min, nebulizer gas: 80 psi and temperature: 40°C.

3.15 Clinical protocol for the treatment of dogs affected by spontaneous osteosarcoma or by high grade sarcoma with peptides released from tumor cells upon *Salmonella* infection.

3.15.1 Primary canine osteosarcoma cells derivation

Primary canine osteosarcoma cells were obtained from dissociation of dog's osteosarcoma specimens. Tissues were minced with a scalpel in a cell strainer. Cells were washed with DMEM (supplemented with 10% FBS, 2 mM L-Glutamine, 100 U/ml Penicillin, 100 mg/ml Streptomycin) and filtered with a cell strainer (100 µM). Cells were counted and cultured at high concentration in complete medium. As soon as cells grew, they were expanded and infected with Ty21a as described above (**Chapter 3.3**). Supernatants derived from untreated tumor cells (ON) and from *Salmonella*-treated tumor cells (Ty21a ON) were then lyophilized. Each vaccination dose consist of supernatant derived from $2x10^6$ cells.

3.15.2 Dog-patients vaccination procedure

Patients undergo standard chemotherapy treatment consisting of 4 cycles of Carboplatin (every 3 weeks). Following the second carboplatin cycle, vaccine is administered for a total of 6 injections: 2 NONE and 4 Ty21a. Only for the first and the second immunization, lyophilized vaccine is solved in Nobivac (used as adjuvant) and given intradermically following Aldara cream administration at the vaccine-injection site. At different time points blood withdraws and DTH test are performed. Description and scheme of the protocol is reported below:

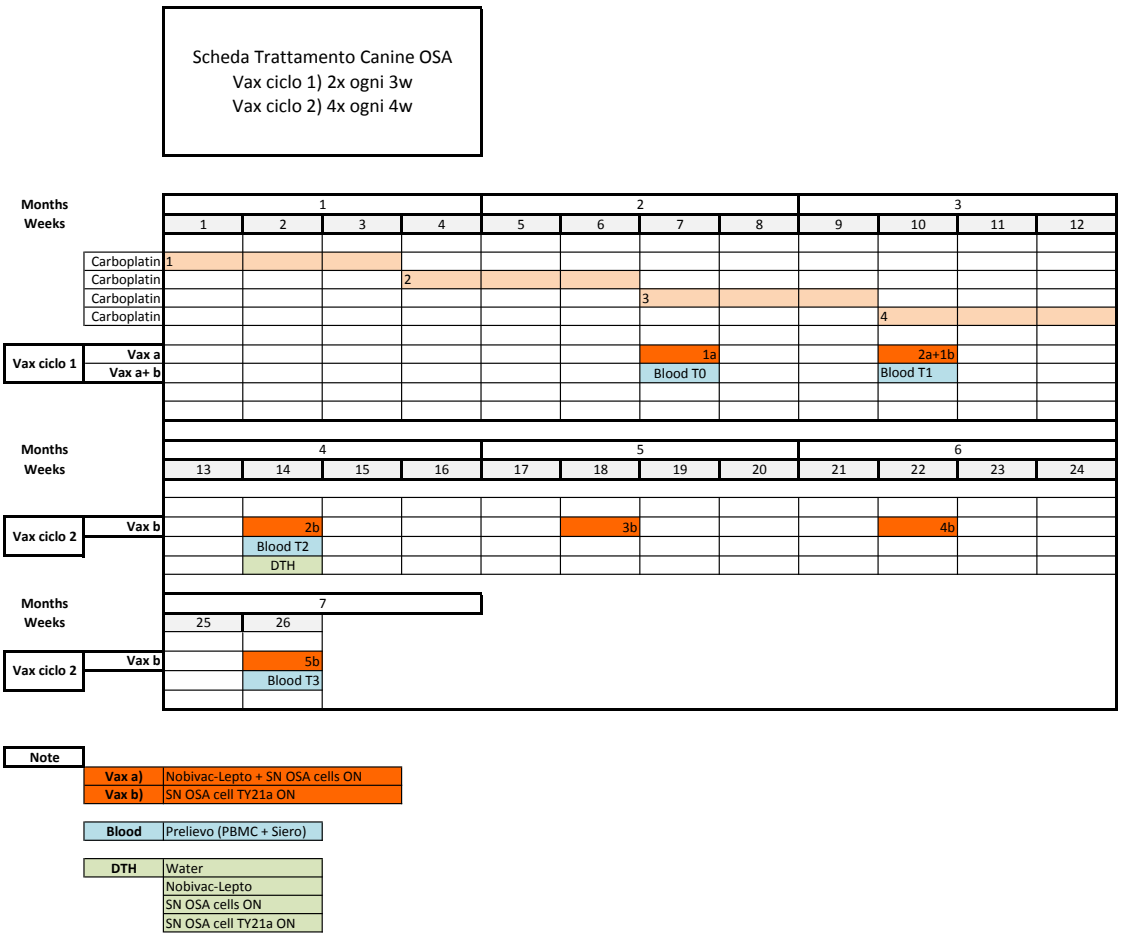

Figure 3-2 Schedule of the clinical trial. OSA and SA patients enrolled in the clinical trial underwent standard chemotherapy cycles (Carboplatin) and were additionally vaccinated as described in the figure. 7-months treatments include vaccinations, DTH test, and blood withdraw for PBMCs isolation and sera analysis.

4. RESULTS

4.1 Murine melanoma B16 cells upon *Salmonella* infection release peptides that if combined as prophylactic vaccine induce a strong antitumor response

4.1.1 Murine melanoma cells infected with *Salmonella* activate membrane hemichannels

Salmonella infection of murine tumor cells leads to the overexpression of Cx43 (Saccheri et al. 2010), the most abundant and ubiquitous component of plasma membrane hemichannel (Neijssen et al. 2005; Mendoza-Naranjo et al. 2007). Bacteria-treated tumor cells have been shown to establish gap junctions (GJ) with dendritic cells (DCs) by the docking of two plasma membrane hemichannels, allowing the transfer of pre-processed antigens from the tumor cells to the DCs (Saccheri et al. 2010). It is known that *Salmonella* up-regulates hemichannels expression on tumor cells, hence, we hypothesized that infection of tumor cells with this bacterium may lead to extracellular release of peptides that could be used as anticancer vaccine.

A necessary condition for peptides release through hemichannels is hemichannel activation (Weber et al. 2004); it has been previously shown that if hemichannels get activated, an hemichannel-dependent ATP release occurs (Kang et al. 2008). Hence to verify whether *Salmonella* infection of tumor cells leads to hemichannels opening we infected the mouse melanoma B16 cell line, a melanocytic and non-immunogenic melanoma cell line (Overwijk & Restifo 2001), and we monitored ATP release. B16 cells were treated with *Salmonella Thiphimurium SL3216AT* for 90 min; the infection was stopped by the addiction of gentamycin and after 4 hours we analysed the extracellular ATP content. Conditioned media from *Salmonella*-infected melanoma cells (B16 AT, **Figure 4-1**) was characterized by a higher amount of ATP compared to medium of untreated cells.

Importantly, the pre-treatment of B16 cells with the hemichannel inhibitor heptanol reduced ATP release to baseline levels. This data suggests that ATP was specifically released through hemichannels. The same findings were obtained treating with *Salmonella* the murine B16-OVA melanoma cell line, a melanoma cell line that expresses the exogenous protein Ovalbumin. Both results demonstrate that *Salmonella* treatment of murine tumor cells leads to hemichannel activation suggesting that peptide release might occur as well.

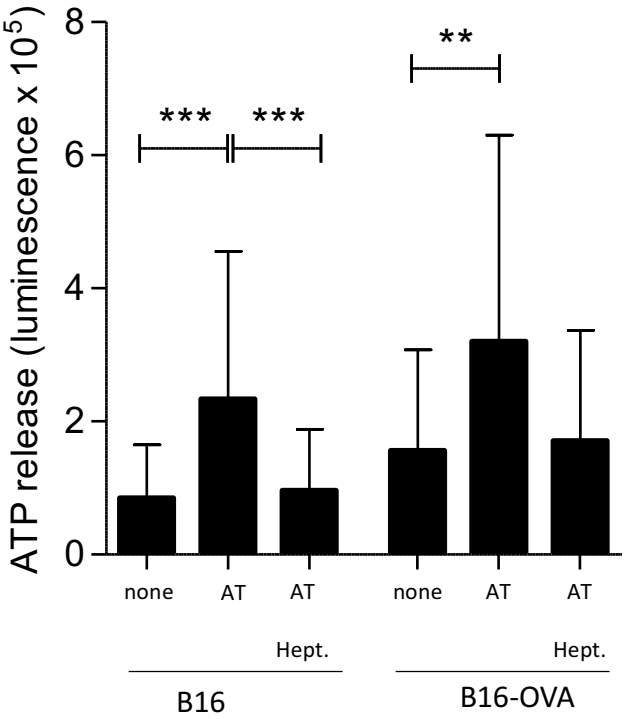

Figure 4-1. Bacteria-treated murine tumor cells functionally open hemichannels. Functional hemichannels opening was assessed performing an ATP assay. Both mouse melanoma cell line B16 and B16-OVA were treated with *Salmonella Thiphimurium SL3216AT* (AT) in presence or absence of the hemichannel blocker heptanol (Hept.). The derived supernatants were analysed for ATP content. ***p<0.05* 1-way-ANOVA test Bonferroni post test, (n=3).

4.1.2 Murine melanoma cells infected with *Salmonella* release potentially immunogenic peptides

Tumor antigens expressed by tumor cells on their MHC molecules are small peptides (7-13 amminoacids) that mainly derive from the intracellular processing of large proteins by proteasome enzymes (Leone et al. 2013). Only peptides that fit into the spatial constrain of MHC pocket can bind to it and only some of these peptides activate an immune response. To assess whether *Salmonella* infection could lead to the extracellular release of immunogenic peptides, we used murine B16-OVA cell line, a cell line that expresses Ovalbumin protein intracellularly. Ovalbumin processing by cell proteasome induces the release of peptides that can be exposed on the cell surface combined with MHC class I and II molecules. Hence, we wanted to address whether following *Salmonella* infection release of OVA-derived peptides could be found in the conditioned media. In order to do so we decided to follow two different strategies. First, we decided to test the ability of B16-OVA supernatants to activate $CD8a^+$ lymphocytes derived from OTI mice. OTI are transgenic mice whose $CD8a^+$ cells are restricted for the recognition of $OVA_{257-264}$ the immunodominant class I peptide derived from the proteasome cleavage of Ovalbumin (Ben-Shahar et al. 1999). Second, knowing the OVA sequence, we wanted to detect OVA-derived peptides by a mass spectrometry approach.

B16-OVA cells were treated with *Salmonella* (as described in **Chapter 3.3**). Briefly, cells were deprived of serum and antibiotics and treated with *Salmonella* for 90 min. Infection was stopped incubating cells with fresh medium added with gentamycin; the lack of serum was maintained for the entire experiment to avoid serum-derived proteins inside cells' supernatants that could interfere during the following analysis. After the overnight incubation, supernatant of *Salmonella*-treated and untreated cells were collected, peptides were enriched following an optimized TCA-based protocol and fractionated by Sep-pak C18 device, a silica-based bonded phase with strong hydrophobicity (as explained in:

Annex 4.5.1). The different fractions were obtained using as elution buffer, increasing percentages of Acetonitrile-based solution, ranging from 5% to 80%. Dendritic cells loaded with *Salmonella*-derived-supernatant-fractions for 4 hours specifically induced IFN-γ production by OTI-CD8a^{+} lymphocytes (**Figure 4-2**). The specific OTI-CD8a^{+} cell activation highlighted in the supernatant the presence of the $OVA_{257-264}$, the most immunogenic class I peptide derived from the proteasome cleavage of Ovalbumin. This suggests that *Salmonella* induces the release of potentially immunogenic peptides from tumor cells.

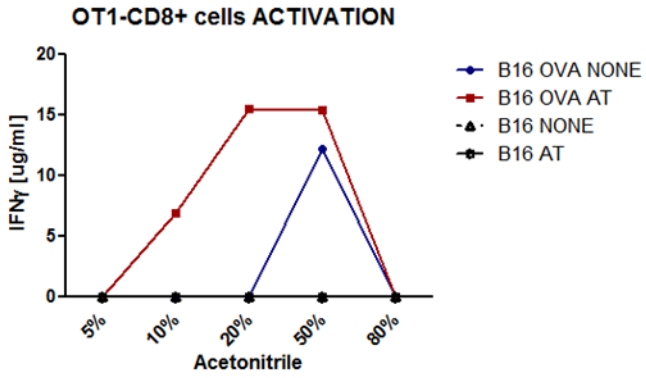

Figure 4-2. B16-OVA cells infected with *Salmonella* release peptides leading to the activation of CD8a^{+}-OTI cells *in vitro*. Murine dendritic cells (D1) were loaded for 4 hours with fractions of supernatants derived from untreated (NONE) or *Salmonella*-infected B16-OVA cells (AT). Following 72 hours of co-culture, OTI-CD8^{+} cells activation was assessed measuring IFN-y release by ELISA. B16 derived supernatants were assessed as negative control. Results of one representative experiment out of four are shown.

The stress induced by 18 hours of starvation of the protocol used could have promoted the release of peptides in the extracellular space even from untreated cells. The percentage of dead cells both in untreated and in *Salmonella* infected cells was detected by FACS using Annexin^{+}PI^{+} staining. The percentage of late apoptotic cells after 18 hours was around

20%; thus, indicating that the presence of $OVA_{257-264}$ in the supernatant of *Salmonella*-infected B16-OVA cells was not due to an augmented cell mortality (**Figure 4-3**). The release of $OVA_{257-264}$ was further confirmed by nano-scale liquid chromatographic tandem mass spectrometry combined with electrospray ionization (nLC-ESI-MS/MS **, Figure 4-4**). OVA-peptide was detected as double charge (m/z=482,28) inside all the fractions that activated OTI-CD8a^{+} cells. nLC-ESI-MS/MS spectrum of (m/z 482.28, z = +2) confirmed $OVA_{257-264}$ identity (sequence: SIINFEKL).

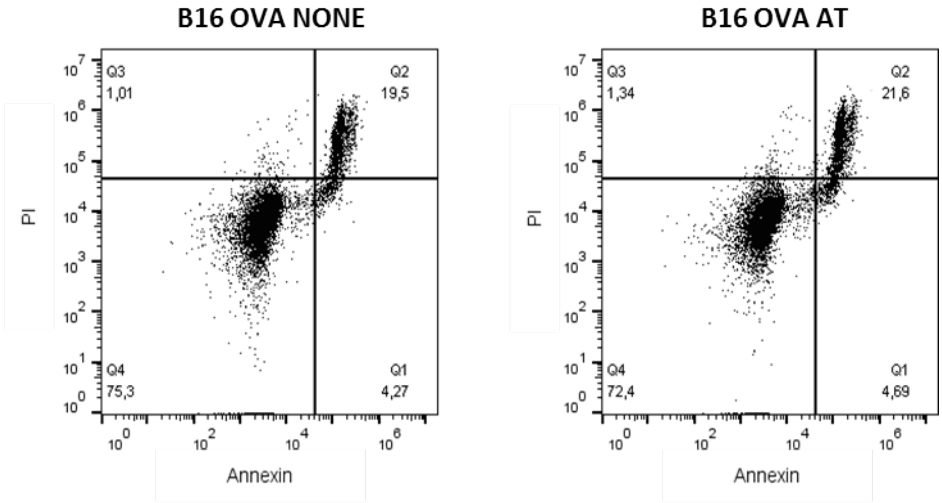

Figure 4-3*Salmonella* treatment of B16-OVA cells do not alter cell vitality. Representative Annexin staining performed to check mortality of cells at the end of protocol used to induce peptides release by tumor cells: thus after 18 hours from *Salmonella* infection, during which cells are maintained in starvation. Vital cells are showed as Annexin-PI- cells, cells undergoing apoptosis mark as Annexin+PI- while necrotic cells stain as Annexin+PI+.

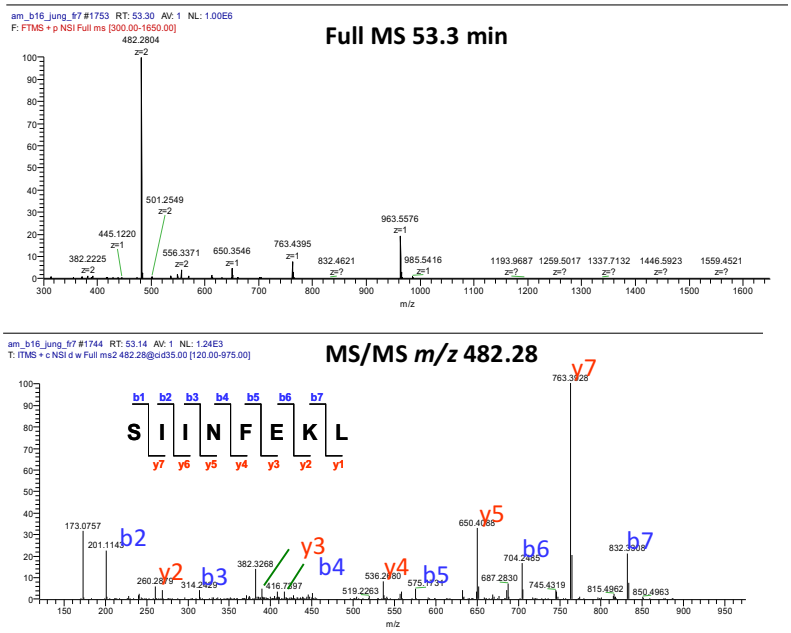

Figure 4-4. B16-OVA cells infected with *Salmonella* release peptides among which the immunogenic OVA-derived peptide SIINFEKL. Full nLC-ESI spectrum [300-1650 Da] at 53.3 min of B16-OVA-derived supernatant. $OVA_{257-264}$ (sequence: SIINFEKL) is mostly detected as double charge m/z=482.28 z=2. nLC-ESI-MS/MS spectrum of (m/z 482.28, z = +2) confirmed $OVA_{257-264}$identity.

4.1.3 Dendritic cells loaded with peptides released by *Salmonella*-infected tumor cells boost an immune response *in vivo*

Immunogenicity is the ability of an antigen to boost an immune response tailored against cells that expose that specific antigen. To assess whether the peptides released by tumor cells following *Salmonella* infection are immunogenic, we tested their ability to induce an antitumor response *in vivo*. From an immunologic standpoint, DCs-based immunotherapy carries the highest potential of inducing effective anticancer immune responses since DCs are key players in the activation of T cells (Steinman & Banchereau 2007). Notably DCs process antigens through the immune-proteasome, that differs in structure and function from the proteasome of tumor cells; hence, antigens derived from DCs are not necessarily the same as the ones produced by the tumor cells (Morel et al. 2000). However besides picking up and processing antigens themselves, DCs are also able to acquire exogenous

antigens and to induce T cell activation via cross-presentation (Joffre et al. 2012). Antigens derived from the treatment of B16 cells with *Salmonella* were directly processed by tumor-proteasome therefore they have a high probability to match the ones exposed by tumor cells on their own MHC molecules. Simulating the antigen uptake by DCs that happens *in vivo*, we loaded DCs with the peptides derived from the treatment of tumor cells with *Salmonella* and we used them to immunize mice.

Two different methodologies to concentrate peptides were compared. In the first methodology, supernatant derived from the equivalent of $2x10^6$ *Salmonella*-infected cells was concentrated and desalted using a Sep-Pak-C18 device and the derived peptides were used for each immunization (Vax). In the second methodology, the supernatant derived from the equivalent of $2x10^6$ *Salmonella*-infected cells was simply lyophilized and the derived peptides were dissolved in water and used for each immunization (Lyoph).

We preventively vaccinated 6 weeks old mice (C57J/BL6) three times, specifically at day 0, 4 and 11. Four weeks later, we challenged mice with 10^5 B16 cells (**Figure 4-5A**). Mice immunized with DCs loaded with peptides derived from B16 cells infected with *Salmonella* (DCs Vax and DCs lyoph) showed a trend of delayed tumor growth and a longer overall survival (**Figure 4-5B-D**) compared to the mice vaccinated with DCs alone. The delayed tumor growth was evident particularly in the late phase of growth (**Figure 4-5B**) suggesting that the recall of the immune response induced by the vaccination was not immediate. This might be due to the fact that immunization were performed 4 weeks before tumor cells injection; the antitumor effect became visible in terms of tumor growth delay but eventually the tumor escaped control. No major differences in term of survival were observed between vaccination based on peptides released by tumor cells treated with *Salmonella* that were enriched by lyophilization (DC-lyoph) or by the use of Sep-Pak C18 device (DCs-Vax); thus, both methods are suitable to concentrate peptides. Interestingly vaccination with DCs loaded with two well-known melanoma antigens $Trp2_{180-188}$ $gp100_{25-}$

$_{33}$ induced only a mild tumor growth delay (**Figure 4-5B**) mirrored by a little amelioration in term of survival (**Figure 4-5E**).

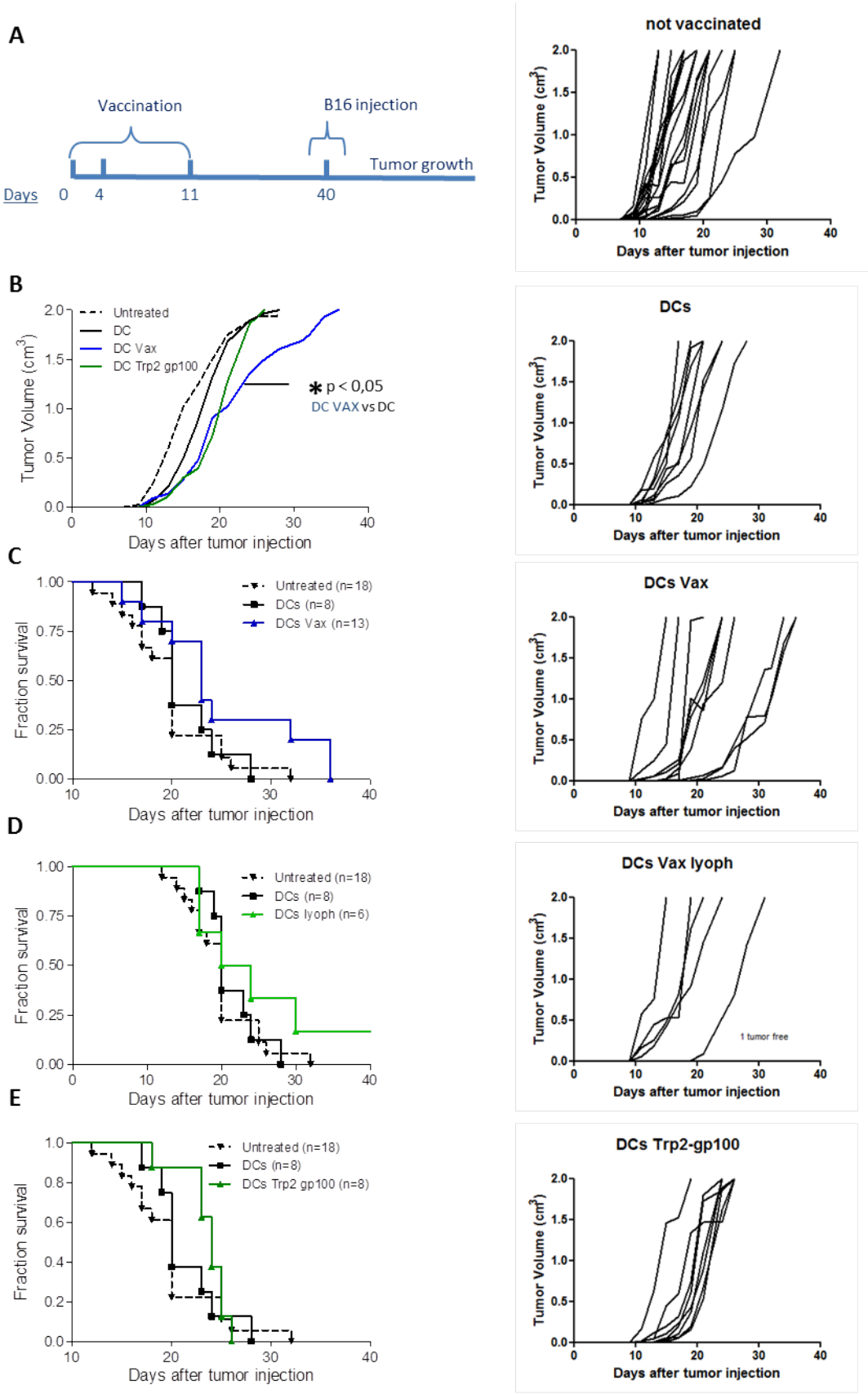

Figure 4-5 Dendritic cells loaded with peptides released by *Salmonella*-treated B16 cells induce an antitumor response *in vivo*. (A) Scheme of the schedule used to assess peptides immunogenicity in vivo. Immunization with dendritic cells loaded with peptides

were performed at day 0, 4 and 11. 10^5 B16 cells were injected subcutaneously at day 40. (B) Tumor volume growth of C57J/BL6 mice that underwent to different immunization protocol. Mice were immunized with dendritic cells alone (DCs), dendritic cells loaded with murine melanoma antigens $Trp2_{180-188}$ $gp100_{25-33}$ (DC Trp2 gp100), dendritic cells loaded with peptides released by of *Salmonella*-treated B16 cells that were lyophilized to be concentrated (DC lyoph), dendritic cells loaded with peptides released by of *Salmonella*-treated B16 cells that were processed on Sep-pak C18 to be concentrated (DC Vax); a group of mice was not immunized (untreated) (C-E) Growth Kaplan–Meier survival curves of C57J/BL6 mice (n=6-12 animals per group) differently vaccinated. Tumor growth was monitored every two days and mice were sacrificed once tumor volume reached cm^3. (Log-rank Mantel-Cox test was performed to assess differences among survival curves. Two way ANOVA followed by Bonferroni post-test *p<0,05 **p<0,01 ***p<0,001)

4.1.4 Peptides release by tumor cells following *Salmonella* infection do not exert an adjuvant effect per se

Peptides released by tumor cells following *Salmonella* infection might have a direct effect on dendritic cells altering their activation status. In order to evaluate the possible adjuvant effect exerted by peptides on DCs, we loaded on a murine dendritic cell line (D1) the supernatant derived from *Salmonella* infected B16 cells and we analyzed the expression of surface activation markers (CD40 and CD86). Activation of D1 was not detectable neither following incubation with supernatant derived from *Salmonella* infection of B16 cells (B16 Vax NS) nor following the incubation with the same supernatant but processed by Sep-Pak C18 (B16 Vax Sep-pak), step that we usually perform to concentrate peptides (**Figure 4-6A**). The same very low percentages of $CD40^+$ or $CD86^+$ cells were detected incubating DCs with supernatant derived from untreated B16 cells (B16 None NS, B16 None Sep-Pak). Consistently we found that peptides released by tumor cells following *Salmonella* infection or by untreated tumor cells do not have any adjuvant effect on human primary dendritic cells: monocyte derived dendritic cells (MoDCs) (**Figure 4-6B**). No significant changes in the percentage of activated MoDCs ($HLA\text{-}DR^+CD86^+CD206^-$) were observed.

In all the tests LPS treatment was performed as positive control to induce DCs activation (**Figure 4-6A-B**).

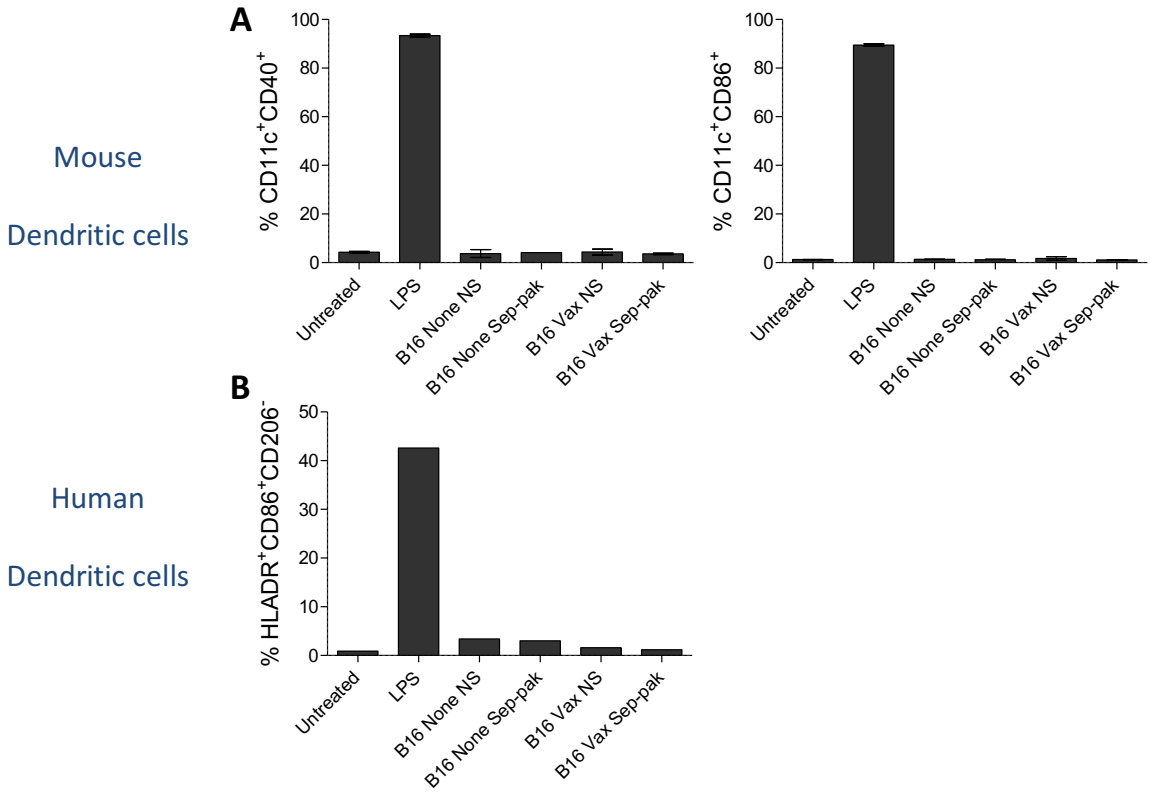

Figure 4-6. Cells supernatants derived from *Salmonella*-treated tumor cells do not activate dendritic cells. Supernatants derived from *Salmonella*-treated melanoma tumor cells (B16 Vax) and untreated cells (B16 None) were collected. Half of their volume was stored untouched (NS- not separated) and the second half was loaded on Sep-Pak C18 membrane (Sep-pak). After washing with 0.01%Formic Acid solution to remove salts, protein and peptides were eluted with 80%Acetonitrile solution. Samples were dried by speed-vacuum and solved in an appropriate volume of dendritic cells (DCs) medium. (A) Both TQ and Sep-pak-derived supernatants were loaded on an established murine dendritic cell line (D1); its activation state was evaluated by the expression of CD40 and CD80 markers. (B) B16/B16 Vax-derived supernatants were also incubated with primary human DCs: monocytes-derived DCs (moDCs); their activation state was determined by the expression of $HLADR^{+}CD86^{+}CD206^{-}$.

4.1.5 *Salmonella* induces tumor cells to release peptides that boost an immune response *in vivo*

A pivotal role in modulating the antitumor effect of immunogenic peptides is exerted by adjuvants since they can tailor the immune response by recruiting immune cells at the immunization site and inducing their activation (Christian Bode 2011; Aucouturier et al. 2002). We tested the amplitude of the antitumor response induced by peptides derived from *Salmonella*-treated-B16 cells (Vax) combined with two different adjuvant formulations: ODN1826 (CpG) and Incomplete Freud's Adjuvant (IFA) + Aldara. ODN1826 is a TLR9 agonist while IFA is an oily solution that allows gradual release of antigens and Aldara (Imiquimod) is a TLR7 agonist. The immunogenicity of peptides derived from untreated cells was also assessed as control (GpG-NONE/IFA Aldara Control). The dose of peptides was the same used for the first experiment thus equivalent to the peptides derived from $2x10^6$ tumor cells (Vax/dose2). In order to evaluate whether peptides' concentration could influence the immune response we also tested a lower and a higher dose of peptides but only combined with IFA and Aldara; respectively peptides derived from $1x10^6$ (Vax/dose1) and $5x10^6$ (Vax/dose3) *Salmonella*-treated B16 cells. The schedule adopted was equivalent to the schedule followed for the first *in vivo* experiment (**Figure 4-5A**).

Mice vaccinated with peptides released by *Salmonella*-treated tumor cells conjugated with CpG (CpG Vax) and with the higher dose of peptides combined with IFA Aldara (IFA-Aldara Vax/dose3) had a significant prolonged survival compared with their control group (respectively CpG and IFA-Aldara) (**Figure 4-7C, F**). The administered doses of peptides positively correlated with the amplitude of the antitumor response both in terms of overall survival (**Figure 4-7D-F**) and tumor growth delay (**Figure 4-8B**). Peptides derived from untreated cells (Control), either conjugated with CpG or IFA-Aldara, had no effect on tumor growth (**Figure 4-8-A,B**) suggesting once more that the antitumor response induced

by IFA-Aldara Vax/dose3 and CpG Vax rely on the peptides specifically release by tumor cells following *Salmonella* infection.

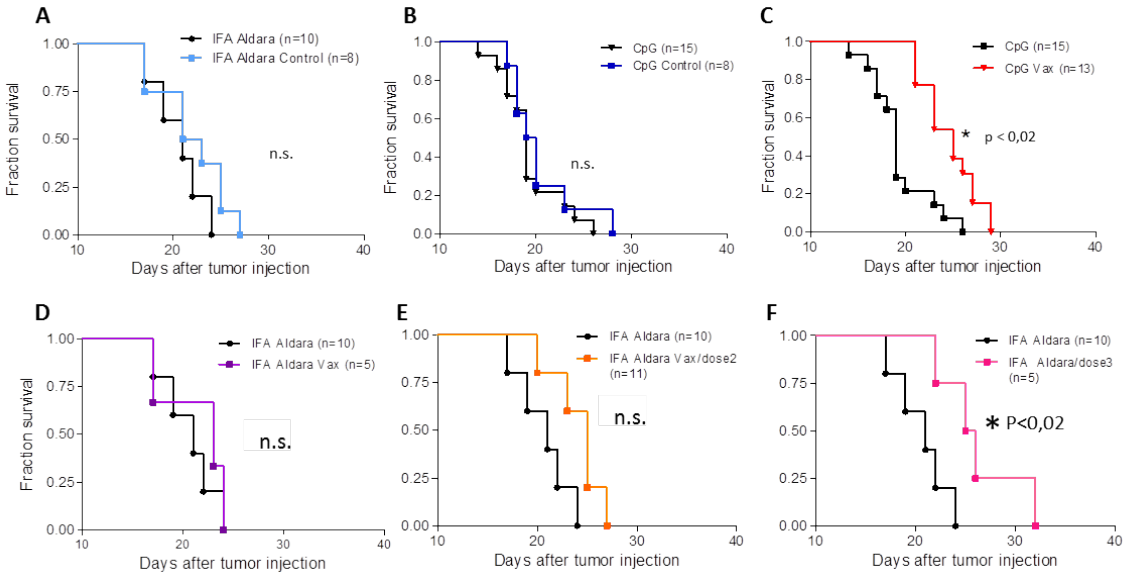

Figure 4-7. Peptides released by *Salmonella*-treated B16 cells in combination with either IFA-Aldara or CpG induce an antitumor response *in vivo*. Kaplan–Meier survival curves of C57J/BL6 mice vaccinated with peptides derived from untreated cells (Control) in combination with IFA-Aldara (A) and CpG (B). Survival curve of mice vaccinated with peptides derived from $2x10^6$ B16 cells infected with *Salmonella* and combined with CpG (C). Survival curves of mice vaccinated with increasing doses of peptides derived from *Salmonella* infected B16 cells, $1x10^6$ cells (D), $2x10^6$ (E), $5x10^6$ (F), combined with IFA-Aldara. (Log-rank Mantel-Cox test was performed to assess differences among tumor growth curves).

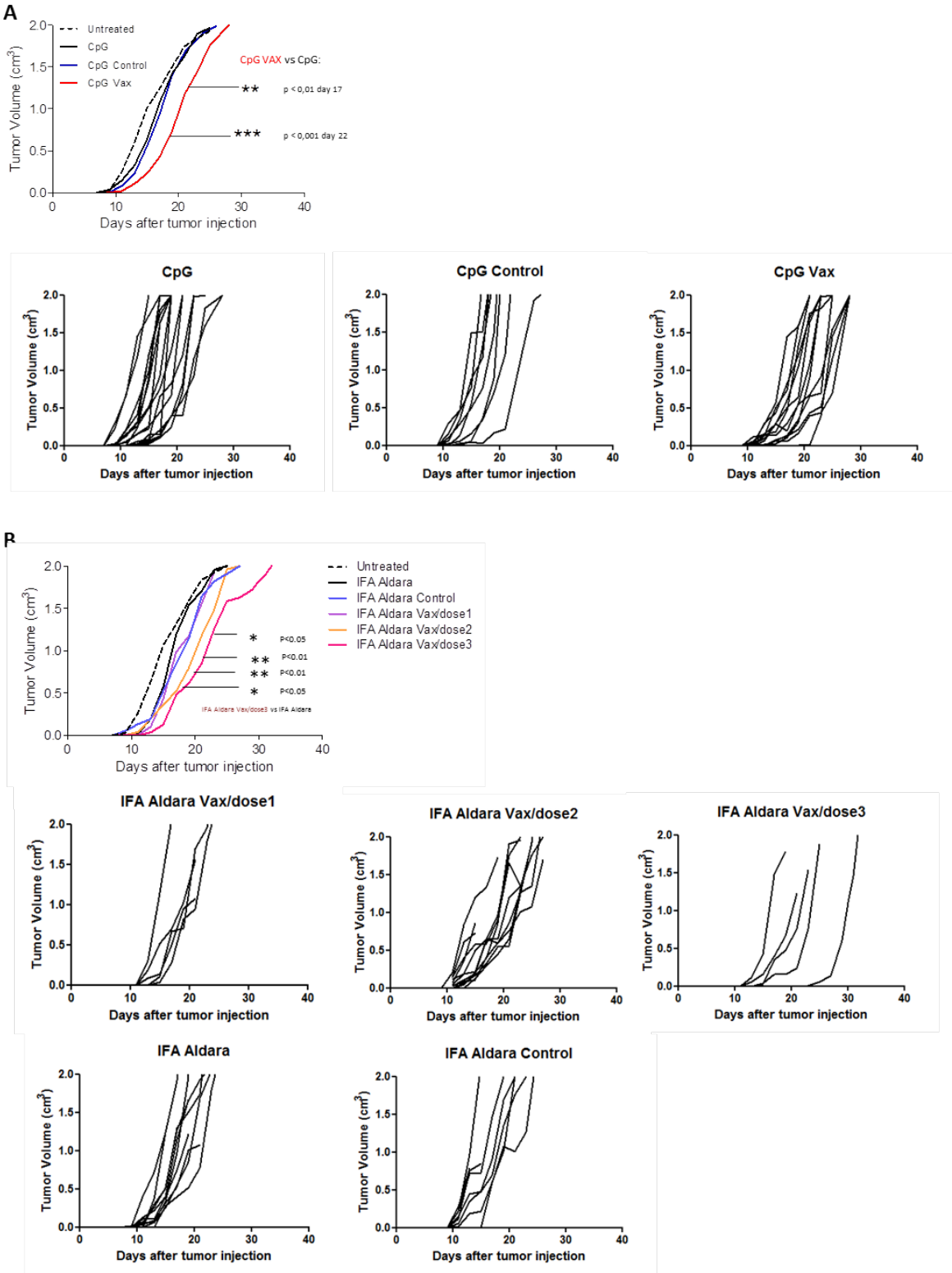

Figure 4-8. Peptides released by *Salmonella*-treated B16 cells in combination with either IFA Aldara or CpG induce an antitumor response *in vivo*. C57J/BL6 mice were vaccinated subcutaneously 3 times (at day 0, 4 and 11) and then at day 40, 10^5 B16 cells were injected at the flank opposite to the vaccination. Tumor growth was assessed every two days measuring the x and the y dimension. (**A**) Tumor growth curves of C57J/BL6

mice (n =8+) vaccinated with peptides combined with CpG. Mice vaccinated with peptides derived from untreated cells (CpG Control), with peptides derived from $2x10^6$ B16 cells infected with *Salmonella* (CpG VAX), with CpG alone (CpG). Tumor growth of not vaccinated mice is represented as black dashed line. (**B**). Tumor growth curves of C57J/BL6 mice vaccinated with peptides combined with IFA-Aldara. Mice vaccinated with increasing doses of peptides derived from *Salmonella* infected B16 cells, $1x10^6$ cells (Vax/dose1), $2x10^6$ (Vax/dose2), $5x10^6$ (Vax/dose3), vaccinated with supernatant of untreated cells (IFA-Aldara Control), vaccinated with IFA-Aldara alone (IFA-Aldara). Tumor growth of not vaccinated mice is represented as black dashed line. (Two way ANOVA followed by Bonferroni post-test *p<0,05 **p<0,01 ***p<0,001)

4.2 Human melanoma cell lines infected with *Salmonella* release peptides that induce the expansion of CD8-T cell from peripheral blood mononuclear cells that specifically kill human melanoma cells in vitro.

4.2.1 *Salmonella* infection of tumor cells induces a hemichannel-mediated peptide release

Salmonella induces mouse tumor cells to release immunogenic peptides that stimulate an antitumor immune response *in vivo*. We asked whether *Salmonella* could exert the same effect on human tumor cells. To address this question, we took advantage of the T2 cell *in vitro* system, suitable to assess peptide-enrichment inside the *Salmonella*-conditioned media (Hosken & Bevan 1990). T2 cells are HLA-A0201 restricted lymphoblastic cells that are deficient for the transporter associated with antigen processing (TAP) (Leone et al. 2013; Durgeau et al. 2011). Without TAP-mediated transport of cytosolic peptides into the endoplasmic reticulum (ER), assembled class I complexes are structurally unstable and retained only transiently at the cell surface. However once T2 cells are exposed to a solution containing peptides capable to bind HLA-A0201 molecule, surface HLA are stabilized (Hosken & Bevan 1990). The expression of HLA-A0201 molecules detected the surface of T2 cells is proportional to the number of antigens inside the solution in which are cultured.

To evaluate whether *Salmonella*-treated tumor cells released HLA-A0201-binding peptides, we treated both the human colon cancer cell line HT29 and the human melanoma cell line SkMel24, with the vaccine strain of *Salmonella enterica serovar Typhi* (Ty21a); then, the conditioned-medium was added to T2 cells (**Figure 4-9A**). T2 cells cultured with the supernatant from *Salmonella*-infected SkMel24 cells showed a significantly higher expression of HLA-A0201 compared to T2 cells cultured with conditioned media of untreated cells (**Figure 4-9B**). Interestingly, peptide enrichment was completely lost once

the hemichannel blocker heptanol was added to the system, suggesting that peptide release was mainly hemichannel-mediated. We hypothesize that the *Salmonella*-induced peptide release might be a shared mechanism among tumour cells since it also occurred in human adenocarcinoma HT29 cells infected with *Salmonella Ty21a* (**Fig.4-9B**). To confirm that the higher HLA-A0201 expression on T2 cells correlated with the higher antigen concentration inside the supernatants, we loaded T2 cells with two different concentrations of the HLA-A0201-resctricted peptide Mart-1 (Kawakami et al. 1994); also in this case the higher amount of Mart-1 lead to a higher HLA-A0201 signal (**Fig.4-9B**).

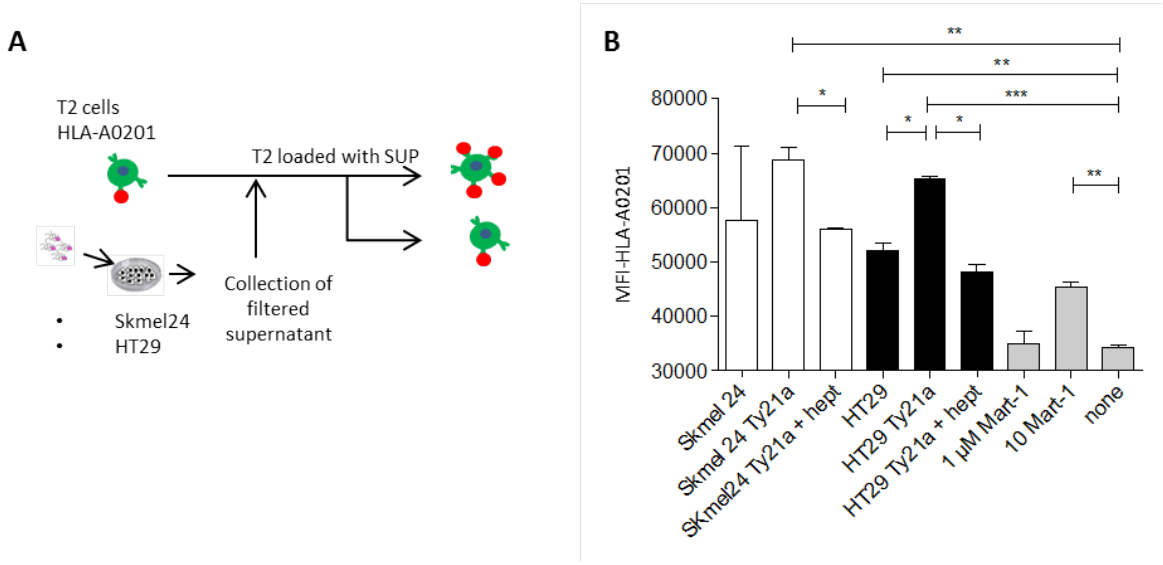

Figure 4-9. *Salmonella*-treated tumor cells release peptides through hemichannels. Functional hemichannels opening was assessed performing a T2 binding assay. **A** Scheme of the performed T2 assay. **B** Human melanoma cells (Skmel24) and adenocarcinoma cell line (HT29) were treated with *Salmonella enterica serovar Typhi (Ty21a)* and the derived supernatants were added to T2 cells. As a positive control, an increasing amount of Mart-1 peptide was added to T2 cells. HLA-A0201 expression was detected after 24 hours of incubation. (The Student's t-test was used for statistical analysis*$p<0.05$,**$p<0.01$, ***$p<0.001$, (n=4)).

4.2.2 Peptides released by 62438 human melanoma cell line upon *Salmonella* infection induce the expansion of CD8-T cell from PBMCs

We showed that both human and mouse tumor cells can release peptides once stimulated with *Salmonella*; in order to verify whether among the peptides released by human tumor cells some are immunogenic, we tested their capability to activate antigen-specific-$CD8^+$ T cells starting from peripheral blood mononuclear cells (PBMCs) of healthy donors. Indeed, in the blood of healthy people there are circulating $CD8^+$ T-lymphocytes whose TCR recognize tumor antigens; since the frequency is estimated to be very low (Gros et al. 2016), usually several stimulations with a known tumor antigen are required to expand a specific $CD8^+$ T cell population. We infected the HLA-A2-restricted human melanoma cell line 62438 with *Salmonella enterica* serovar Typhi (Ty21a) and we used the derived supernatant to stimulate PBMCs isolated (**Chapter 3.9**) from blood of an HLA-$A2^+$ healthy donor. In parallel, we stimulated PBMCs with the known HLA-A2 restricted melanoma antigen Mart-1. Every 10 days $CD8^+$ lymphocytes were enriched by magnetic column separation and further stimulated with HLA-A2-matched irradiated PBMCs loaded either with Mart-1 or with peptides released by Ty21-infected 62438 cells. At every stimulation, we tested the capacity of the $CD8^+$ lymphocytes stimulated by peptides released by 62438 cells (CTL2_SUP) to recognize antigens presented by 62438 (the tumor cells from where peptides-were derived). Increasing frequencies of IFN-ɣ expressing $CD8^+$ lymphocytes were detected over time in response to their co-culture with 62438 cells (**Figure 4-10**). Moreover after 4 stimulations, CTL2_SUP had a mild cytotoxic response against 62438 cells (**Figure 4-11**) further proved by the augmented expression of the degranulation marker CD107a (**Figure 4-10**-3^{rd} stimulation). For the Delfia-cytotoxicity test (**Figure 4-11**) two different ratios of effector cells (CTLs) and target cells (62438) were assessed; respectively 25:1 and 12.5:1. The observed killing activity correlated with the number of effector cells used in the test. Importantly, the activation of $CD8^+$

lymphocytes against 62438 was specifically mediated by the recognition of HLA-antigen complex as the same lymphocytes did not get activated once incubated with 62428, a melanoma 62438 cell-derivative lacking HLA-A2 molecule. Clusters formed by the activated $CD8^+$ T cells were clearly visible; Mart-1-induced clusters were usually larger and expanded more rapidly than the clusters stimulated by peptides released by tumor cells following *Salmonella* infection (**Figure 4-12**).

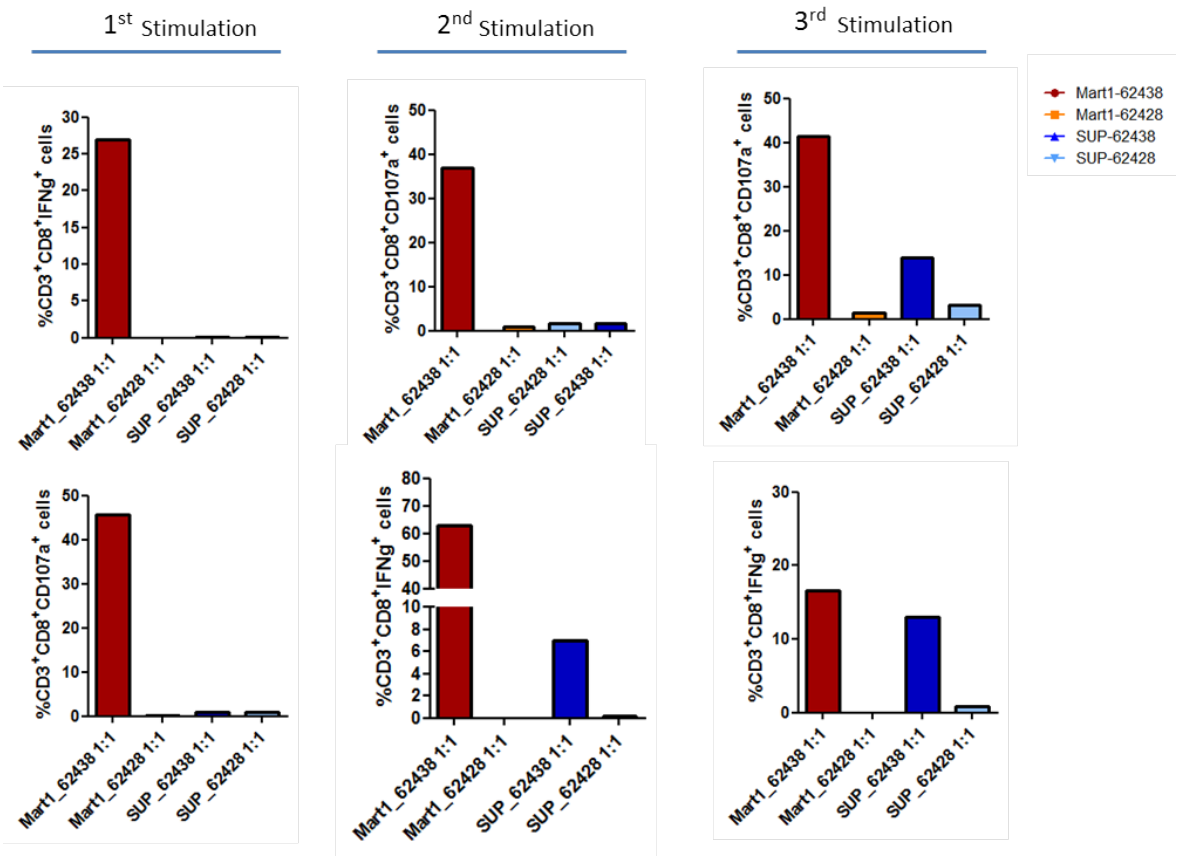

Figure 4-10. Peptides released by human melanoma cells following *Salmonella* infection induce the expansion of $CD8^+$ T cells from healthy donor's PBMCs. Peptides released by *Salmonella* infected human melanoma 62438 cells were used to stimulate PBMCs isolated by the blood of healthy donors (SUP). In parallel the melanoma antigen Mart-1 was used to stimulate the expansion of $CD8^+$ T cells as positive control (Mart-1). At every stimulation aliquots of expanded $CD8^+$ lymphocytes were co-cultured with 62438 tumor cells at 1:1 ratio (from where peptides-were derived) and their activation was assessed measuring IFN-ɣ and CD107 expression. HLA-negative human melanoma cells line 62428 were used to verify the specificity of the activation. Each graph referrers to one independent experiment.

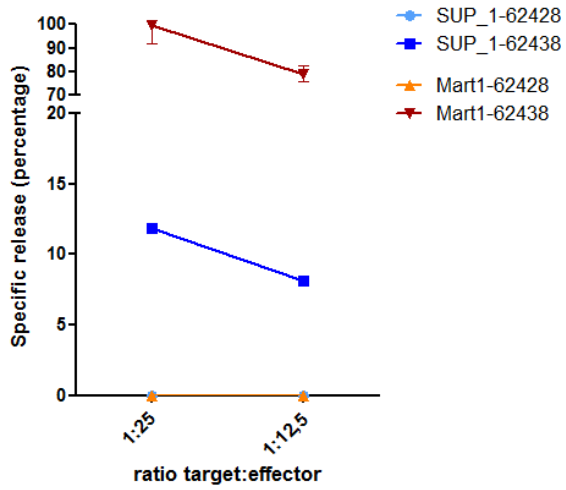

Figure 4-11. Peptides released by human melanoma cells following *Salmonella* infection induce the expansion of CD8$^+$ T cells that kill tumor cells from where peptides were derived. Peptides released by *Salmonella* infected human melanoma 62438 cells were used to stimulate PBMCs isolated by the blood of healthy donors (SUP). In parallel, the melanoma antigen Mart-1 was used to stimulate the expansion of CD8$^+$ T cells as positive control (Mart-1). After three stimulations, expanded CD8$^+$ lymphocytes were co-cultured with 62438 tumor cells and their killing ability was assessed by Delfia assay using two different ratios of effector:target cells (1:25 and 1:12.5). Samples were tested in duplicates. HLA-negative human melanoma cells line 62428 were used to verify the specificity of the killing. Graph referrers to one independent experiment.

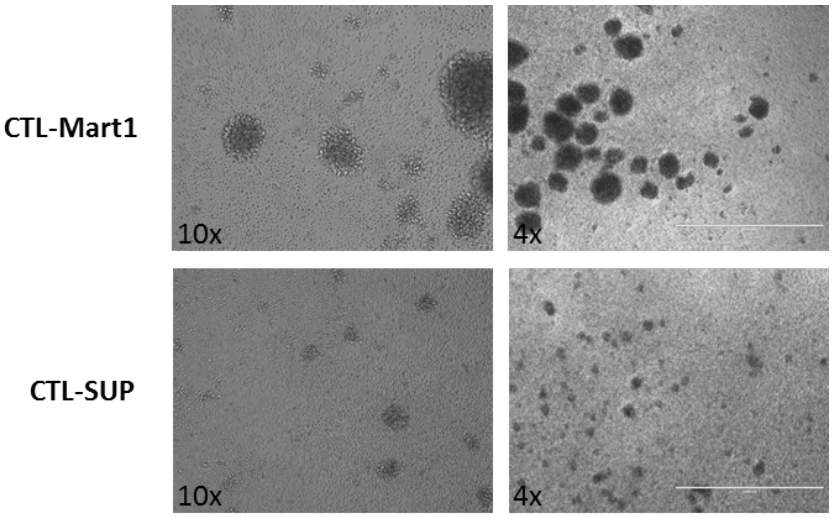

Figure 4-12. Peptides released by human melanoma cells following *Salmonella* infection induce the expansion of CD8$^+$ T. Pictures of representative clusters formed stimulating healthy donor's PBMCs with peptides derived from *Salmonella* infected 62438

human melanoma cell line (CTL-SUP) and with the known melanoma antigen Mart-1 (CTL-Mart-1).

4.3 From bench to patients: translating our vaccine strategy into clinical practice

4.3.1 *Salmonella*-derived peptides-based vaccine prolongs survival of osteo/sarcoma affected dogs

To translate our immunotherapy vaccine strategy into a patient anticancer treatment, we started to collaborate with a veterinary clinic. Dogs with osteosarcoma and high-grade sarcoma are being treated with an autologous vaccine formulation with the purpose of promoting a specific antitumor response, that can prevent tumor relapse and increase survival. Osteosarcoma (OSA) is the most common bone primary tumor in dogs, comprising up to 85% of all reported bone neoplasia (Mirabello et al. 2009). Median survival times approach 4–5 months with amputation alone (Mirabello et al. 2009), and adjuvant chemotherapy improves median survival times to 8–12 months (Selmic et al. 2014). Despite the use of various chemotherapy protocols and novel treatment approaches, clinically meaningful improvements in survival have not been achieved and 90% of dogs die of metastatic disease within 2 years from treatment (Wycislo & Fan 2015). Differently high grade sarcoma (SA) dog patient's life expectancy is between 3 and 6 months from diagnosis (Dennis et al. 2011; Frezza et al. 2017). The clinical trial protocol is explained in details in the method section (**Chapter 3.15.2**) and schematically represented in **Figure 4-13**. Briefly, patients diagnosed with OSA or high-grade SA were surgically operated for tumor resection; we derived SA/OSA cells from patient's tumor biopsy, kept them in culture and infected them with *Salmonella*. Cell supernatants were filtered and lyophilized to be combined with a veterinary adjuvant (Leptospirosis vaccine) and a topically delivered TLR9-agonist Imiquimod (Aldara) for the first 2 immunizations while they were solubilized in water for the following 4 immunizations. In total 6 intramuscular vaccinations were performed after 4 cycles of chemotherapy. As tumor cell-isolation was not successful in two patients (OSA0 and OSA42), these were treated with a heterologous

vaccine formulation. Our choice is supported by data from literature that show how heterologous vaccines can induce a higher immune response than autologous once (Schadendorf et al. 2000; Selvaraj 2014).

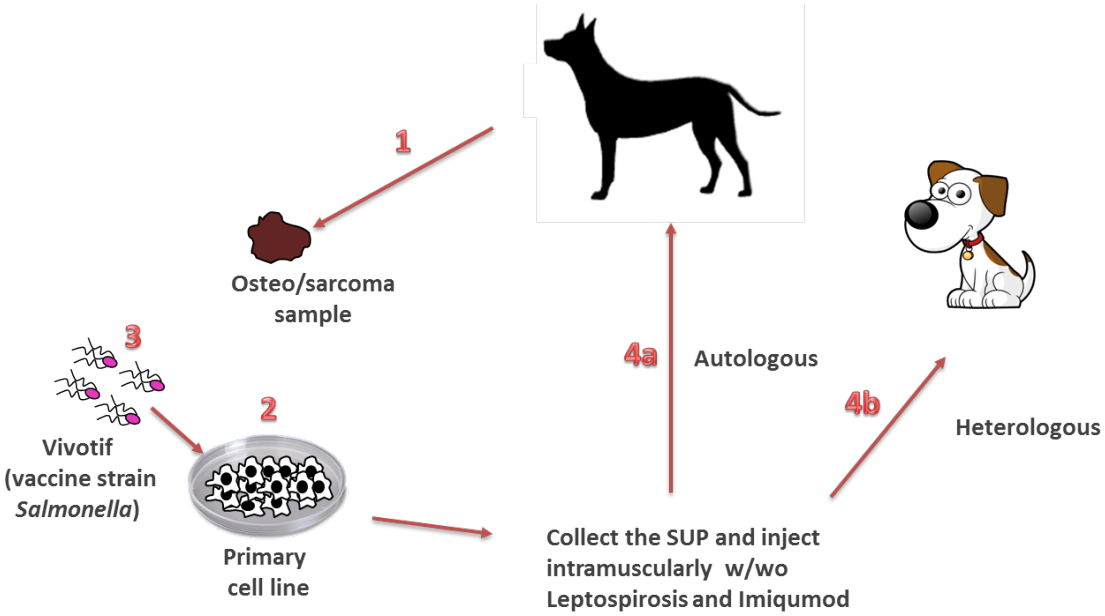

Figure 4-13. Pipeline of the clinical trial. Dog patients diagnosed with OSA or high-grade SA were surgically operated for tumor resection (1); SA/OSA cells from patient's tumor biopsy were derived (2) and kept in culture to infect them with *Salmonella*(3). Cell supernatants were filtered and lyophilized to be either combined with Leptospirosis vaccine and a topically delivered Imiquimod or solved in water; vaccinations were performed either in autologous setting (4a) or in heterologous setting (4b).

Since our collaboration started, eleven patients have been treated, eight with osteosarcoma and three with high grade sarcoma (**Figure 4-14**). Of the osteosarcoma patients, one is still under vaccination, four died before completing the vaccination, two out of three patients that completed the vaccination died within the life expectancy period (367 and 390 days after diagnosis) and one patient had a long overall survival, dying after 653 days for reasons not related to the tumor. With regard to the sarcoma affected dogs, one patient is alive and still within life expectancy period while one patient died without improvement of the overall survival; the third patient is alive after more than 1400 days and survived also

to a recurrence of disease that was again treated with vaccination, showing that a marked antitumor response had been promoted.

Patient	Breed	Diagnosis		VAX			Survival (from diagnosis)
OSA0	Terranova	osteosarcoma	December 15, 2012	Heterologous	March 11, 2013	Completed	dead after 653
OSA1	Amstaff	osteosarcoma	January 18, 2013	Autologous	April 3, 2013	5 out of 6	dead after 224
OSA8	Meticcio	osteosarcoma	December 1, 2013	Autologous	March 27, 2014	5 out of 6	dead after 229 days
OSA17	Meticcio	osteosarcoma	November 21, 2014	Autologous	April 2, 2015	4 out of 6	dead afteer 186
OSA 23	Greyhound	Osteosarcoma	November 24, 2015	Autologous	March 1, 2016	5 out of 6	Dead after 269
OSA 25	Rottweiler	osteosarcoma	February 16, 2016	Autologous	September 5, 2016	Completed	dead after 367
		metastasis onset (lung)	October 1, 2016	Autologous	January 5, 2017	Completed	
OSA29	Tosa Inu	osteosarcoma	July 7, 2016	Autologous	January 12, 2017	Completed	dead after 390
OSA42	Border Collie	osteosarcoma	July 7, 2017	Heterologous		on going	164
SA5	Pitbull	sarcoma	November 1, 2013	Autologous	February 17, 2014	Completed	1502
		sarcoma relapse	November 2015	Autologous	February 20, 2016	Completed	
SA32	Beagle	sarcoma	December 13, 2016	Autologous	May 20, 2017	4 out of 6	dead after 241
SA35	Cocker Spaniel	sarcoma	January 4, 2017	Autologous	December 1, 2017	Completed	342

Figure 4-14. List of the patients involved in the clinical trial. In a clinical setting, dogs affected by spontaneous high-grade sarcoma or osteosarcoma have been treated with vaccines obtained following our strategy. Primary ostosarcoma/sarcoma cells were obtained from the dissociation of patient's tumor specimen and were treated with *S. thyphimurium*. Dogs were administered with the derived vaccine following four carboplatin cycles (**Chapter 3.15.2**).

4.3.2 Dog patients' overall survival correlates with the presence of circulating tumor specific lymphocytes.

Dog patients were constantly monitored during the clinical trial. Blood (from where PBMCs were derived) and sera samples were taken at different time points in order to perform an adequate immune-monitoring. In details, blood withdraws were done during the first three vaccinations and at the end of the vaccination protocol (4 months since the beginning). SA5 can be considered the patient that better responded to the therapy; two years after the vaccination protocol, a sarcoma relapse occurred but following a second

cycle of vaccination the prognosis is stable and the patient is healthy. The level of circulating lymphocytes able to respond to tumor cells was assessed performing a CD107a assay in which IFN-ɣ staining was included. Total PBMCs isolated before Sa5 was included in the clinical trial (Sa5 T0) and at the end of the first vaccination protocol (Sa5 T3) were co-cultured for 5 hours with Sa5 tumor cells in a ratio 5:1 in presence of the golgi stop monensine. Frequency of circulating anti-tumor lymphocytes was induced by the vaccines (**Figure 4-15**). Indeed, at the end of the vaccination protocol a higher percentage of $CD8^+$ T cells were activated in response to the co-culture with Sa5-tumor cells (**Figure 4-15A,B**) expressing both IFN-ɣ and CD107a (marker of cytotoxicity). Similar levels of circulating antitumor $CD8^+$ lymphocytes were detected when a sarcoma relapse was diagnosed (Sa5 Tmet0, **Figure 4-15A,B**) and at the end of the second vaccination protocol (Tmet2). Interestingly, also an antitumor specific response mediated by CD4 lymphocytes was boosted by the vaccine (**Figure 4-15C,D**). The percentage of $CD4^+$IFN-$ɣ^+$ cells was higher at the end of the immunization protocol (Sa5 Tmet2) than at the beginning (Sa5 T0). Contrarily to what we observed in terms of $CD8^+$ lymphocytes response, a low level of antitumor $CD4^+$ T cells was detected at the moment of sarcoma relapse diagnosis; positively the second immunization protocol increased the circulating anti-tumor $CD4^+$ T cells (**Figure 4-15C,D**).

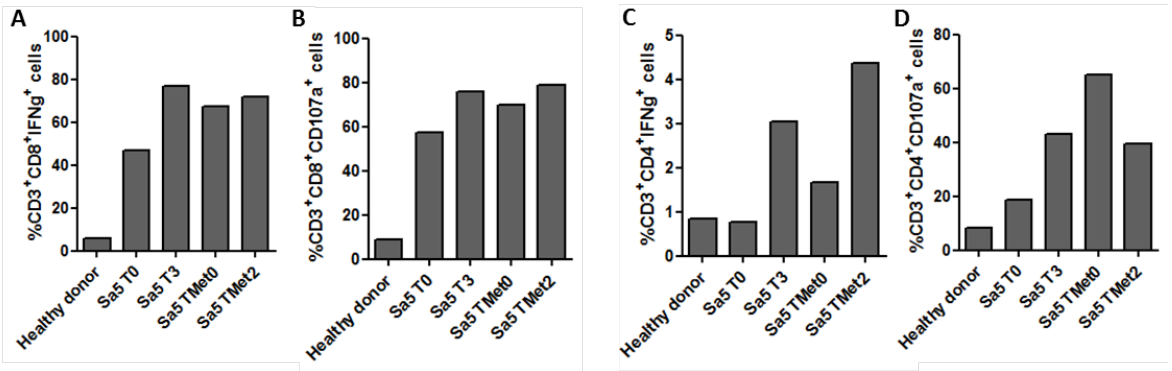

Figure 4-15. Vaccination of sarcoma patient with peptides derived from *Salmonella* treated patient's derived tumor cells boosted the expansion of specific antitumor lymphocytes. The ability of circulating lymphocytes that recognize patient's tumor cells was assessed for the duration of the clinical trial. Total PBMCs were co-cultured with tumor cells at a ratio (PBMCs:tumor) cells of 5:1 for 5 hours. CD107a antibody was added for the duration of the protocol while intracellular staining for IFN-ɣ expression together with the staining to distinguish $CD4^+$ $CD8^+$ subpopulation was performed at the end of the protocol.

Moreover, we observed that circulating lymphocytes of Sa5 at the end of the immunization protocol had acquired also the ability to kill tumor cells (**Figure 4-16A**). Total PBMCs were co-cultured for 1h30min with Batda-labelled-tumor cells and their killing ability was assessed by Delfia assay (**Chapter 3.13.2**) using different ratio of effector:target cells (1:50 1:25 1:12,5 and 1:6,125). Lymphocytes' cytotoxic effect was also observed after sarcoma relapse (**Figure 4-16B**) but the percentage of specific release didn't increase over the time of the second immunization protocol.

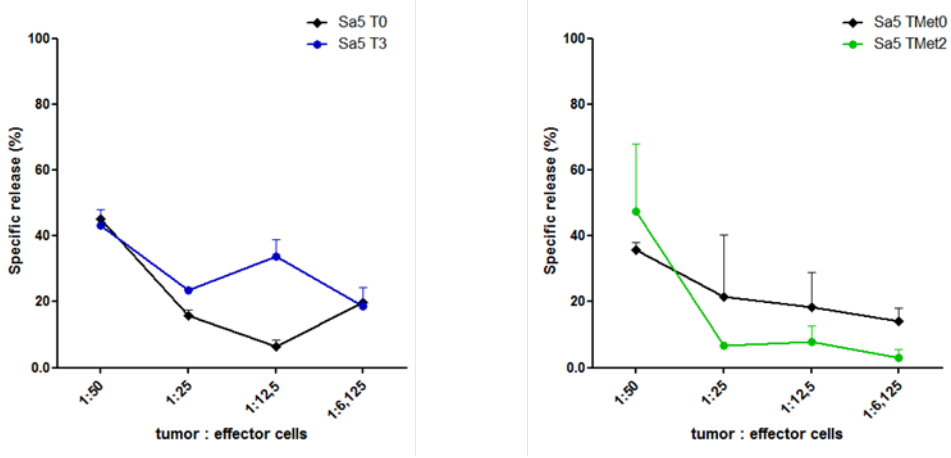

Figure 4-16. Vaccination of sarcoma patient with peptides derived from *Salmonella* treated patient's derived tumor cells boosted the expansion of lymphocytes able to kill tumor cells. The ability of circulating lymphocytes to recognize and kill patient's tumor cells was assessed for the duration of the clinical trial. Total PBMCs were co-cultured for 90 min with tumor cells and their killing ability was assessed by Delfia assay (**Chapter 3.13.2**) using different ratio of effector:target cells (1:50 1:25 1:12.5 and 1:6.125).

While $CD8^+$ T lymphocytes are the principal mediator of an antitumor cytotoxic response, $CD4^+$ T cells are responsible for B cell activation that leads to immunoglobulin production. Consistent with the finding that the vaccination leads Sa5 to boost an antitumor $CD4^+$ T cell response (**Figure 4-15C,D**), a specific antitumor humoral response was equally induced by the vaccination (**Figure 4-17**).

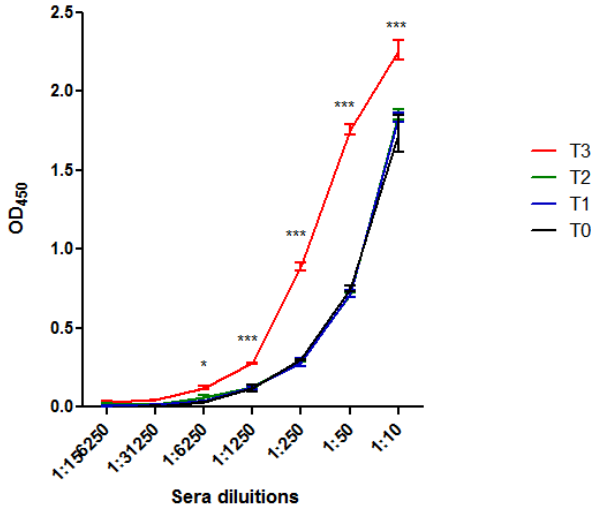

Figure 4-17. Vaccination of sarcoma patient with peptides derived from *Salmonella* treated patient's derived tumor cells induced a humoral response against tumor cells. The content of tumor cell-specific IgG in the serum of Sa5 was assessed for the duration of the clinical trial. T0=before entering the clinical trial; T1=after one vaccination; T2=after two vaccinations; T3=after four vaccinations. *$p<0.05$ ***$p<0.001$ 2-way-ANOVA Bonferroni post-test to compare T3vsT0.

4.4 Unravelling vaccine composition by mass spectrometry-based approach

4.4.1 Identification of the peptides released by *Salmonella* treated tumor cells: samples preparation for mass spectrometry analysis.

Salmonella induces the release of immunogenic peptides from tumor cells. Their identification will allow the development of a vaccine formulation of antigens with a strong antitumor immunity. To achieve this goal, we compared peptides released by *Salmonella*-treated tumor cells with those released by untreated tumor cells and developed a list of immunogenic peptide candidates. Due to the complexity of supernatant composition low and high molecular weight peptides were separated with a 10KDa centrifugation filter (filter aided sample preparation, FASP) and differently analysed. Low molecular weight fraction was concentrated in a centrifuge vacuum concentrator and soon acquired by nLC-MS, while high molecular weight fraction, containing mainly proteins, underwent enzymatic treatment before acquisition (see pipeline **Figure 4-18**). The MS-based peptidomic approach we developed and the strategy that we propose to identify both tumor antigens and neoantigens are explained in the next chapter. Even though we believe that antigens and neoantigens (included in the low molecular weight fraction) are responsible for the induction of the antitumor response, a role of the proteins included in the high molecular weight fraction cannot be excluded. Indeed, proteins might exert an adjuvant function in vivo or might be taken up and processed by DCs thus contributing to the antitumor specific immune response.

4.4.2 Strategy to identify tumor antigens and neoantigens released by tumor cells following *Salmonella* infection

Aiming to identify tumor antigens among the peptides released after *Salmonella* infection we performed a mass-spectrometry based proteomic study via a Data Dependent Analysis

(DDA) methodology coupled with direct database search. Briefly, the 15 most abundant precursor ions detected by the mass spectrometer in a survey scan per millisecond (MS1) are selected for fragmentation (MS2). The resulting fragmented ions recorded are searched against Uniprot databases to have sequences identified, using two independent Database search engine. MaxQuant was used as platform to detect proteins and peptides significantly different in supernatant derived from *Salmonella* treated and untreated cells imposing a supervised analysis and a Student-T test statistical analysis. Proteome Discoverer coupled with Mascot were applied only to the low molecular weight fractions of samples derived from *Salmonella* treatment to identify peptides and to access the MS2 scan list of all annotated and non-annotated peptides. Theoretically, with this DDA-approach, we can identify all the tumor antigens whose sequence is derived from normally expressed proteins. Both tumor associated antigens (TAA), that are peptides normally encoded by the normal genome but aberrantly expressed by tumor cells (i.e. overexpressed) and cancer testis antigens (CTAs), that are peptides belonging to developmental protein whose expression is re-stored by cancer cells, can hence be identified. On the contrary, neoantigens, that are mutated peptides generated by non-synonymous mutations or other genetic alterations, and the recently identified spliced antigens that arise from post translational splicing (Hanada et al. 2004; Vigneron 2004; Warren et al. 2006), cannot be easily identified by this approach due to the fact that their sequence differs from normally expressed peptides (Mishto & Liepe 2017). These antigens have been so far identified tailoring the phase of database searching on customized databases of peptides usually derived from exome sequencing data but this approach is time consuming and suffers of false sequence assignment. With the aim to overcome drawbacks associated to this strategy, we followed a different pipeline (**Figure 4-18**); after DDA-analysis we focused on the MS1 scan. All detected signals were considered as features, meaning a combination of mass-charge ratio (m/q) and retention time (RT). Then we used XCMS software

(Tautenhahn et al. 2012) to determine the features whose levels were significantly higher in the supernatant derived from *Salmonella*-treated tumor cells compared with supernatant of untreated tumor cells. We identified features belonging to three different categories:

1) Category1 (Cat1): Peptides that underwent MS2 fragmentation and that were identified as true PSM (Peptides Sequence Match) by the data base searching engine Proteome Discoverer coupled with Mascot.

2) Category 2 (Cat2): Peptides that underwent fragmentation but were not annotated by Proteome Discoverer due to the parameters imposed in the search, suggesting that they might be either PTM-modified peptides or mutated peptides. A further ranking of these features was done on the basis of the comparison between the retention time (RT) associated to the matched m/z value in order to exclude false positive features. If the difference between the RT attributed by XCMS and the RT showed by PD was less than 2 minutes, features were ranked as ClassA; if the same difference was in-between 2 and 4 minutes features were included in ClassB; eventually, if the difference was higher than 4 minutes features were excluded from the analysis.

3) Category 3 (cat3): MS1 features that, although highlighted as specific for *Salmonella*-treatment by XCMS, were not fragmented. This might be due either to a poor ionization of the peptide that leads to its exclusion from the fragmentation step (intrinsic drawback of short peptides that lack basic amino acids residues) or simply to an exclusion driven by the DDA mode where the selection of precursor ions is stochastic since it follows an intensity dependent heuristics (Caron et al. 2015). These features included exclusively in the MS1 scan and described as over-represented in *Salmonella*-derived supernatant might be still promising for the identification of modified or mutated tumor antigens and thus might be targeted by further MS analysis tailored for their identification. This category includes also instrumental ‘noise’, namely features that have an MS trace although they are not analytes.

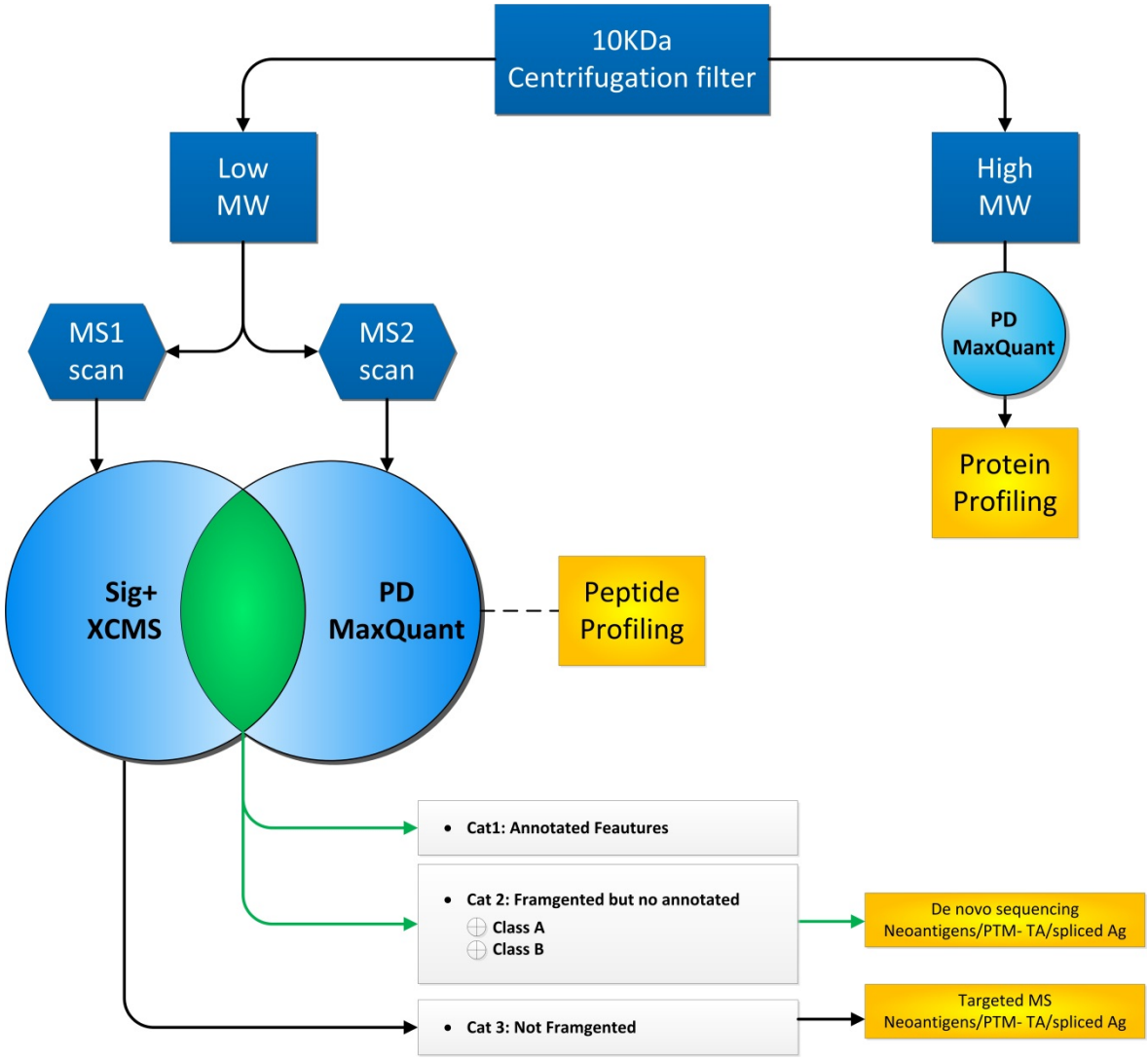

Figure 4-18. Pipeline of the peptidomic analysis

4.4.2.1 Feasibility of the proposed pipeline

In order to evaluate the feasibility of our strategy we analyzed by XCMS features derived from a standard protein analysis. We chose tryptic digestion of bovine serum albumin (BSA), and compared features detected by XCMS to a blank sample (features derived from a buffer run). Before proceeding with the categorization of the features detected by XCMS as BSA-specific we assessed the overlap between all the features detected by XCMS (MS1 scan) and all the PSM revealed by Proteome Discoverer/Mascot. 15% of the overall features overlapped at the m/z level (**Figure 4-19**) but the majority of the features appeared

to be software specific. These can be considered as 'noise' intrinsic of both softwares. In most of DDA studies only a small portion of PSMs (20% - 40%) represents plausible matches and is annotated while the remaining are considered as 'noise' (Jeong et al. 2012). This percentage can be lower if a pure protein is analyzed. Taking into account that XCMS applies to a specific algorithm to filter and identify peaks from the MS1 scan and to match peaks across samples, its noise is reasonably different from the noise of classical data base searching engine as Mascot, MaxQuant or SEQUEST. The overlap at m/z level was scored for all the peptidomic studies performed to characterize supernatants derived from melanoma cells that are discussed below. Similarly to what we observed for BSA-analysis, the overlap between all the features detected by XCMS (MS1 scan) and all the PSM revealed by Proteome Discoverer/Mascot was around 15% (ranging in between 18%-28%, data not shown).

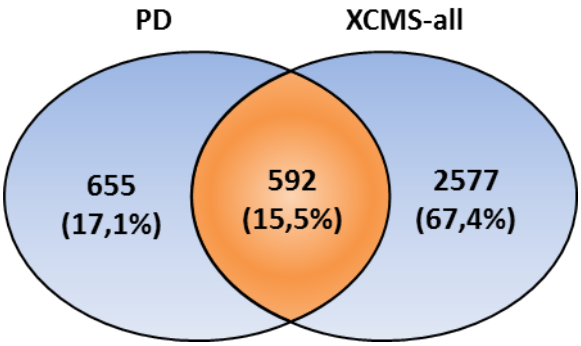

Figure 4-19. Overlap between analysis based on MS1 scan and MS2 scan is 15%. Venny diagram representing the overlap at m/z level between MS2 scan list (all PSM showed by PD) and the list of features revealed by XCMS (based on MS1 scan).

We then proceeded investigating the 496 features (pvalue<0.01 fold change>3 Intensity precursor>$2x10^6$) detected by XCMS as overrepresented inside the BSA sample compared to the blank. Comparing at m/z level these 496 significant features with the MS2 scan revealed by Proteome Discoverer we observed a 30% of overlap (149 on 496 total significant features, **Figure 4-20**). The analysis of the true PSM of BSA detected by PD was in line with that expected for a pure protein (13%, 234 on 1240 total PSM). 14,8% of

these true PSM were in common with XCMS (36 annotated features on 234 total PSM). This percentage represents 24% of the significant features detected by XCMS (36 out of 149 total significant and overlapping features). The remaining 85% of the true PSM is scored in our proposed pipeline by MaxQuant/PD while the remaining 76% of the significant features revealed by XCMS could be potential neoantigens and PTM-modified antigens and will be further investigated. In conclusion, following our proposed pipeline for two-group comparison that combines the analysis of classical database searching engine with the analysis of the features at MS1-level, we are not losing information but, on the opposite, we are gaining knowledge of features that otherwise would not be accessible.

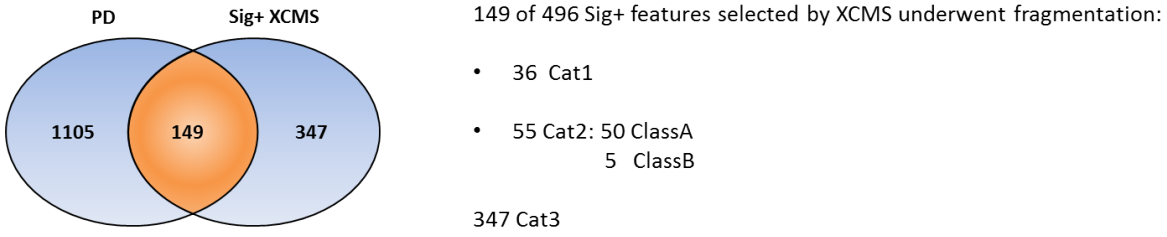

Figure 4-20. 30% of the features selected as overrepresented in BSA sample overlap with the MS2 scan list. 496 BSA-features were selected by XCMS imposing pvalue<0.01, fold change>3 Intensity precursor>$2x10^6$. 149 out of 496 (30%) were overlapping with the MS2 scan list revealed by PD.

4.4.2.2 Identification of peptides released by murine melanoma B16 cell line

Vaccination of mice with peptides released by murine melanoma B16 cells upon *Salmonella* infection boosted a strong antitumor response that significantly delayed the growth of B16 tumor cells injected in the flank of the mice (**Figure 4-7**). Three sets of supernatants tested in vivo were analyzed by mass spectrometry. Briefly, low molecular weight peptides inside cell's supernatants were separated by proteins using a 10KDa centrifugation filter and analyzed by nLC-ESI-MS^2 (see pipeline**, Figure 4-18**).

23 peptides were identified as specifically released following *Salmonella* infection (**Figure 4-21**). A Gene Ontology (GO) Cellular Component analysis showed that several proteins, to which the selected peptides belonged to, are found in the focal adhesion or as components of ribosomes (**Figure 4-22**) and we observed an enrichment of proteins dedicated to mRNA transport, mRNA stability regulation and protein translation (**Table 4-1**). Our attention focused on a peptide belonging to Cofilin, a protein already described to be a source of human tumor antigen. This same peptide was found to be expressed also by 3 different human melanoma cell lines and primary human melanoma cells (Gloger et al. 2016) and to be identified by proteomic analysis in the MHC-binding peptidome of human breast and pancreatic cancer cell lines (Antwi et al. 2009). NetMHC4.0 predicted this Cofilin peptide to be a good binder of murine MHC class I molecules H2Kk and H2Kd (IC50<3000nM).

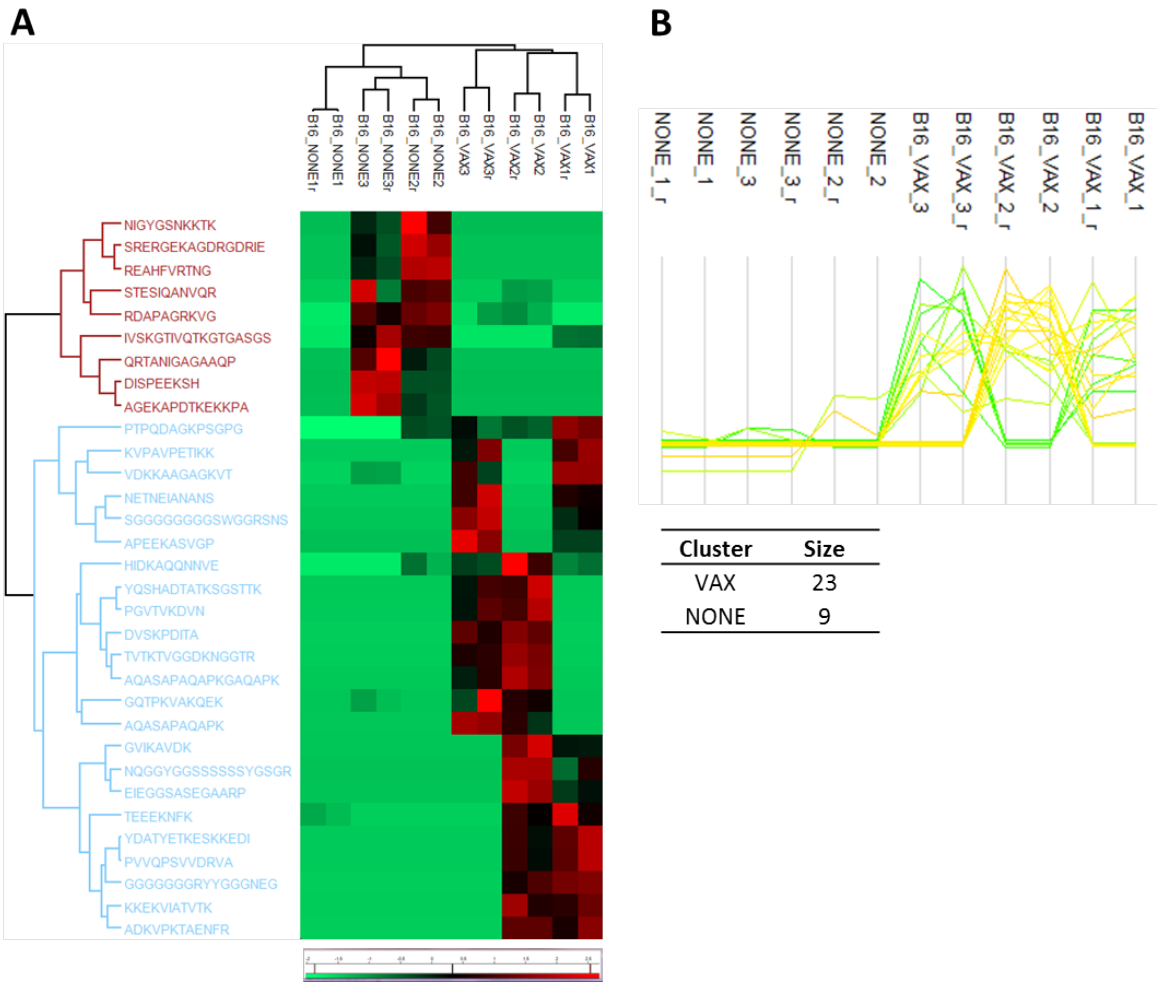

Figure 4-21. Profiling peptides specifically released by murine B16 melanoma cells upon *Salmonella* infection: results from data base searching engine. Three B16-supernatants that were tested *in vivo* were analyzed through nLC-MS: control supernatants (None) and the ones derived from *Salmonella* treated B16 cells (Vax). Each supernatant was analyzed in duplicate, shown as -bis. A. HeatMap that shows 23 identified peptides significantly more abundant in Vax supernatants; analyses were performed with MaxQuant software on the identified peptides. *P <0.05. Red color: up-regulated. Green color: down-regulated B. Graph representing the distribution of the intensity of the 23 Vax-specific peptides

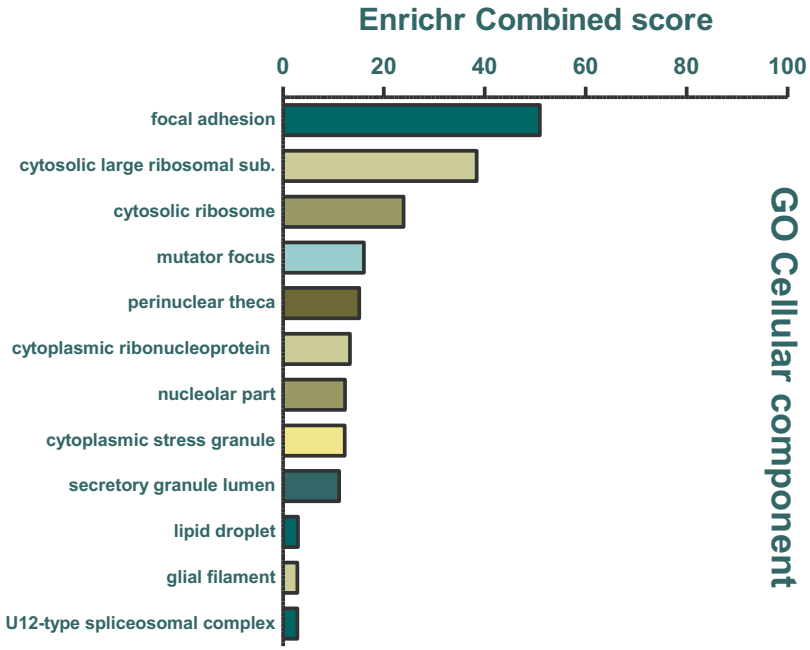

Figure 4-22. Peptides released by murine B16 melanoma cells upon *Salmonella* infection belong to proteins mainly found at the level of focal adhesion and as components of ribosomes. Gene Ontology (GO) Cellular Component analysis applied to the 23 peptides identified as released specifically following *Salmonella* infection. Combined score calculated by EnrichR tool is plotted for each GO-Cellular component category.

Reactome 2016

Index	Name	P-value	Adjusted p-value	Z-score	Combined score
1	Translation_Homo sapiens_R-HSA-72766	1.704e-14	8.075e-13	-2.03	64.36
2	Eukaryotic Translation Elongation_Homo sapiens_R-HSA-156842	2.163e-14	8.075e-13	-2.00	62.92
3	Peptide chain elongation_Homo sapiens_R-HSA-156902	1.339e-14	8.075e-13	-1.97	62.79
4	GTP hydrolysis and joining of the 60S ribosomal subunit_Homo sapiens_R-HSA-72706	9.878e-14	1.844e-12	-1.98	59.18
5	L13a-mediated translational silencing of Ceruloplasmin expression_Homo sapiens_R-HSA-156827	9.145e-14	1.844e-12	-1.94	58.16
6	3' -UTR-mediated translational regulation_Homo sapiens_R-HSA-157279	9.145e-14	1.844e-12	-1.93	57.90
7	Eukaryotic Translation Initiation_Homo sapiens_R-HSA-72613	1.661e-13	2.326e-12	-1.94	57.06
8	Cap-dependent Translation Initiation_Homo sapiens_R-HSA-72737	1.661e-13	2.326e-12	-1.93	56.84
9	Viral mRNA Translation_Homo sapiens_R-HSA-192823	1.980e-12	2.464e-11	-1.85	49.78
10	Selenocysteine synthesis_Homo sapiens_R-HSA-2408557	2.550e-12	2.596e-11	-1.85	49.46

KEGG 2016

Index	Name	P-value	Adjusted p-value	Z-score	Combined score
1	Ribosome_Homo sapiens_hsa03010	6.508e-11	1.432e-9	-1.75	40.96
2	RNA transport_Homo sapiens_hsa03013	0.01387	0.1526	-1.84	7.88
3	PI3K-Akt signaling pathway_Homo sapiens_hsa04151	0.04918	0.1874	-2.02	6.07
4	Legionellosis_Homo sapiens_hsa05134	0.05622	0.1874	-1.79	5.16

Table 4-1. Peptides released by murine B16 melanoma cells upon *Salmonella* infection belong to proteins mainly involved in protein translation. Pathway knowledge analysis with KEGG2016 and Reactome2016 databases was applied to the 23 peptides identified as released specifically following *Salmonella* infection. Tabs show the statistically significant enriched pathways and the associated scores calculated by EnrichR tool.

In order to evaluate the presence of peptide candidates as neoantigens or posttranslational modified tumor antigens we analyzed the differences at the level of MS1 scan between samples derived from *Salmonella* treated or untreated B16 cells (following the pipeline shown in **Figure 4-18**). 79 features were found to be over represented in samples derived from *Salmonella* treatment of tumor cells (**Figure 4-23**). 39 of them overlapped with the list of total PSM (**Figure 4-23**); among them 2 were already annotated spectra with the

search parameter imposed (Cat1) and 6 features belonging to Cat2 were candidates positive to undergo de-novo sequencing (Cat2). The non-overlapping fraction, is composed of 40 features that will be further investigated with a target data acquisition (TDA) mode to force the Mass Spectrometer to fragment them. As additional control, we verified by Proteome Discoverer if some of the peptides released by B16 cells following *Salmonella* infection were belonging to *Salmonella* itself. The few peptides found to belong to *Salmonella* were not present in these lists as they were neither erroneously assigned by MaxQuant nor included among the selected significant features by XCMS.

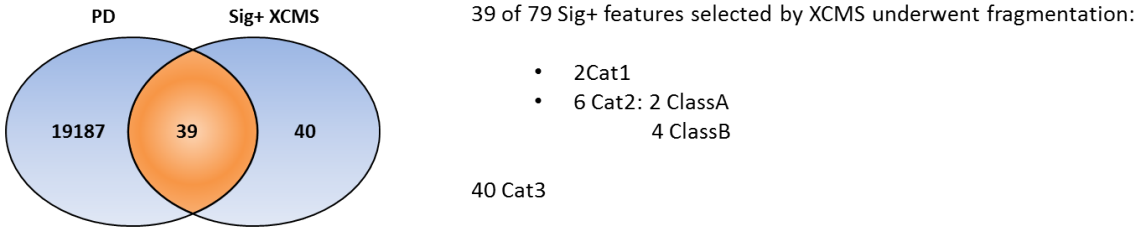

Figure 4-23. 50% of the features selected as overrepresented by XCMS in *Salmonella*-derived sample overlap with the MS2 scan list. 79 features specific for *Salmonella*-treatment were selected by XCMS imposing pvalue<0.01, fold change>3 Intensity precursor>$2x10^6$. 39 out of 79 (50%) were overlapping with the MS2 scan list revealed by PD.

4.4.2.3 Identification of peptides released by human melanoma 62438 cell line

Supernatant derived from the infection of human melanoma 62438 cell line with *Salmonella* allowed the expansion of $CD8^+$ T cells from healthy donor's PBMCs (**Figure 4-10**). Moreover expanded lymphocytes were able to activate a cytotoxic response against 62438 cells that was mediated by the recognition of HLA-peptide complex (**Figure 4-11**). Peptide candidates to be responsible for $CD8^+$T cells expansion were identified by mass spectrometry analyzing cell supernatants derived from three biological replicates.

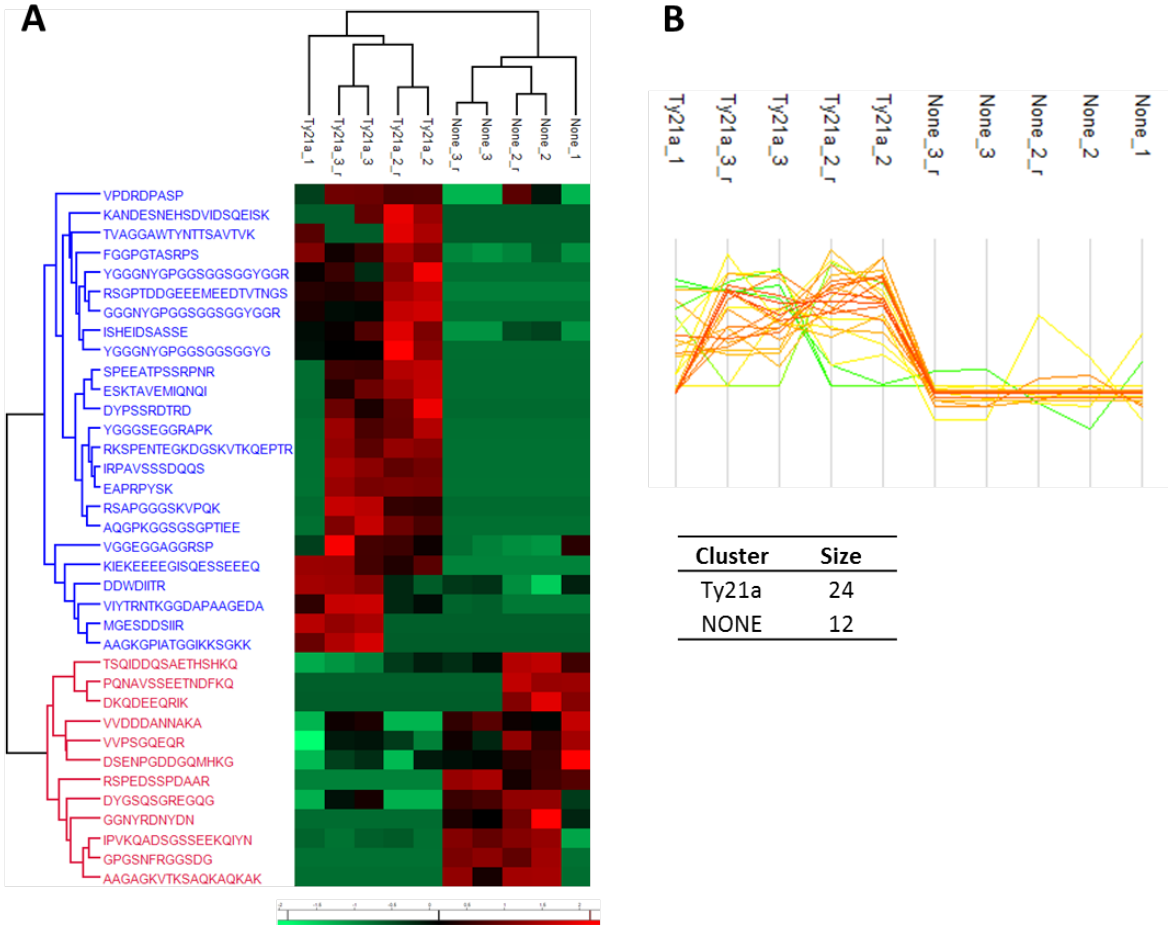

Figure 4-24. Profiling peptides specifically released by human 62438 melanoma cells upon *Salmonella* infection: results from data base searching engine. Three 62438-supernatants that were tested for expansion of $CD8^+$ T cells from healthy donor PBMCs (**Chapter 4.2**) were analyzed through nLC-MS both control supernatants (None) and the ones derived from *Salmonella* treated 62438 cells (Ty21a). Each supernatant was analyzed in duplicate, identified as -r. **A**. HeatMap that shows 24 identified peptides significantly more abundant in Ty21a-supernatants; analysis were performed with MaxQuant software on the identified peptides. *P <0.05. Red color: up-regulated. Green color: down-regulated **B**. Graph representing the distribution of the intensity of the 24 Ty21a-specific peptides.

Comparing peptides detected inside the supernatant of untreated 62438 cells with supernatant derived from *Salmonella* infected 62438 cells, 24 peptides were found to be over-represented in this second condition (**Figure 4-24**). Cellular-Component Gene Ontology analysis (**Figure 4-25**) showed that proteins to which peptides belonged to are

mainly localized at the focal adhesion; some are instead either nuclear or cytoplasmic ribosomal subunit, other belong to supraspliceosomal complexes. Interestingly Reactome and KEGG databases highlighted the enrichment of proteins involved either in pathways triggered by infection or in peptide chain elongation and splicing processes (**Table 4-2**).

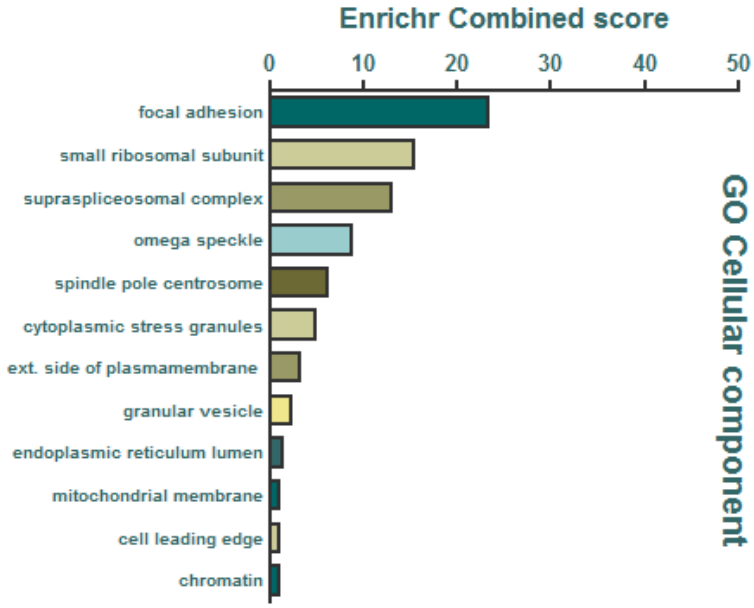

Figure 4-25. Peptides released by 62438 cells upon *Salmonella* infection belong to proteins mainly found at the level of focal adhesion, as components of ribosomes or spliceosomal complex. Gene Ontology (GO) Cellular Component analysis applied to the 24 peptides identified as specifically released following *Salmonella* infection. Combined score calculated by EnrichR tool is plotted for each GO-Cellular component category.

Reactome 2016

Index	Name	P-value	Adjusted p-value	Z-score	Combined score
1	Infectious disease_Homo sapiens_R-HSA-5663205	0.00002507	0.001074	-2.40	25.46
2	Peptide chain elongation_Homo sapiens_R-HSA-156902	0.00009000	0.001074	-1.96	18.23

KEGG 2016

Index	Name	P-value	Adjusted p-value	Z-score	Combined score
1	Ribosome_Homo sapiens_hsa03010	0.0003821	0.002292	-1.75	13.74
2	Spliceosome_Homo sapiens_hsa03040	0.008608	0.02582	-1.77	8.43

Table 4-2. Peptides released by 62438 cells upon *Salmonella* infection belong to proteins mainly involved in protein translation. Pathway knowledge analysis with

KEGG and Reactome databases was applied on the 24 peptides identified as specifically released following *Salmonella* infection. Tabs show the statistically significant enriched pathways and the associated scores calculated by EnrichR tool.

XCMS showed that 159 features were over-represented inside the supernatant derived from *Salmonella* infection of 62438. 49 out of 159 overlapped with features also present inside the MS2 scan (**Figure 4-26**). 5 features were found to be fragmented and already associated to a sequence (Cat1) while 21 features have been fragmented but not assigned to any sequence (Cat2). Importantly these 21 features could be further characterized by a de-novo sequencing. The 110 features whose m/z did not overlap with any PSMs will be further investigated following a target data acquisition (TDA) mode to define their identity. To conclude this analysis we verified by proteome discoverer if some of the peptides released by 62438 following *Salmonella* infection were belonging to *Salmonella*. The few peptides found to belong to *Salmonella* even in this case were neither erroneously assigned by MaxQuant nor included among the selected significant features by XCMS.

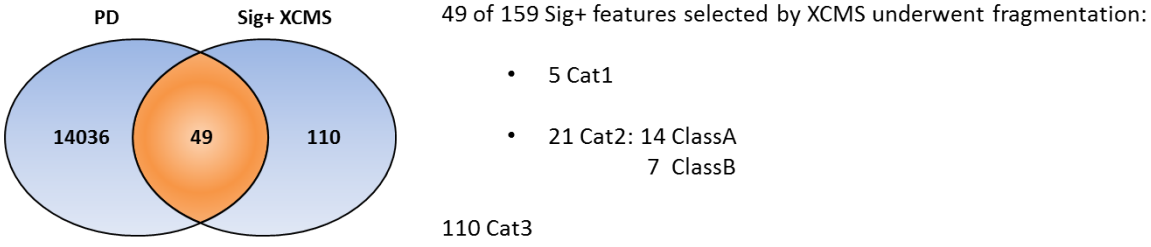

Figure 4-26. 32% of the features selected as overrepresented by XCMS in *Salmonella*-derived sample overlap with the MS2 scan list. 159 features specific of *Salmonella*-treatment were selected by XCMS imposing pvalue<0.01, fold change>3 Intensity precursor>$2x10^6$. 49 out of 159 (32%) were overlapping with the MS2 scan list revealed by PD.

4.4.2.4 Identification of peptides released by patients-derived human melanoma cells.

We demonstrated that *Salmonella* induces the release of immunogenic peptides by both murine and human tumor cell lines. Peptide candidates to be responsible of the immunogenicity were identified by mass spectrometry approach combining two different strategies in order to identify both non mutated tumor antigens and PTM-tumor antigen/neoantigens/spliced antigens (see pipeline **Figure 4-18**). The same pipeline could be used on cells directly derived from patient's tumor cells with the aim to identify novel tumor antigens and neoantigens to be included in vaccine formulation to be administered to patients to boost an antitumor response. To verify the feasibility of this strategy we derived primary tumor cells from melanoma biopsies, we infected them with *Salmonella* and we went through a MS-based peptidomic analysis of the released peptides. Peptides over-represented in supernatants derived from *Salmonella*-infected tumor cells clustered together and separately from peptides released by untreated tumor cells (**Figure 4-27**) although they were derived from melanoma cells of three different patients. This suggests that *Salmonella* induces the release of peptides that are shared among patients affected by the same tumor type. 115 peptides were selected to be specific of *Salmonella* treatment. Proteins to which these selected-peptides belonged to are mainly located at focal adhesion or belong to cytosolic ribosomal protein (**Figure 4-28**). They participate to several steps of the translational processes impacting on the mRNA splicing, on its subsequent transport from nuclei to ribosomal protein, protein translation and protein transport. KEGG and Reactome analysis highlighted also the enrichment of proteins that are involved in pathways activated in response to bacterial infection (**Table 4-3**). Since we have previously performed an MS-based peptidomic study on peptides released by the human melanoma cell line 62438, we wondered whether some of the selected peptides were found to be released also by primary patients-derived melanoma cells. We found 3 peptides

commonly released after *Salmonella* infection (**Figure 4-4**). They belonged to Nucleophosmin (NM1) protein and to the high mobility group protein (HMG-I/HMG-Y), both involved in pathways activated in response to a pathogen, while the third peptide is involved in the translation process and belongs to the translation machinery-associated protein 7 (TMA7). Interestingly peptides derived from NM1 and TMA7 were predicted to be strong binders of the HLA-A0301; IC_{50} lower than 500nM were calculated by NetMHC4.0 (**Figure 4-4**) either for the entire sequence or for shorter portions of the sequenced peptides. HMG-I-peptide was predicted to be a mild binder of HLA-B4001 (IC_{50}<1000nM). Moreover, we found NM1-peptide to be described as an HLA-binder in two different studies (Bassani-Sternberg et al. 2015; Pearson et al. 2016). Furthermore, TMA7 protein is already known as a source of tumor antigens but the peptide-sequence we found has not been described yet. This finding further proves that infection of tumor cells with *Salmonella* promote cancer cells to release immunogenic peptides.

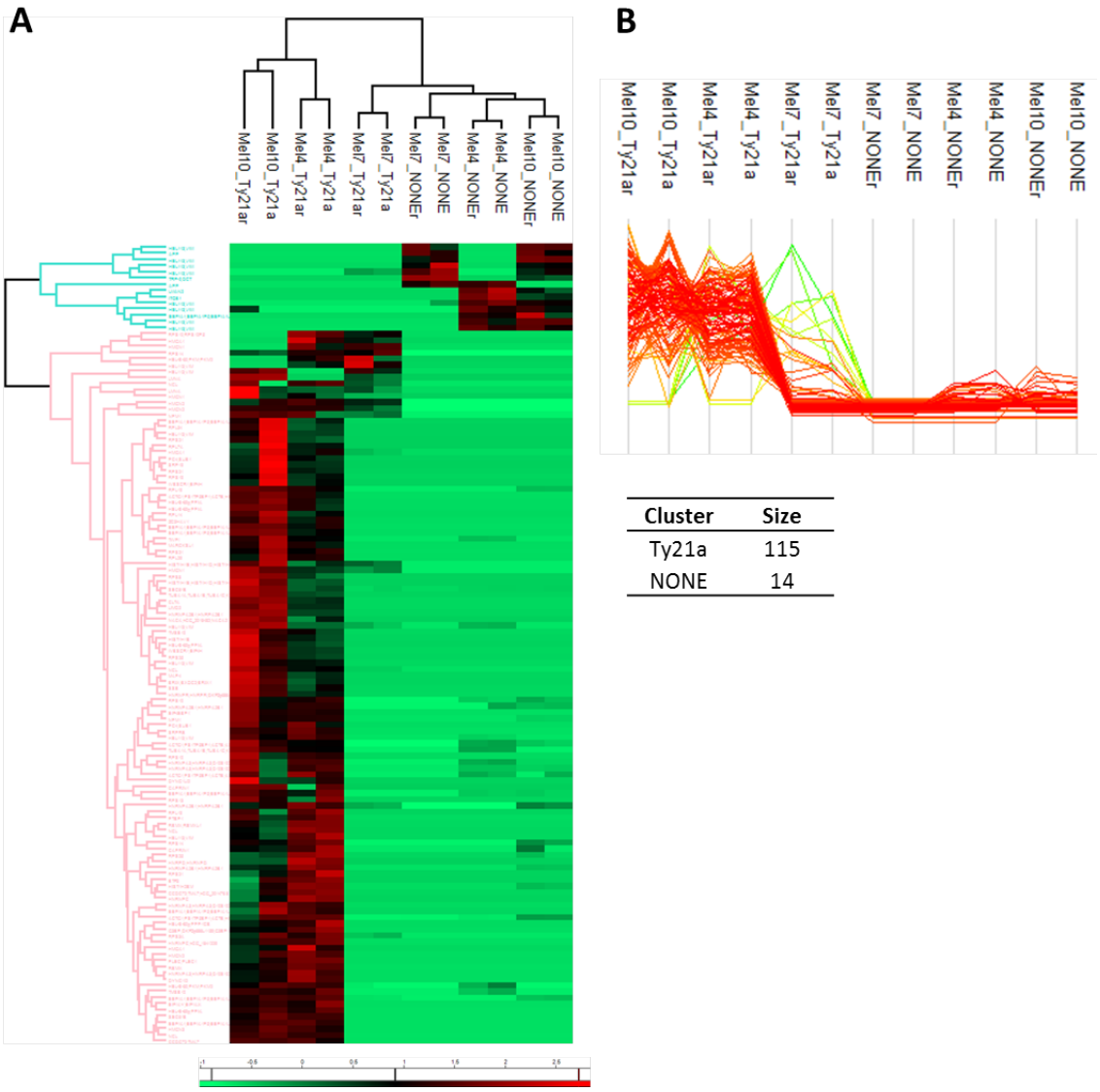

Figure 4-27. Profile of peptides specifically released by human patients-derived melanoma cells upon *Salmonella* infection: results from data base searching engine. Supernatants of three different patients-derived melanoma cells (Mel1, Mel4, Mel7) were analyzed through nLC-MS both control supernatants (None) and the ones derived from *Salmonella* treated melanoma cells (Ty21a). Each supernatant was analyzed in duplicate, identified as -r. A. HeatMap that shows 115 identified peptides significantly more abundant in Ty21a-supernatants; analysis were performed with MaxQuant software on the identified peptides. *P <0.05. Red color: up-regulated. Green color: down-regulated B. Graph representing the distribution of the intensity of the 115 Ty21a-specific peptides.

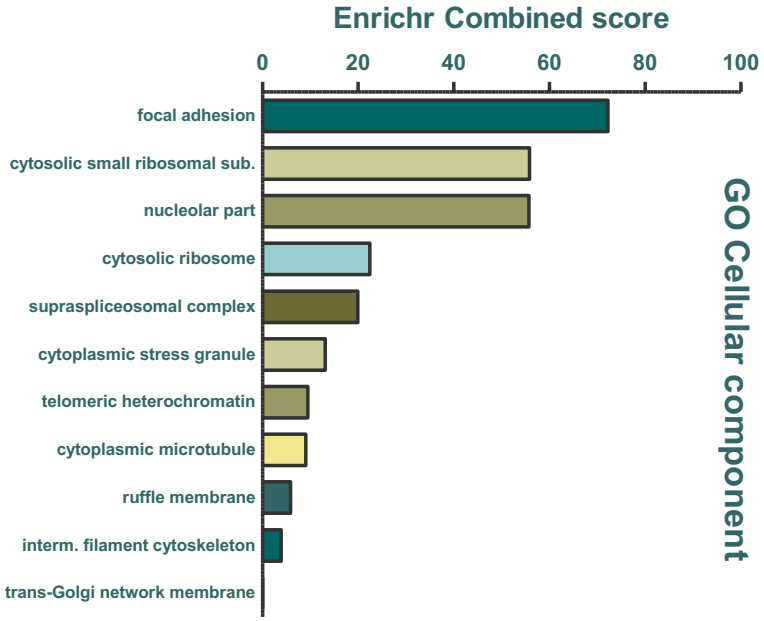

Figure 4-28. Peptides released by patients-derived melanoma cells upon *Salmonella* infection belong to proteins mainly found at the level of focal adhesion, as component of ribosomes or spliceosomal complex. Gene Ontology (GO) Cellular Component analysis applied on the 115 peptides identified as specifically released following *Salmonella* infection. Combined score calculated by EnrichR tool is plotted for each GO-Cellular component category.

Reactome 2016

Index	Name	P-value	Adjusted p-value	Z-score	Combined score
1	Translation_Homo sapiens_R-HSA-72766	2.229e-24	4.948e-22	-2.04	110.99
2	SRP-dependent cotranslational protein targeting to membrane_Homo sapiens_R-HSA-1799339	2.328e-23	2.584e-21	-1.99	103.88
3	Eukaryotic Translation Elongation_Homo sapiens_R-HSA-156842	7.788e-21	4.322e-19	-1.99	92.17
4	Peptide chain elongation_Homo sapiens_R-HSA-156902	3.274e-21	2.423e-19	-1.95	91.86
5	Eukaryotic Translation Initiation_Homo sapiens_R-HSA-72613	3.019e-19	9.574e-18	-1.95	83.03
6	Cap-dependent Translation Initiation_Homo sapiens_R-HSA-72737	3.019e-19	9.574e-18	-1.94	82.72
7	Viral mRNA Translation_Homo sapiens_R-HSA-192823	2.676e-19	9.574e-18	-1.88	80.52
8	Influenza Life Cycle_Homo sapiens_R-HSA-168255	3.910e-18	7.233e-17	-2.00	80.21
9	Selenocysteine synthesis_Homo sapiens_R-HSA-2408557	4.346e-19	1.072e-17	-1.87	79.08
10	Eukaryotic Translation Termination_Homo sapiens_R-HSA-72764	4.346e-19	1.072e-17	-1.86	78.75

KEGG 2016

Index	Name	P-value	Adjusted p-value	Z-score	Combined score
1	Ribosome_Homo sapiens_hsa03010	2.029e-16	1.035e-14	-1.75	63.09
2	Protein export_Homo sapiens_hsa03060	0.00004578	0.001167	-1.56	15.57
3	Phagosome_Homo sapiens_hsa04145	0.0001066	0.001812	-1.66	15.17
4	Pathogenic Escherichia coli infection_Homo sapiens_hsa05130	0.0006326	0.008066	-1.74	12.81
5	Salmonella infection_Homo sapiens_hsa05132	0.002308	0.02354	-1.61	9.75
6	Vasopressin-regulated water reabsorption_Homo sapiens_hsa04962	0.007972	0.05729	-1.74	8.42
7	Apoptosis_Homo sapiens_hsa04210	0.008986	0.05729	-1.78	8.39
8	Spliceosome_Homo sapiens_hsa03040	0.007974	0.05729	-1.65	7.97
9	Vibrio cholerae infection_Homo sapiens_hsa05110	0.01060	0.06006	-1.61	7.33
10	RNA transport_Homo sapiens_hsa03013	0.01562	0.07968	-1.65	6.86

Table 4-3. Peptides released by patients-derived melanoma upon *Salmonella* infection belong to proteins mainly involved in protein translation and in pathway activated in response to infection. Pathway knowledge analysis with KEGG and Reactome databases was applied to the 115 peptides identified as specifically released following *Salmonella* infection. Tabs show the statistically significant enriched pathway and the associated scores calculated by EnrichR tool.

	Sequence	Gene names	Protein names	HLA-binding prediction (NetMHC 4.0)		
seq1	AAGKGPIATGGIKKSGKK	CCDC72;TMA7	Translation machinery-associated protein 7	HLA-A0301	<500	strong
seq2	KIEKEEEEGISQESSEEEQ	HMGA1	High mobility group protein HMG-I/HMG-Y	HLA-B4001	<1000	mild
seq3	RSAPGGGSKVPQK	NPM1	Nucleophosmin	HLA-A0301	<500	strong

Table 4-4. Human 62438 melanoma cell line and patients-derived melanoma cells release identical peptides upon *Salmonella* infection. Three peptides were found to be equally released by human melanoma 62438 cells and patients-derived melanoma cells upon *Salmonella* infection. Of each peptide, sequence, gene name, protein name and the predicted HLA binding are described.

By the analysis of the features we observed 269 signals that specifically correlated with *Salmonella* treatment (**Figure 4-29**); 177 of these features overlapped with the list of PSM and among these 11 were already annotated while 76 (44 ranked as ClassA and 30 as ClassB) were selected for further de novo sequencing approach. The 92 features whose m/z did not overlap with the m/z of the total PSMs were selected to be further added to an inclusion list for a TDA mass spectrometry analysis aimed to identify them.

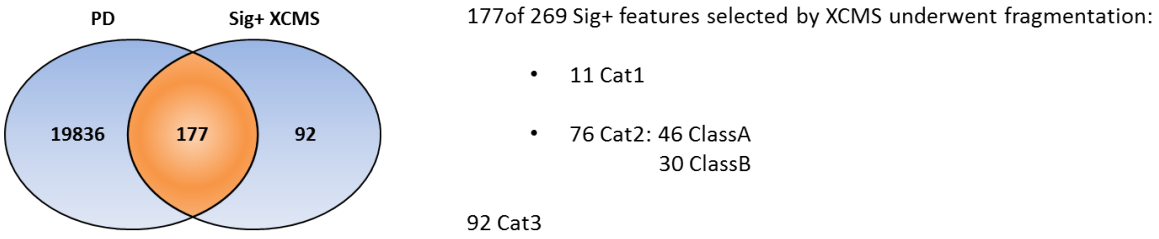

Figure 4-29. 60% of the features selected as overrepresented by XCMS in *Salmonella*-derived sample overlap with the MS2 scan list. 269 features specific of *Salmonella*-treatment were selected by XCMS imposing pvalue<0.01, fold change>3 Intensity precursor>$2x10^6$. 177 out of 269 (60%) were overlapping with the MS2 scan list revealed by PD.

4.4.2.5 Identification of peptides released by dog patient-derived melanoma cells treated with Salmonella.

In collaboration with a veterinarian clinic we had the opportunity to receive one dog-patient melanoma biopsy. As we did for osteosarcoma and high-grade sarcoma patients, we isolated tumor cells from the melanoma biopsy, we kept them in culture and infected them with *Salmonella* Ty21a. An MS-based peptidomic analysis was performed to identify peptide composition of the conditioned-supernatants. The same pipeline described to analyze peptides released by murine and human melanoma cells treated with *Salmonella* was applied also in this case. Peptides derived from untreated or *Salmonella*-treated tumor cells clustered separately and 243 peptides were selected as specific of *Salmonella* treatment (**Figure 4-30**). These selected peptides belonged to proteins mainly located at the cell focal adhesion or at the level of proteasome structure or inside stress-associated granules (**Figure 4-31**). This GO-Cell Component observation was in accordance to what we stated analyzing peptides released by both murine and human melanoma cells upon *Salmonella* infection. In agreement with the previous analysis, proteins were described to be involved in mRNA to protein-translation process, mRNA splicing, protein transport and in pathways activated following bacterial infection (**Table 4-5**). In addition to what we previously found, KEGG tool stated a significant enrichment for proteins associated to gap junction pathway (**Table 4-5**).

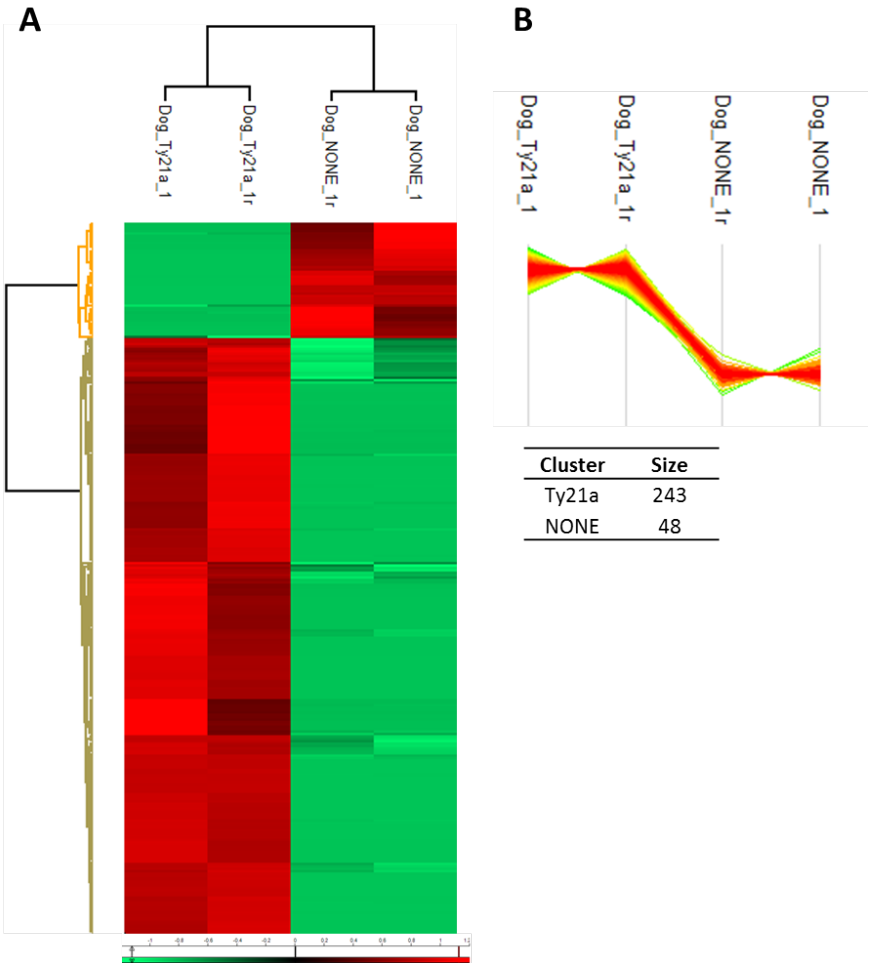

Figure 4-30. Profile of peptides specifically released by dog patients-derived melanoma cells upon *Salmonella* infection: results from data base searching engine. Supernatants of dog patient-derived melanoma cells were analyzed through nLC-MS both control supernatants (None) and the ones derived from *Salmonella* treated melanoma cells (Ty21a). Each supernatant was analyzed in duplicate, identified as -r. A. HeatMap that shows 243 identified peptides significantly more abundant in Ty21a-supernatants; analysis was performed with MaxQuant software on the identified peptides. *P <0.05. Red color: up-regulated. Green color: down-regulated B. Graph representing the distribution of the intensity of the 243 Ty21a-specific peptides.

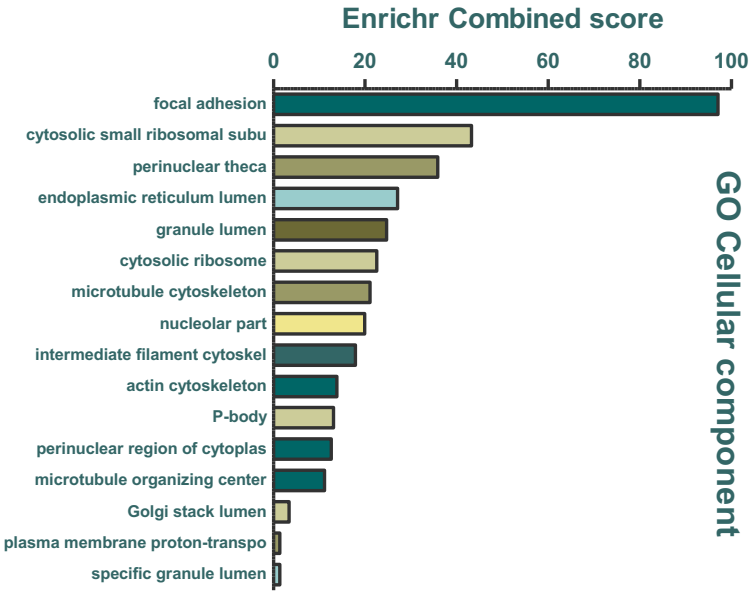

Figure 4-31. Peptides released by dog patients-derived melanoma cells upon *Salmonella* infection belong to proteins mainly found at the level of focal adhesion, as component of ribosomes or in the ER-lumen. Gene Ontology (GO) Cellular Component analysis applied on the 243 peptides identified as specifically released following *Salmonella* infection. Combined score calculated by EnrichR tool is plotted for each GO-Cellular component category.

KEGG 2016

Index	Name	P-value	Adjusted p-value	Z-score	Combined score
1	Ribosome_Homo sapiens_hsa03010	1.183e-13	7.807e-12	-1.75	51.97
2	Pathogenic Escherichia coli infection_Homo sapiens_hsa05130	0.00005381	0.001776	-1.82	17.93
3	ECM-receptor interaction_Homo sapiens_hsa04512	0.0002557	0.004680	-1.65	13.66
4	Phagosome_Homo sapiens_hsa04145	0.0002836	0.004680	-1.63	13.35
5	Gap junction_Homo sapiens_hsa04540	0.004423	0.05181	-1.68	9.12
6	Proteoglycans in cancer_Homo sapiens_hsa05205	0.007145	0.05895	-1.83	9.05
7	Focal adhesion_Homo sapiens_hsa04510	0.007024	0.05895	-1.77	8.78
8	Protein digestion and absorption_Homo sapiens_hsa04974	0.004710	0.05181	-1.57	8.41
9	Platelet activation_Homo sapiens_hsa04611	0.01087	0.07971	-1.71	7.71
10	Apoptosis_Homo sapiens_hsa04210	0.01571	0.09428	-1.73	7.19

Reactome 2016

Index	Name	P-value	Adjusted p-value	Z-score	Combined score
1	SRP-dependent cotranslational protein targeting to membrane_Homo sapiens_R-HSA-1799339	1.334e-16	4.168e-14	-2.00	73.16
2	Peptide chain elongation_Homo sapiens_R-HSA-156902	2.807e-16	4.168e-14	-1.95	69.74
3	Eukaryotic Translation Elongation_Homo sapiens_R-HSA-156842	5.812e-16	4.168e-14	-1.96	68.91
4	Viral mRNA Translation_Homo sapiens_R-HSA-192823	2.807e-16	4.168e-14	-1.91	68.38
5	Selenocysteine synthesis_Homo sapiens_R-HSA-2408557	4.368e-16	4.168e-14	-1.91	67.38
6	Eukaryotic Translation Termination_Homo sapiens_R-HSA-72764	4.368e-16	4.168e-14	-1.90	67.10
7	Nonsense Mediated Decay (NMD) independent of the Exon Junction Complex (EJC)_Homo sapiens_R-HSA-975956	5.812e-16	4.168e-14	-1.91	66.87
8	Formation of a pool of free 40S subunits_Homo sapiens_R-HSA-72689	1.499e-15	9.404e-14	-1.90	64.82
9	GTP hydrolysis and joining of the 60S ribosomal subunit_Homo sapiens_R-HSA-72706	5.759e-15	2.224e-13	-1.92	62.91
10	3' -UTR-mediated translational regulation_Homo sapiens_R-HSA-157279	5.128e-15	2.145e-13	-1.89	62.10

Table 4-5. Peptides released by dog patients-derived melanoma cells upon *Salmonella* infection belong to proteins mainly involved in protein translation and in pathway activated in response to infection. Pathway knowledge analysis with KEGG and Reactome databases was applied to the 243 peptides identified as specifically released following *Salmonella* infection. Tabs show the statistically significant enriched pathways and the associated scores calculated by EnrichR tool.

Feature analysis by XCMS showed that 1313 were overrepresented in supernatant derived from *Salmonella* treated tumor cells (**Figure 4-32**). 322 of them were overlapping with the list of features detected by Proteome Discoverer software; among them, 24 were unambiguously annotated (Cat1) while 175 (119 were ranked as ClassA and 56 as ClassB) belong to Cat2. 10 out of 175 of the significant features were found to be peptides belonging to *Salmonella*; hence they were excluded from the selection-list and 151 were eventually taken under consideration for de-novo sequencing analysis. The 991 non overlapping features (Cat3) could be targeted by future MS-based peptidomic analysis to get their MS2 spectrum.

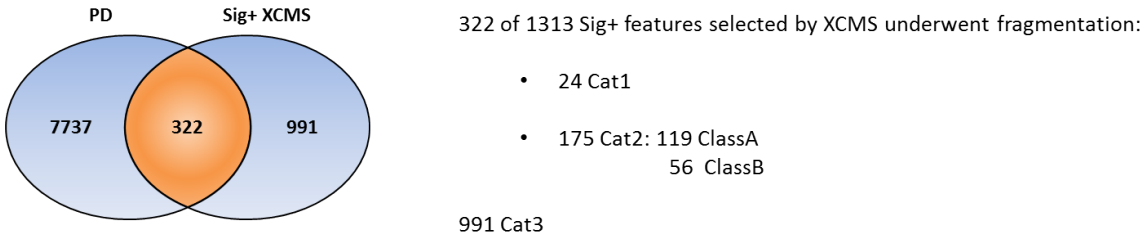

Figure 4-32. 40% of the features selected as overrepresented by XCMS in *Salmonella*-derived sample overlap with the MS2 scan list. 1313 features specific of *Salmonella*-treatment were selected by XCMS imposing pvalue<0.01, fold change>3 Intensity precursor>$2x10^6$. 322 out of 1313 (40%) were overlapping with the MS2 scan list revealed by PD.

4.4.3 Identification of proteins inside *Salmonella*-derived supernatants

Aiming to properly characterize the cell supernatant derived in response to cell infection with *Salmonella* the MS-based peptidomic analysis described above was done in parallel with a proteomic analysis (see pipeline **Figure 4-18**). The high molecular weight fraction deriving from FASP procedure was digested with trypsin and analyzed by nLC-MS. For technical reasons the analysis of the proteins derived from 62438 human melanoma cell line couldn't be performed. The analysis of proteins derived from melanoma cells, both mouse B16, human-patient and dog-patient-derived cells are described below.

4.4.3.1 Murine melanoma B16 cells: protein analysis

Three sets of supernatants derived from murine melanoma B16 cells that were tested *in vivo* were analyzed by mass spectrometry. The proteomic analysis revealed that two out of three supernatants derived from cells treated with *Salmonella* clusterd together (**Figure 4-21**). The third *Salmonella*-derived sample resulted overall poor of signals; the lack of most of the proteins that well profile the other two *Salmonella*-derived samples weights more than the shared proteins.

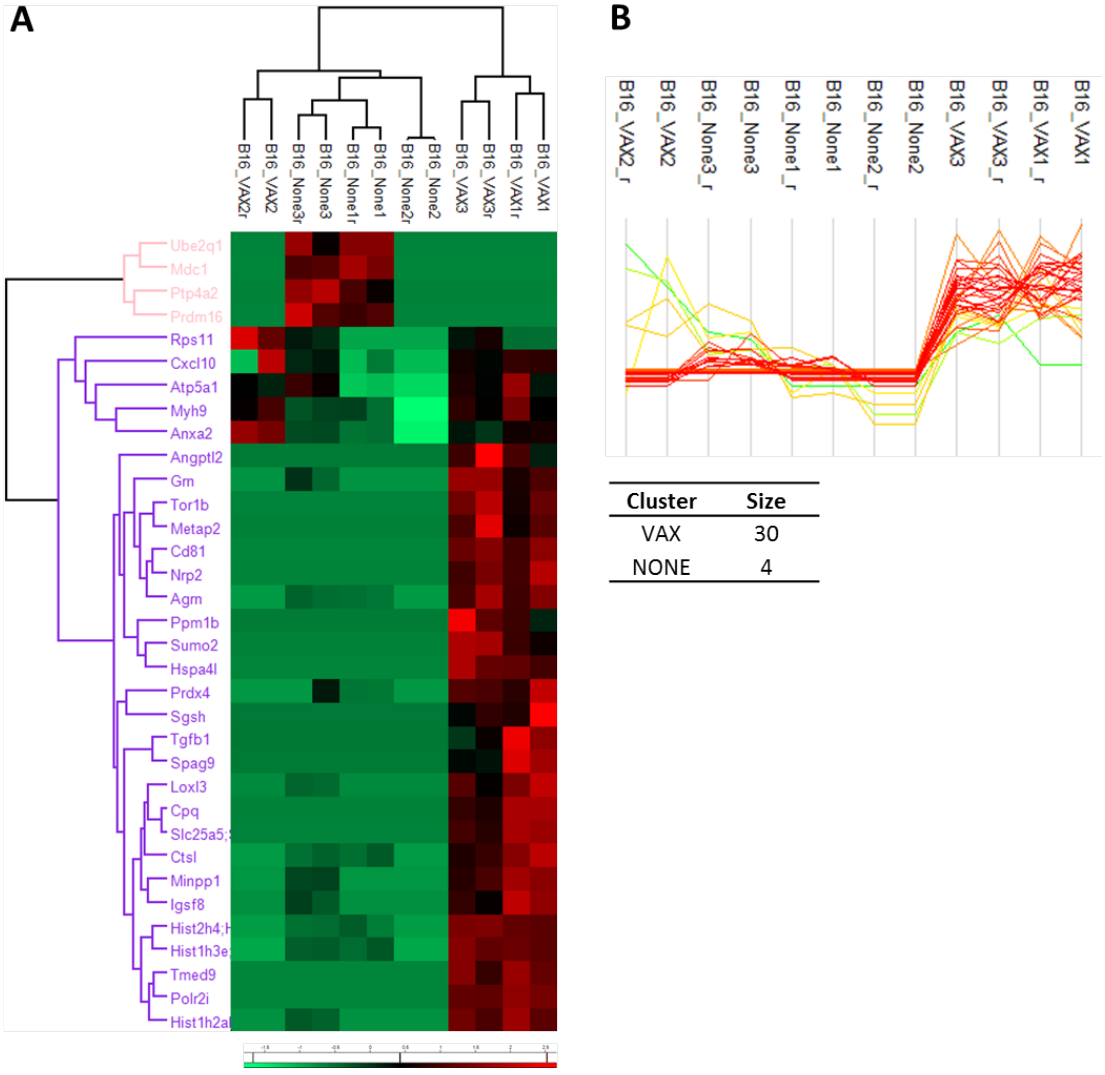

Figure 4-33. Profile of proteins overrepresented in supernatants derived from *Salmonella*-infected B16 melanoma cells. Protein content of supernatants of murine B16 melanoma cells were analyzed through nLC-ESI-MS^2 both control supernatants (None) and the ones derived from *Salmonella* treated melanoma cells (AT). Each supernatant was

analyzed in duplicate, identified as -r. A. HeatMap that shows 30 identified proteins significantly more abundant in AT-supernatants; analysis was performed with MaxQuant software on the identified proteins. *P <0.05. Red color: up-regulated. Green color: down-regulated B. Graph representing the distribution of the intensity of the 30 AT-specific proteins.

The proteins selected as specific of *Salmonella* stimuli are mainly associated to stress response (**Table 4-6**). Some proteins are involved in pathways activated by infection; the overrepresentation of pathways like Huntingon disease and Rheumatoid arthritis suggest that some proteins are involved in disfunctional intracellular acitvity: endocytosis, accumulation of unfolded proteins. Interestingly there is an enrichment of proteins involved in lysosome and the lysosomal degradation of glycoprotein. None of the proteins representative of *Salmonella* treatment was found by the peptidomic analysis done on the low molecular fraction discussed in **Chapter 4.4.2.2**. This suggests that peptides selected by the peptidomic study do not derive from the degradation of proteins inside cells supernatant.

KEGG 2016

Index	Name	P-value	Adjusted p-value	Z-score	Combined score
1	Malaria_Homo sapiens_hsa05144	0.002448	0.09636	-1.96	11.80
2	Huntington's disease_Homo sapiens_hsa05016	0.002965	0.09636	-1.88	10.92
3	Rheumatoid arthritis_Homo sapiens_hsa05323	0.008026	0.1739	-1.72	8.29
4	Lysosome_Homo sapiens_hsa04142	0.01458	0.2071	-1.70	7.18
5	Systemic lupus erythematosus_Homo sapiens_hsa05322	0.01739	0.2071	-1.65	6.67
6	Parkinson's disease_Homo sapiens_hsa05012	0.01912	0.2071	-1.65	6.52
7	Alcoholism_Homo sapiens_hsa05034	0.02941	0.2389	-1.73	6.09
8	Proteoglycans in cancer_Homo sapiens_hsa05205	0.03702	0.2545	-1.81	5.95
9	MAPK signaling pathway_Homo sapiens_hsa04010	0.05576	0.2545	-1.74	5.03
10	HTLV-I infection_Homo sapiens_hsa05166	0.05692	0.2545	-1.67	4.78

Reactome 2016

Index	Name	P-value	Adjusted p-value	Z-score	Combined score
1	Developmental Biology_Homo sapiens_R-HSA-1266738	0.0009560	0.05773	-2.37	16.46
2	HS-GAG degradation_Homo sapiens_R-HSA-2024096	0.0004487	0.05773	-2.13	16.41
3	Infectious disease_Homo sapiens_R-HSA-5663205	0.001727	0.05773	-2.36	15.01
4	Extracellular matrix organization_Homo sapiens_R-HSA-1474244	0.0008048	0.05773	-2.10	14.98
5	Influenza Infection_Homo sapiens_R-HSA-168254	0.001366	0.05773	-2.06	13.57
6	Disease_Homo sapiens_R-HSA-1643685	0.004143	0.08438	-2.30	12.64
7	Non-integrin membrane-ECM interactions_Homo sapiens_R-HSA-3000171	0.001804	0.05773	-1.99	12.57
8	Elastic fibre formation_Homo sapiens_R-HSA-1566948	0.001720	0.05773	-1.92	12.25
9	Assembly of collagen fibrils and other multimeric structures_Homo sapiens_R-HSA-2022090	0.002965	0.06887	-1.96	11.38
10	Heparan sulfate/heparin (HS-GAG) metabolism_Homo sapiens_R-HSA-1638091	0.002965	0.06887	-1.92	11.16

Table 4-6. Proteins overrepresented in supernatants of B16 cells treated with *Salmonella* are mainly involved in pathways activated in response to stress. Pathway knowledge analysis with KEGG and Reactome databases was done on the 30 proteins found specifically in *Salmonella*-derived cells' supernatants. Tab shows the statistically significant enriched pathways and the associated scores calculated by EnrichR tool.

4.4.3.2 Human patients-derived melanoma cells: protein analysis

Protein content of supernatants derived from primary patients-derived melanoma cells treated with *Salmonella* was analyzed and resulted clustering separately from proteins derived from untreated cells (**Figure 4-34**). The selected proteins are mainly involved in stress-response to infection, in metabolic dysfunctional pathway and in transcriptional misregulation (**Table 4-7**). Similar observations were done for the proteins analysis of mouse melanoma cells (**Table 4-6**), while at peptidomic level (**Chapter 4.4.2.3**), the significant peptides arising from the analysis were not overlapping with the proteins found in the high molecular weight fraction.

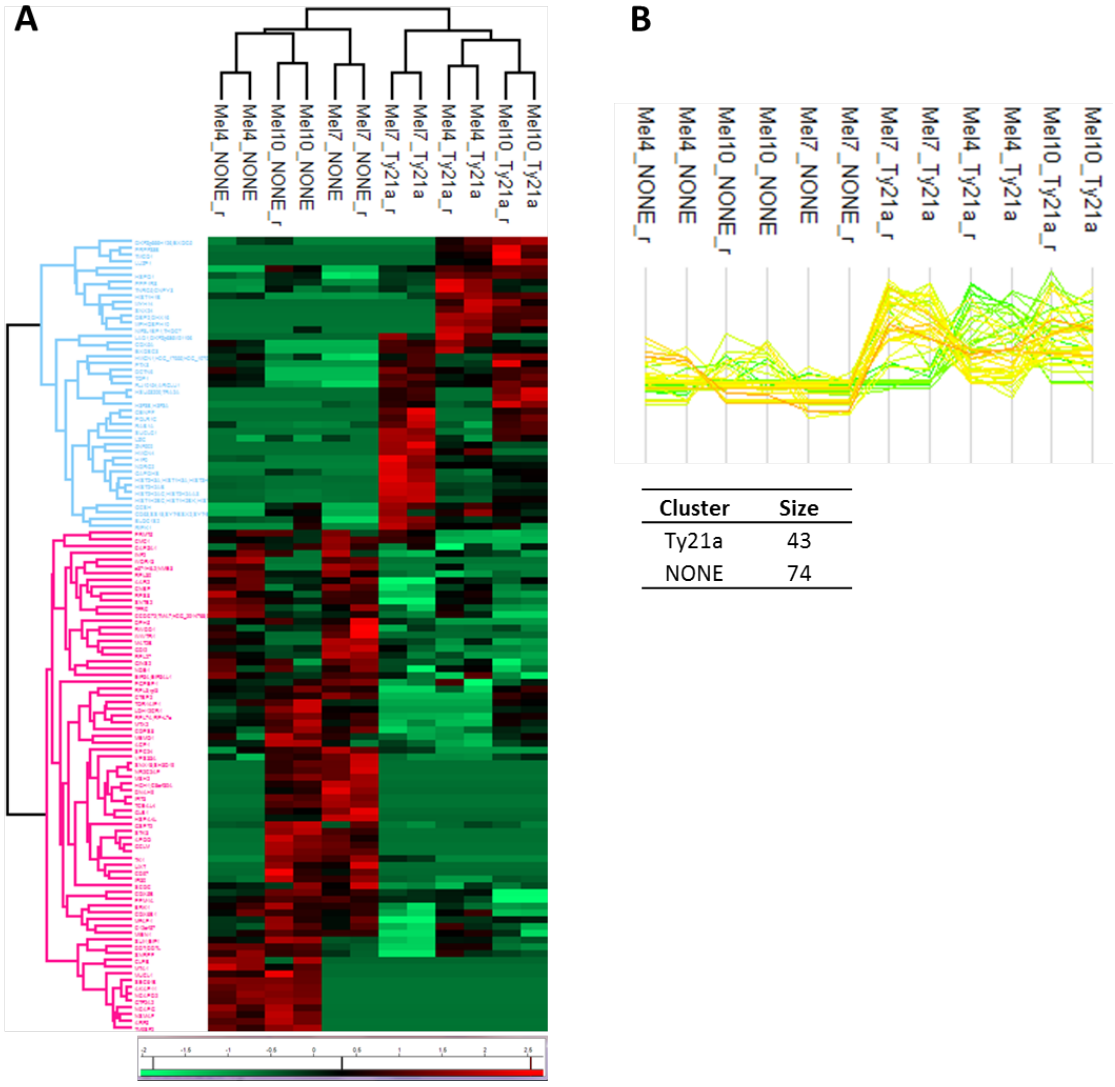

Figure 4-34. Profile of proteins overrepresented in supernatants derived from patients-melanoma cells infected with *Salmonella*. Protein content of supernatants of

human patient-derived melanoma cells were analyzed through nLC-ESI-MS^2 both control supernatants (None) and the ones derived from *Salmonella* treated melanoma cells (Ty21a). Each supernatant was analyzed in duplicate, identified as -r. A. HeatMap that shows 43 identified proteins significantly more abundant in Ty21a-supernatants; analysis was performed with MaxQuant software on the identified proteins. *P <0.05. Red color: up-regulated. Green color: down-regulated B. Graph representing the distribution of the intensity of the 43 Ty21a-specific proteins.

KEGG 2016

Index	Name	P-value	Adjusted p-value	Z-score	Combined score
1	Systemic lupus erythematosus_Homo sapiens_hsa05322	0.000008020	0.0003288	-1.75	20.50
2	Alcoholism_Homo sapiens_hsa05034	0.00003134	0.0006425	-1.88	19.47
3	Legionellosis_Homo sapiens_hsa05134	0.005684	0.07769	-1.84	9.49
4	Cytosolic DNA-sensing pathway_Homo sapiens_hsa04623	0.007628	0.07819	-1.63	7.94
5	RNA degradation_Homo sapiens_hsa03018	0.01089	0.08927	-1.74	7.88
6	Transcriptional misregulation in cancer_Homo sapiens_hsa05202	0.05254	0.2400	-1.63	4.81
7	Epstein-Barr virus infection_Homo sapiens_hsa05169	0.06438	0.2400	-1.70	4.67
8	RNA polymerase_Homo sapiens_hsa03020	0.06361	0.2400	-1.38	3.81
9	Metabolic pathways_Homo sapiens_hsa01100	0.1075	0.2939	-1.66	3.71
10	Propanoate metabolism_Homo sapiens_hsa00640	0.06361	0.2400	-1.24	3.42

Reactome 2016

Index	Name	P-value	Adjusted p-value	Z-score	Combined score
1	RNA Polymerase I Chain Elongation_Homo sapiens_R-HSA-73777	0.000005549	0.0002564	-2.07	24.99
2	DNA Damage/Telomere Stress Induced Senescence_Homo sapiens_R-HSA-2559586	0.000006375	0.0002564	-2.00	23.98
3	B-WICH complex positively regulates rRNA expression_Homo sapiens_R-HSA-5250924	0.000005951	0.0002564	-1.99	23.96
4	Cellular Senescence_Homo sapiens_R-HSA-2559583	0.00001883	0.0003492	-2.18	23.69
5	HDACs deacetylate histones_Homo sapiens_R-HSA-3214815	0.000006820	0.0002564	-1.98	23.52
6	RHO GTPases activate PKNs_Homo sapiens_R-HSA-5625740	0.000006820	0.0002564	-1.93	22.99
7	RNA Polymerase I Promoter Clearance_Homo sapiens_R-HSA-73854	0.00001752	0.0003492	-1.95	21.31
8	NoRC negatively regulates rRNA expression_Homo sapiens_R-HSA-427413	0.00001493	0.0003492	-1.89	20.98
9	RNA Polymerase I Transcription_Homo sapiens_R-HSA-73864	0.00002043	0.0003492	-1.93	20.88
10	Negative epigenetic regulation of rRNA expression_Homo sapiens_R-HSA-5250941	0.00001752	0.0003492	-1.87	20.49

Table 4-7. Proteins overrepresented in supernatant of patients-derived melanoma cells treated with *Salmonella* are mainly involved in pathways activated in response to stress. Pathway knowledge analysis with KEGG and Reactome databases was done on the 43 proteins found specifically in *Salmonella*-derived cells' supernatants. Tabs show the statistically significant enriched pathways and the associated scores calculated by EnrichR tool.

4.4.3.3 Dog-patient derived melanoma cells: protein analysis

Proteins overrepresented in supernatant derived from Dog-patient melanoma cells treated with *Salmonella* clustered well and separately from proteins found in supernatant of untreated cells (**Figure 4-35**). 467 proteins were defined specific of samples derived from *Salmonella* treatment and, as we observed analyzing proteins derived from mouse and human samples, proteins were enriched for pathways associated to stress-response to infection and metabolic dysfunctional pathways. In addition to what we observed with the analysis of mouse and human samples, some proteins found in dog samples are involved in protein translation (spliceosome and ribosome) and protein processing inside the endoplasmic reticulum (**Table 4-8**). 5 proteins were found to overlap with the peptidomic analysis: Semaphorin3G, HistonH3, Tubulin-α-chain, Ribosomal protein P0, Serum amyloid A protein. The peptides belonging to these five proteins that have been found by the peptidomic analysis, might be the results of protein degradation.

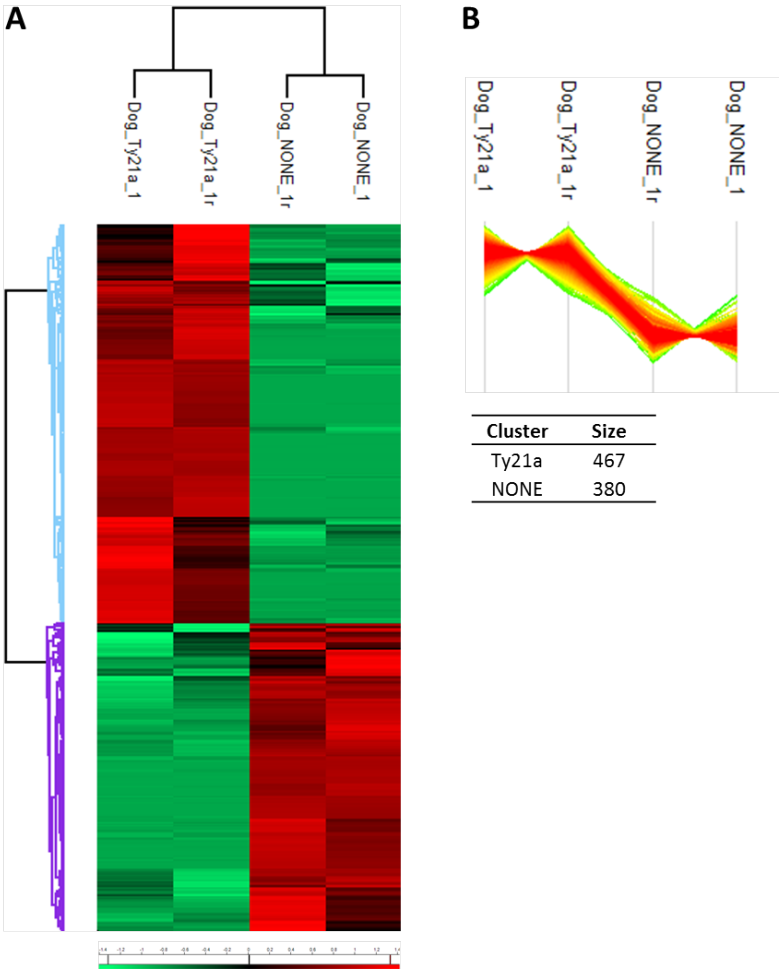

Figure 4-35. Profile of proteins overrepresented in supernatants derived from dog patient-derived melanoma cells infected with *Salmonella*. Protein content of supernatants of dog patient-derived melanoma cells were analyzed through nLC-MS both control supernatants (None) and the ones derived from *Salmonella* treated melanoma cells (Ty21a). Each supernatant was analyzed in duplicate, identified as -r. **A**. HeatMap that shows 467 identified proteins significantly more abundant in Ty21a-supernatants; analysis were performed with MaxQuant software on the identified proteins. *P <0.05. Red color: up-regulated. Green color: down-regulated B. Graph representing the distribution of the intensity of the 467 Ty21a-specific proteins.

KEGG 2016

Index	Name	P-value	Adjusted p-value	Z-score	Combined score
1	Spliceosome_Homo sapiens_hsa03040	1.266e-14	2.989e-12	-1.80	57.49
2	Proteasome_Homo sapiens_hsa03050	9.740e-11	1.149e-8	-1.69	38.90
3	Endocytosis_Homo sapiens_hsa04144	0.00001427	0.001069	-1.91	21.34
4	Protein processing in endoplasmic reticulum_Homo sapiens_hsa04141	0.00001858	0.001069	-1.74	18.98
5	RNA transport_Homo sapiens_hsa03013	0.00002264	0.001069	-1.77	18.93
6	Metabolic pathways_Homo sapiens_hsa01100	0.0004302	0.01258	-1.86	14.44
7	Pyruvate metabolism_Homo sapiens_hsa00620	0.0001996	0.007850	-1.66	14.15
8	Regulation of actin cytoskeleton_Homo sapiens_hsa04810	0.0007903	0.01696	-1.67	11.95
9	Shigellosis_Homo sapiens_hsa05131	0.0004875	0.01258	-1.49	11.36
10	Salmonella infection_Homo sapiens_hsa05132	0.0005331	0.01258	-1.46	10.98

Reactome 2016

Index	Name	P-value	Adjusted p-value	Z-score	Combined score
1	Processing of Capped Intron-Containing Pre-mRNA_Homo sapiens_R-HSA-72203	9.188e-14	7.865e-11	-2.16	64.78
2	AUF1 (hnRNP D0) binds and destabilizes mRNA_Homo sapiens_R-HSA-450408	3.167e-13	1.355e-10	-2.17	62.51
3	Cell Cycle, Mitotic_Homo sapiens_R-HSA-69278	3.107e-11	3.655e-9	-2.43	58.84
4	Metabolism of proteins_Homo sapiens_R-HSA-392499	3.844e-12	1.097e-9	-2.14	56.14
5	Host Interactions of HIV factors_Homo sapiens_R-HSA-162909	4.269e-11	3.655e-9	-2.20	52.47
6	Regulation of activated PAK-2p34 by proteasome mediated degradation_Homo sapiens_R-HSA-211733	2.345e-11	3.655e-9	-2.10	51.43
7	Regulation of Apoptosis_Homo sapiens_R-HSA-169911	3.107e-11	3.655e-9	-2.11	51.11
8	Regulation of mRNA stability by proteins that bind AU-rich elements_Homo sapiens_R-HSA-450531	3.991e-11	3.655e-9	-2.10	50.25
9	Hh mutants that don't undergo autocatalytic processing are degraded by ERAD_Homo sapiens_R-HSA-5362768	1.152e-10	7.588e-9	-2.18	49.82
10	mRNA Splicing - Major Pathway_Homo sapiens_R-HSA-72163	1.016e-11	2.175e-9	-1.96	49.72

Table 4-8. Proteins overrepresented in supernatant of dog melanoma cells treated with *Salmonella* are mainly involved in pathways activated in response to stress. Pathway knowledge analysis with KEGG and Reactome databases was done on the 467 proteins found specifically in *Salmonella*-derived cells' supernantants. Tabs show the statistically significant enriched pathways and the associated scores calculated by EnrichR tool.

4.5 Annex

4.5.1 Assessment of OVA-peptides inside supernatants derived from *Salmonella* treatment of B16-OVA cells: samples preparation optimization.

In order to analyze by mass spectrometry the supernata nts derived from *Salmonella* treated B16-OVA cells to detect OVA peptides we had to find a suitable protocol. Importantly we had to find the way to remove salts that could interfere with mass spectrometry analysis and to concentrate peptides instead of proteins in order to increase the probability to detect $OVA_{257-264}$ among all the released peptides. For these purposes, we loaded a precise volume of medium derived from untreated cells with 20ug $OVA_{257-264}$ and tested two different peptide-enrichment protocols (**Figure 4-36**). The first strategy was based on chemical precipitation of protein (TCA-mediated), while the second was based on protein exclusion by size (using Centricon device). Following this step of peptide-enrichment, desalting and fractionation procedures were performed through the use of Sep-Pak C18, a silica-based bonded phase with strong hydrophobicity. Fractions were obtained by eluting peptides with an increasing percentage of Acetonitrile solution (5% 10% 20% 50% 80%) and peptides-enrichment efficiency was evaluated by MS. As shown by MALDI spectra of two of the derived Acetonitrile-fractions (**Figure 4-37**), samples obtained by TCA-mediated procedure were characterized by a higher number of signals. Moreover, the MS signal associated to $OVA_{257-264}$ (m/z=963,5) obtained by the TCA-mediated protocol was more intense than the one obtained by Centricon-based procedure (**Figure 4-37**). In agreement with these observations, DCs loaded with TCA-derived fractions induced a stronger activation of $CD8^+$-OTI lymphocytes (**Figure 4-38**), leading them to produce IFN-γ. On the basis of all these results we selected the TCA-mediated protocol to proceed with the analysis.

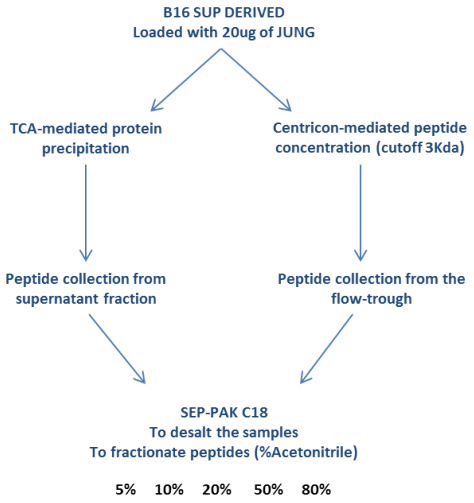

Figure 4-36. Pipeline of the strategy followed to optimize the analysis of B16-OVA-derived supernatant. Two different protocol for peptides enrichment were assessed: either a Centricon-mediated or a TCA-mediated. Following peptides' concentration step, required to favour OVA-peptides detection, salts removal and fractionation of the peptides based on different percentages of acetonitrile were performed using Sep-Pak C18 device.

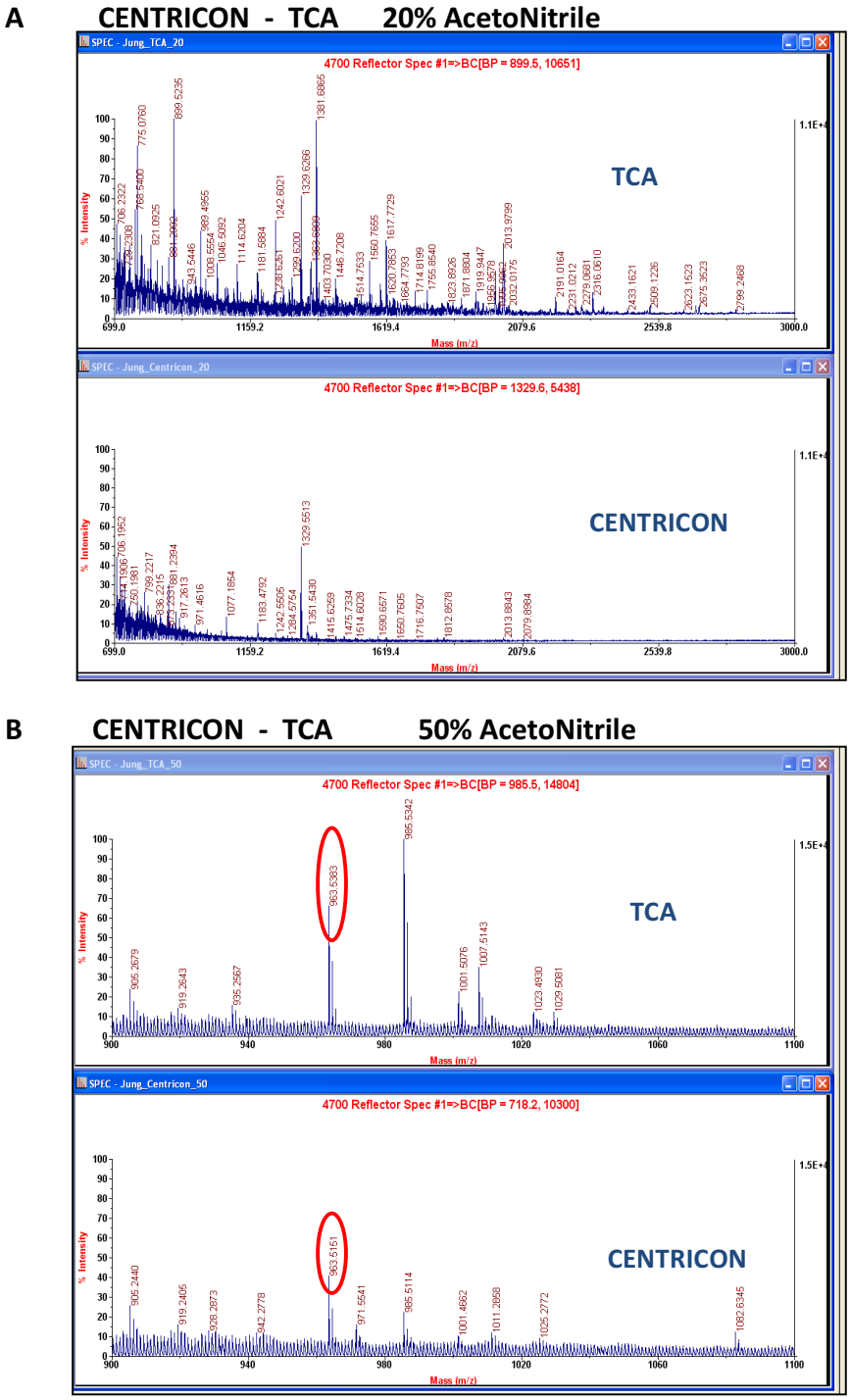

Figure 4-374. A TCA-based protocol performed to enrich peptides is more efficient than a Centricon-based protocol. With the aim to concentrate peptides starting from the supernatant of cells-treated with *Salmonella*, two different strategies were assessed. Peptides were enriched either by a TCA-based protocol, through which protein were precipitated incubating sample over night with a 13% of cold TCA, or by size exclusion with a Centicon cut-off 10KDa. The two differently obtained samples were then loaded on SepPakC18 to be desalted and fractionated with different percentages of Acetonitrile.

Fractions derived from elution with 20% and 50% acetonitrile solution were crystallized on alpha-ciano-hydroxycinnamic acid matrix and analyzed by MALDI. $OVA_{257-264}$ (m/z=963,5) peptide is marked with a red circle.

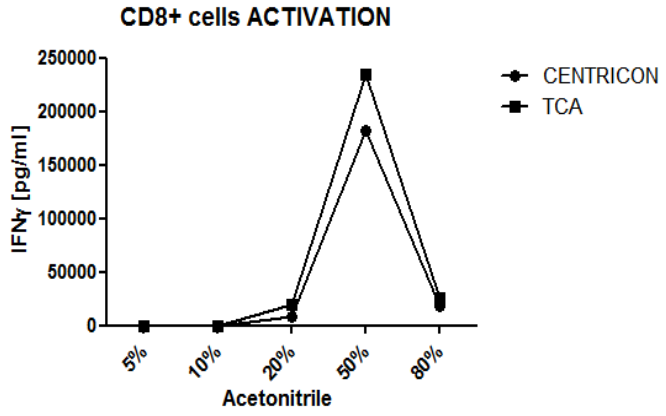

Figure 4-38 A TCA-based protocol performed to enrich peptides is more efficient than a Centricon-based protocol. With the aim to concentrate peptides starting from the supernatant of cells-treated with *Salmonella*, two different strategies were assessed. The first strategy is based on chemical precipitation of protein (TCA-mediated) while the second is based on protein exclusion by size (Centricon device). Following peptide-enrichment, both desalting and fractionation procedures were performed by the use of Sep-Pak C18. All the derived fractions were loaded on murine DCs for 4 hours and then cells were co-cultured with $CD8^+$lymphocytes isolated by the spleen of OTI mice. Following 72 hours lymphocytes activation was assessed measuring IFN-ɣ release by ELISA.

4.5.2 Assessment of *Salmonella*-derived supernatant composition by mass spectrometry approaches: samples overview by MALDI and SACI-ESI-MS.

The MS-based peptidomic study to identify antigens released by *Salmonella* treated tumor cells (**Chapter 4.4**) was preceded by an overall characterization of the samples' composition. An aliquot of them was dedicated to a SACI/ESI-MS analysis (Albini et al. 2015) (**Chapter 3.14.3**). Since sample ionization is obtained at a low voltage, the observed chemical noise was low (gaining in sensitivity) and we could detect a wide m/z range (low, medium, and high molecular weight compounds). As shown in **Figure 4-39**, the profile of the supernatant derived from *Salmonella*-treated tumor cells (B16 Vax) was largely

different from the profile of the supernatant of untreated cells (B16 NONE). B16 Vax samples are enriched in signals associated to multi-polimers and peptides, approximately 90% of the detectable. The remaining 10% is associated to lipids suggesting that lipids might contribute to the antitumoral effect of the vaccine either being a source of lipid-antigens or exerting an adjuvant effect. B16 NONE samples are instead characterized by signals of low intensity distributed all along the m/z.

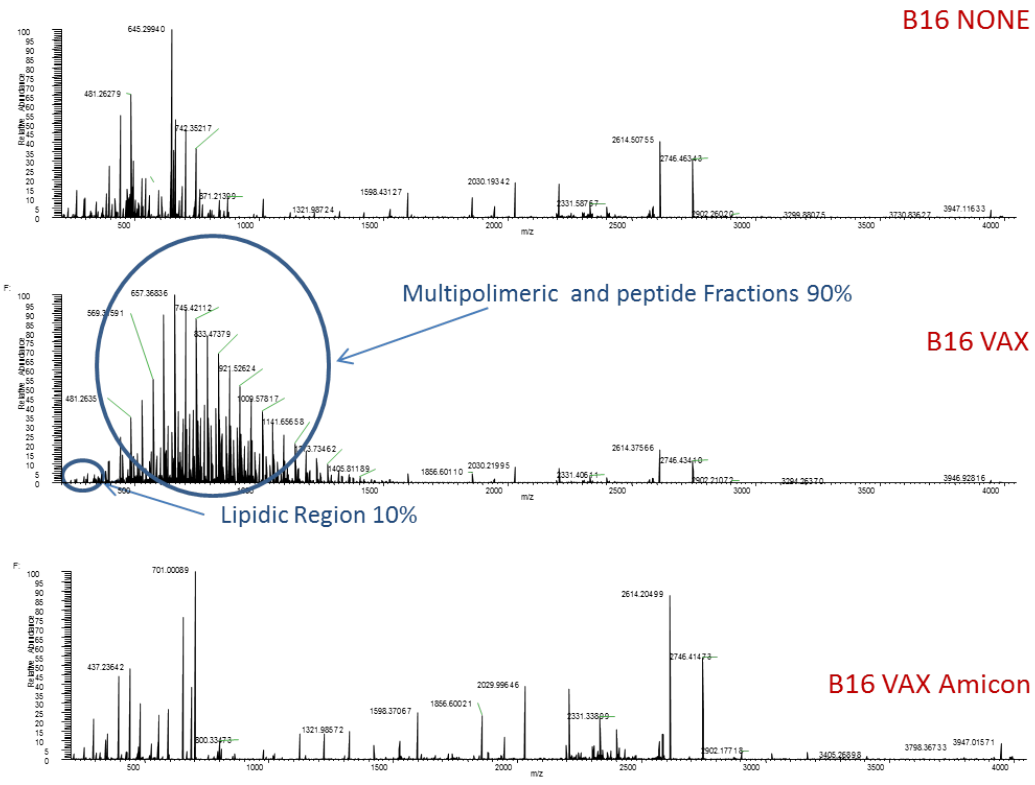

Figure 4-39 Supernatant derived from *Salmonella*-treated B16 cells have a unique profile in term of Lipid-polimer and peptide composition detected by SACI-ESI-MS. Supernatants derived from *Salmonella*-treated B16 cells (B16 Vax), by untreated cells (B16 NONE) and by B16 Vax after FASP procedure were analysed by SACI-ESI-MS.

With the perspective to perform a peptidomic analysis (**Chapter 4.4**), being aware of the complex composition of the *Salmonella* derived supernatants, we decided to process samples by a 10KDa centrifugation filter (Filter aided sample preparation, FASP) in order to separate high from low molecular weight peptides to then proceed by nLC-ESI-MS^2 of

both fractions (as explained in the pipeline **Figure 4-18**). MALDI spectra show the complexity of the samples along the applied procedure (**Figure 4-40**). Sinapinic acid matrix, that favours proteins crystallization instead of peptides crystallization, highlighted the efficiency of protein removal exerted by FASP device since nearly to zero proteins were detected inside B16 Vax FASP sample compared to both B16 NONE and B16 VAX samples (**Figure 4-40A**). At the opposite, alpha-ciano-hydroxycinnamic acid matrix that favors the crystallization of low molecular weight proteins showed that peptides inside FASP-derived samples were abundant and possibly detected even at higher resolution if compared with peptides acquired on the same matrix from the initial and unprocessed supernatant (either B16 Vax and B16 NONE samples) (**Figure 4-40B**). FASP-derived samples were also analysed by SACI-ESI-MS. FASP allow to have multipolimeres removed in favour of peptides signals (**Figure 4-40**).

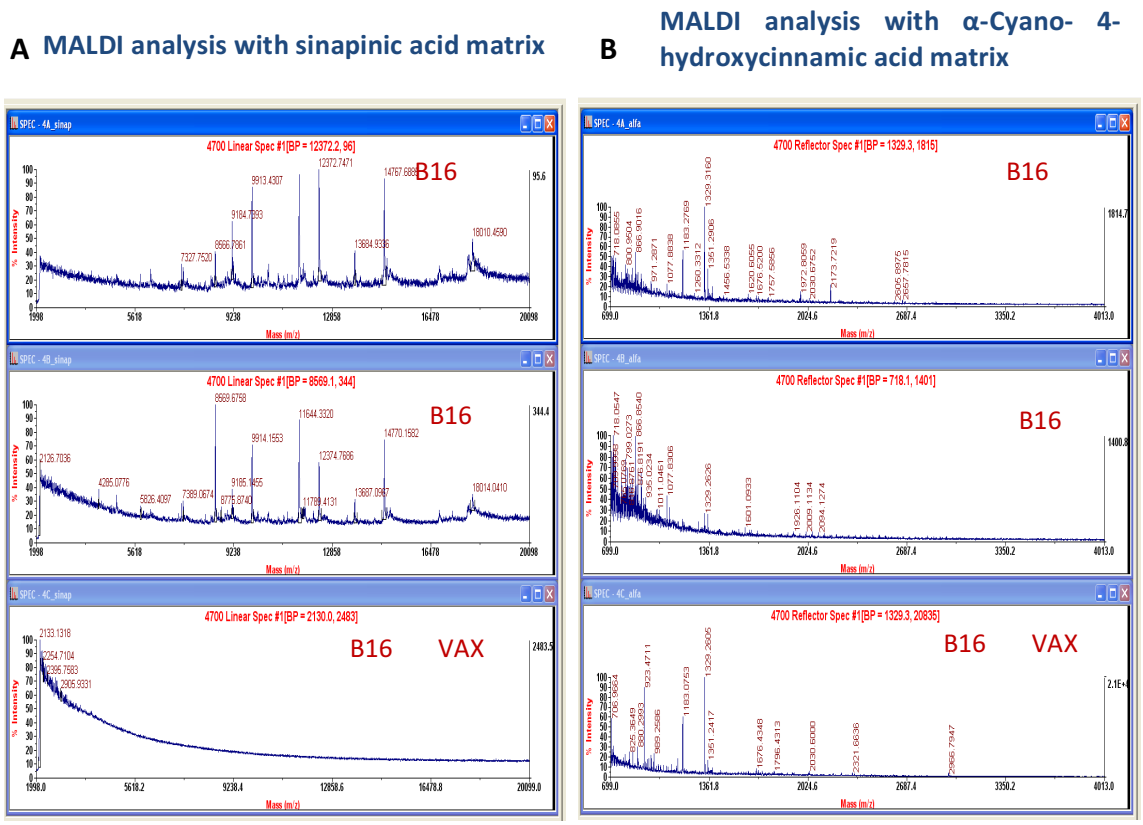

Figure 4-40 Supernatant derived from *Salmonella* treated B16 cells are enriched in peptides. Protein composition of supernatant derived from *Salmonella* treated or untreated B16 cells was assessed before and after being processed on FASP devices (cut-off 10KDa).

Samples were crystalized either on sinapinic acid matrix (A) or on alpha-ciano-hydroxycinnamic acid matrix (B) and then acquired by MALDI-TOF.

4.5.3 Lipids released by murine melanoma B16 cells upon *Salmonella* infection can activate iNKT cells

Mass spectrometry analysis of supernatants derived from *Salmonella* infected B16 cells revealed the presence of lipids (**Figure 4-39**). Sep-pak C18 device used to concentrate peptides before proceeding with mice immunization enables to remove salts but is conservative with lipids. Invariant NK-T cells activation is based on the recognition of specific lipids by the CD1d invariant receptor (Brennan et al. 2013). Upon activation iNKT cells produce IL2 and can mediate a cytotoxic response. Taking advantage of a murine hybridoma (generated by the fusion of a iNKT cell with a thymoma (Schümann et al. 2007)), we tested whether the supernatants derived from *Salmonella* infected tumor cells were able to stimulate iNKT activation. We generated dendritic cells from the bone marrow of wild type C57J/BL6 mice (BMDCs), we loaded them with cell's supernatant either derived following *Salmonella* infection (B16 VAX) or by untreated cells (B16 NONE), and we then added iNKT-hybridoma to the culture. B16 NONE supernatant didn't have any effect on iNKT hybridoma cells since the IL2 production was the same as the one associated to the negative control (consisting of iNKT incubated with BMDCs without stimuli). VAX samples instead were able to stimulate a mild but significant IL2 production by iNKT hybridoma cells (**Figure 4-41**) indicating that iNKT activation might be also induced in vivo and iNKT cells might be involved in the antitumor response. IL2 release following αGal stimulation was monitored as a positive control.

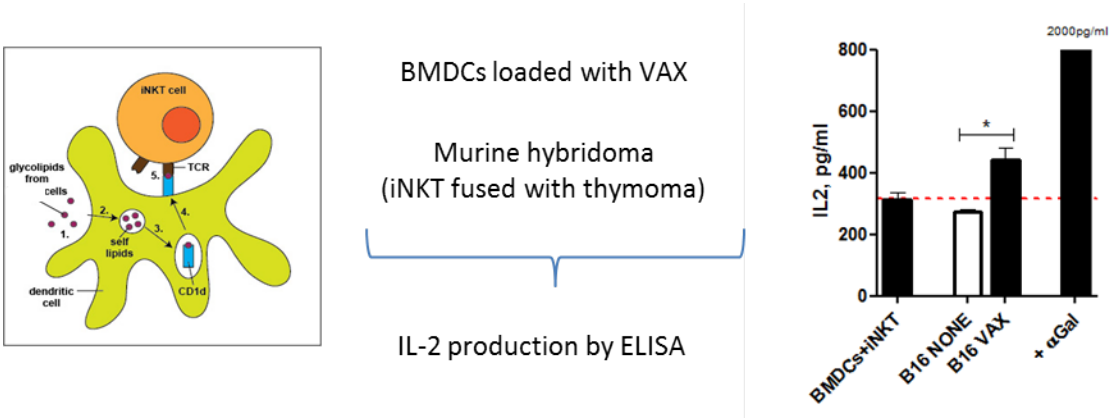

Figure 4-41. Supernatants-derived from murine melanoma cells treated with *Salmonella* can activate iNKT cells. iNKT hybridoma cells were cocultured with bone marrow derived dendritic cells (BMDCs) in presence of different stimuli: supernatant derived from untreated cells (B16 NONE), supernatant derived from *Salmonella* treated B16 cells (B16 Vax), αGal, or left un-stimulated (BMDCs+iNKT). After 48hours IL-2 production was assessed by ELISA. (The Student's t-test was used for statistical analysis *p=0,0285*).

5. DISCUSSION

In this work we provide evidence that *Salmonella* infection of tumor cells promotes the release of antigens that, once administered with selected adjuvant following a prophylactic schedule, induced an antitumor response either in a mouse model of non-immunogenic melanoma B16, or in dog patients suffering from spontaneous osteosarcoma or high grade sarcoma. We also proposed a novel mass-spectrometry based approach that enables to identify the sequence of neoantigens and spliced tumor antigens that otherwise wouldn't be accessible.

Starting from a previous finding of the laboratory by Saccheri and colleagues (Saccheri et al. 2010) that showed that *Salmonella* infection of mouse melanoma cells promoted a gap junction mediated transfer of immunogenic peptides from tumor cells toward dendritic cells, we proved that the same *Salmonella* stimulus induced both murine and human cell lines to release peptides in the extracellular space through plasma membrane hemichannels. If the ATP assay allowed us to verify that *Salmonella* promoted the opening of hemichannels of murine cells, by the T2 binding assay, frequently used to validate the antigenicity of peptides, we demonstrated that peptides released by *Salmonella*-infected human melanoma cells are of the correct size to be loaded on HLA molecules and hence are potential antigens. Moreover, peptide release is hemichannel-dependent as it is completely blocked by heptanol, a hemichannel blocker.

Furthermore, taking advantage of a well-established murine cell model to monitor antigen processing, B16OVA, we showed that among the peptides released by tumor cells upon *Salmonella* infection some were well-described antigens. Indeed B16OVA cells released the most immunogenic ovalbumine-derived class I peptide, $OVA_{257-264}$.

All these compelling evidence about the presence of antigens inside the supernatant of tumor cells treated with *Salmonella* lead us to assess their immunogenicity in a preclinical model of melanoma. Mice vaccinated three times with LPS-activated DCs loaded with

peptides released by B16 cells treated with *Salmonella* had a longer overall survival than mice vaccinated with unloaded DCs. Furthermore DCs loaded with the mixture of peptides released by B16 cells upon *Salmonella* stimulus had a stronger effect than DCs loaded with two B16-tumor antigens $Trp2_{180\text{-}188}$ $gp100_{25\text{-}33}$ showing that our vaccine formulation possibly contains antigens more immunogenic than $Trp2_{180\text{-}188}$ and $gp100_{25\text{-}33}$. Our results are promising considering that B16 cells are poorly immunogenic; although 180 druggable mutations have been estimated by the B16-mutanome study of Castle and colleagues (Castle et al. 2012), mice immunized with irradiated tumor cells are not protected from a subsequent challenge with B16 cells (Dranoff et al. 1993); this is mainly due to the fact that this melanoma cell line expresses MHC class I very poorly and do not express MHC class II (Seliger et al. 2001; Overwijk & Restifo 2001). Of notice, Schreus and colleagues were instead able to obtain a partial but consistent mice survival vaccinating them with DC loaded with Trp2 (Schreurs et al. 2000); the shorter schedule adopted, meaning the time in between immunization and B16 challenge, together with the higher number of DC used for the immunization procedures may have favored the induction of a protective immune response. From an immunologic standpoint, DC-based immunotherapy carries the highest potential of inducing effective anticancer immune responses as it provides cytokines and co-stimulatory molecules necessary to activate naïve-T cell in an antigen specific manner. Nevertheless, one major drawback of DC-based approaches is that, once applied in the clinics for therapeutic purposes, they require leukapheresis, processing and culturing of peripheral PBMCs, therefore allowing a limited number of vaccinations and long preparation time. Improvement for patients has been achieved through the use of therapeutic DC-based vaccines as recently reported by Gross and colleagues (Gross et al. 2017) but, since they rely on patient-derived DCs they imply high costs for a not shareable procedure. To set us as close as possible to a feasible and less demanding clinical setting and aiming to provide a vaccine with neoantigens shared among patients, we conjugated

peptides released by *Salmonella* treated B16 cells with adjuvants and assessed them as DC-free vaccines.

Incomplete Freud Adjuvant (IFA)-based vaccines are water-in-oil emulsions of antigen in mineral oil and mannide monooleate as a surfactant; IFA is thought to induce local inflammation and forms a depot that protects antigen from degradation and slowly releases it to antigen presenting cells (Aucouturier et al. 2002). Its safety has been early clarified by Rosenberg studies (Rosenberg et al. 1998) while its adjuvant efficacy has been debated. Haileilmichaeil and colleagues showed that IFA-based vaccination turns the vaccination site into a persistent source of T cell priming thus preventing their tumor localization while causing their dysfunction and deletion (Hailemichael et al. 2013). On the contrary Kenter and colleagues showed that synthetic long peptides combined with IFA, specifically Montanide 51, gave clinical benefits to patients affected by Vulvar Intraepithelial Neoplasia (VIN) (Kenter et al. 2009). To overcome any possible drawback related to IFA it has been proposed to administer the emulsion of peptides together with a TLR-agonist as CpG (TLR-9 agonist, (Speiser et al. 2005)) or poly (I:C) (TLR-3 agonist, (Sabbatini et al. 2012) or with CpG and Imiquimod (TLR-9 and TLR-7 agonists, (Goldinger et al. 2012)). We chose to administer peptides in emulsion with IFA together with the Imiquimod and, separately, to assess peptides immunogenicity in solution with CpG ODN 1826 alone. Peptides in emulsion with the IFA and a subsequent stimulation with Aldara cream (Imiquimod) induced an ample antitumor response and mice showed a peptide-dose dependent benefit in terms of overall survival. A significant retardation of tumor growth together with an ameliorated overall survival was also observed immunizing mice with peptides released by *Salmonella*-treated B16 cells combined with CpG ODN 1826, a TLR-9 agonist. The two chosen adjuvants were able to induce an immune response of similar amplitude in terms of both tumor growth retardation and overall survival. Moreover they were as efficient as DCs in boosting the antitumor response thus indicating that DCs as

adjuvants are not an advantage. We obtained following both procedures significant positive results but further investigations are needed to decipher whether different immune cell populations were activated by the two adjuvant formulations. Possibly, we could further enhance vaccine effect combining peptides with all the three adjuvants together; indeed the percentage of central memory T cells responsible of a long term immune response (Hendriks et al. 2000) have been shown to be further augmented in patients, combing IFA with CpG and Imiquimod (Goldinger et al. 2012).

All of the therapeutic vaccinations we performed, either DC-dependent or DC-free, although increasing the survival time against B16 melanoma, did not guarantee a complete tumor rejection and all animals ultimately succumbed to the disease. As discussed earlier, this could be due to the low immunogenicity of B16 cells but also to the rapid growth of this tumor cell line which possibly did not allow for a time sufficient to generate an effective immune response; moreover the induction of anergy or other immune escape/suppressor mechanisms cannot be excluded. As it happens during melanoma progression in humans, PDL-1 is overexpressed by B16 cells during tumor growth (Kleffel et al. 2015) leading to anergic tumor infiltrating lymphocytes; on the contrary, differently from human melanoma, B16 cells however, do not respond to checkpoint blockade (Twyman-Saint Victor et al. 2015), either to a single antibody treatment (CTLA-4, PD-1, PDL-1) or to a combinatorial use of these antibodies. It has been shown instead that coupling radiotherapy to CTLA-4 and PD-1 monoclonal antibodies lead to 80% of mice survival (Twyman-Saint Victor et al. 2015) proving that MHC-class I down regulation, reverted by radiotherapy, is the other tumor-escape mechanism, not less relevant than T cell effectors anergy, that needs to be considered once designing a novel immunotherapy approach. In light of the above considerations, the B16 tumor retardation we observed by vaccinating mice with only one type of adjuvant, is significant and might be further

augmented adding both checkpoint blockade to unleash T cells responses and radiotherapy to induce MHC class I expression.

The immunogenicity of peptides released by tumor cells upon *Salmonella* infection was further demonstrated in the human system, by their ability to induce the expansion of tumor specific $CD8^+$ T cells from healthy donor peripheral blood mononuclear cells (PBMCs). Peptides extracellularly released by the human melanoma cell line 62438 induced $CD8^+$ lymphocytes that responded to the tumor of origin, in an HLA-dependent manner both producing IFN-γ and recruiting the degranulation marker CD107a at the cell membrane; in addition, the expanded lymphocyte population killed 62438 cells in an HLA-dependent manner. These results showed not only that peptides released by 62438 cells upon *Salmonella* infection are antigenic but also that healthy patients have circulating lymphocytes that recognize them and expand upon few rounds of stimulation. One among all of the antigens expressed by 62438 melanoma cell line in association with the HLA-class I molecules is Mart-1, also known as Melan-A. Mart-1 is one of the first melanoma tumor antigens described (Kawakami et al. 1994) and is a melanocyte specific melanosomal protein. As high frequency of Mart-1 specific $CD8^+$ circulating T lymphocytes have been described in healthy donors (Pittet et al. 1999) we used this melanoma antigen as positive control for $CD8^+$ lymphocyte expansion. Mart-1 stimulus gave rise to expansion of tumor-specific lymphocytes that were much more activated in response to tumor cells than lymphocytes expanded by tumor-released peptides, following our approach. This might be due to the heterogeneity of lymphocyte clones stimulated by the multiplicity of peptides derived from the treatment of 62438 cells with *Salmonella*. We possibly expanded several antigens-specific lymphocytes that in response to tumor cells competed between each other resulting in an HLA-dependent activation of lower amplitude than the activation of Mart-1 specific lymphocytes. To ultimately assess the tumor-specific-killing ability of the expanded lymphocytes it would be informative to test

them *in vivo*. A possibility is to challenge immune-reconstituted NSG mice (by healthy human PBMCs) with 62438 cells and to test the capacity of adoptively transferred *ex vivo* peptides-expanded-T lymphocytes to counteract tumor growth. As we had the opportunity to receive tumor biopsies of three different melanoma patients from which melanoma cell lines were derived we could perform the same flow of experiments with patients-derived melanoma cells. The results that would be obtained with these primary cells could be relevant to further sustain the translational potential of our immunotherapy strategy.

The collaboration with a veterinary hospital allowed us to verify the feasibility of the immunotherapy approach we are proposing. Osteosarcoma (OSA) and high grade sarcoma (SA) are a two unmet medical needs in veterinary medicine and the same is true for the human tumor counterpart (Mirabello et al. 2009; Bray 2016). As both tumors similarly develop in human and dogs we were further encouraged to assess vaccine effect on dog patients. The main cause of death is tumor metastases in secondary organs; in particular, for osteosarcoma patients, metastases occur mostly in the lung and it has been shown that micrometastasic disease is likely present in approximately 80% of the patients at diagnosis (V.Griend et al, 1996). Cancer vaccine administration soon after surgical intervention was curative for 2 out of 13 patients enrolled; OSA0 affected by osteosarcoma was immunized with an heterologous vaccine and lived more than 600 days after diagnosis while SA5, a high grade sarcoma patient was immunized with an autologous vaccine and is still alive after more than 1400 days from diagnosis. OSA0 was vaccinated with peptides released by the tumor cell line of a second OSA patient due to the non-availability of its own primary tumor cells; the benefit that OSA0 had in terms of overall survival, suggests the presence of shared tumor antigens inside the heterologous administered vaccine and the possibility to develop a universal OSA vaccine. Unfortunately, we did not succeed to stably grow OSA-donor's cells *in vitro* thus the immune-monitoring was possible only for SA5. T-lymphocytes able to produce IFN-γ and CD107 upon tumor stimulation were detected in

peripheral blood of SA5 demonstrating that the vaccine formulation boosted an immune response which was both CD8 and CD4 T cell-mediated. Accordingly, a tumor specific humoral response was detected in SA5 sera and it increased along the immunization schedule. Three patients are still under vaccination, six died before completing the vaccination because of a highly aggressive disease progression, while other four patients completed the vaccination but died without improvement of the overall survival. We have not yet clarified whether the latter four patients developed an antitumor response although they did not benefit of a longer overall survival. The assessment of tumor specific-antibodies in the sera of patients or the responsiveness of PB-lymphocytes upon tumor stimulation will indicate if vaccine was immunogenic but other factors, such as immune escape strategies, interfered with an effective antitumor response. The results of the clinical trial showed a high variability in individual responses to treatments. The choice of not restricting to a narrow, homogenous sample of patients might have contributed to the observed variability. However, we had the striking indication that at least in two cases an antitumor response was induced by the vaccine and that both autologous and heterologous settings are feasible and can be successful.

Reports of successful cancer vaccine therapies have been recently published. Gross and colleagues reported that 19% of nonresectable metastatic melanoma patients that underwent intradermal autologous vaccination with DCs loaded with 4 HLA class I and 6 class II-restricted tumor peptides over two years (Gross et al. 2017) were still alive after 11 years; a result similar to what was observed treating patients with Ipilimumab. A second report, although it dealt with only six high risk melanoma patients, conveyed that vaccination with clinical grade long peptides (SLP) targeting up to 20 neoantigens per patient was feasible, safe and a successful strategy (Ott et al. 2017). Ott and colleagues reported that four out of six patients were disease-free after 25 months while two patients with recurrent disease that were subsequently treated with anti PD-1 experienced complete

tumor protection. This evidence, together with the results of preclinical studies (Yadav et al. 2014; Kreiter et al. 2015), renovated the interest toward cancer vaccines whose potential was underestimated following the discovery of immunocheckpoint blockade and the failures of clinical trials involving vaccines. Together with what we are proposing with our immunotherapy strategy, the novelty of these successful approaches is that they rely on the induction of an antitumor response directed against neoantigens.

Neoantigens, due to a different sequence from self-peptides, minimize immune tolerance thus becoming the best-choice target for an effective antitumor response. Importantly, we set up a mass-spectrometry (MS) method that will enable us the identification not only of neoantigens but also of tumor specific spliced-peptides. Spliced peptides are a recently discovered category of antigens generated by the post translational ligation of two non-adjacent peptides of a parental protein, mediated by the proteasome. Proteasome catalyzed-peptides splicing occurs more frequently than expected (Liepe et al. 2016) and nowadays compelling evidence showed that spliced peptides are often targeted by T lymphocytes both in response to bacterial infection (Platteel et al. 2017) and to mediate an antitumor response being recognized as tumor antigens (Vigneron et al. 2004; Ebstein et al. 2016). Although they have been identified for the first time in 2004 as target of patients-derived tumor infiltrating lymphocytes, their subsequent discovery has been limited by the lack of tools. Their identification was possible only tailoring the phase of database searching of MS analysis on customized databases of peptides in which all the possible spliced peptides (predicted in silico following criteria that limited the number of all the theoretically possible spliced-peptides) were included (Liepe et al. 2016). Reasonably the efficacy of these pioneering methods are limited both to the size and to the accuracy of customized databases; for example trans-spliced peptides cannot be identified. By our proposed MS-approach, combining the analysis by classical database searching engine with the analysis of the features at MS1-level, we gained knowledge of peptides that otherwise would not be

accessible. We used XCMS software (Tautenhahn et al. 2012) to determine the MS1-features whose levels were significantly higher in supernatants derived from *Salmonella*-treated tumor cells compared with supernatants of untreated tumor cells. Then, overlapping the selected MS1 features with the MS2 scan we obtained a list of features that were not identified by common available databases and thus were likely to be enriched of neoantigens, spliced tumor antigens and PTM peptides. De novo sequencing procedures will allow us to identify their sequence.

Although the results of the novo sequencing data are not available yet, the classical database searching engine analysis highlighted that *Salmonella*-treated tumor cells release non-mutated potentially immunogenic peptides. The analysis of the peptides released by B16 cells showed the presence of Cofilin, described to be an antigen potentially shared by different tumor types. It has indeed been found expressed both on three different human melanoma cell lines and on primary human melanoma cells (Gloger et al. 2016), and furthermore, it has been identified as HLA-binder of both human breast and pancreatic tumor cell lines (Antwi et al. 2009). The analysis of the peptides released by patient-derived melanoma cells and human melanoma cell lines unraveled three peptides that although deriving from different melanoma cells were equally released specifically upon *Salmonella* infection. NM1 and TMA7 are strong HLA binders while HMG-I is a good HLA binder suggesting that they can potentially be immunogenic. Furthermore NM1 has been already described as expressed on HLA molecules of a lymphoblast cell line (Bassani-Sternberg et al. 2015; Pearson et al. 2016). Both the non-mutated peptides selected by canonical database searching engine and the peptides that will be deciphered by the novo sequencing procedure will be prioritized on the basis of the predicted-HLA-binding affinity. Only the good binders will be synthesized and their immunogenicity will be assessed either *ex vivo* or *in vivo*: we will be testing the ability of the peptides to expand

T-lymphocytes from healthy donor PBMCs able to recognize and kill tumor cells *in vitro* and *in vivo*, similarly to what I previously discussed.

A Gene Ontology (GO) Cellular Component analysis applied to the peptides found to be overrepresented in the supernatant of both murine, human and dog tumor cells treated with *Salmonella* showed that several of them belonged to proteins found at the level of focal adhesion and as components of ribosomes; we observed an enrichment of proteins dedicated to mRNA transport, mRNA stability regulation and protein translation. These findings are a further indication that peptides released by tumor cells upon *Salmonella* infection are prone to bind to HLA molecules; indeed previous studies highlighted that ribosomes-derived peptides but also proteins involved in translational processes and nucleosomal proteins are particularly well presented on HLA molecules (Bassani-Sternberg et al. 2015). A possibility that we still need to address is whether among the released peptides upon *Salmonella* infection, non-common antigens as tumor epitopes associated with impaired peptide processing (TEIPPs) are found (Seidel et al. 2012). These peptides although derive from housekeeping proteins are not presented by normal cells and can evade both central and peripheral immune tolerance; thus they could be efficiently targeted by a cancer vaccine immunotherapy (Oliveira et al. 2011; Lampen et al. 2010).

An issue to consider once proposing a peptide-based anticancer vaccine strategy is the autoimmunity that might be induced following immunization. Peptides might indeed boost an aberrant immune response against endogenously HLA-associated peptides instead of inducing an antitumor-specific immune response. None of the mice vaccinated with peptides released by B16 cells upon *Salmonella* infection developed vitiligo (white skin patches that are due to the disappearance of melanocytes). Moreover the clinical trial that involves dogs affected by both high grade sarcoma and osteosarcoma demonstrated the safety of the vaccination. Of note, none of the enrolled patients had a positive reaction to Delayed Type Hypersensitivity (DTH) test. Erythema or induration after 48-72 hours was

never revealed thus indicating that none of the peptides included in the vaccine formulation induced a strong and immediate immune response but also that autoimmunity reactions can be excluded.

The mechanism by which *Salmonella* induces tumor antigen release still remains elusive. Using a hemichannels blocker we demonstrated that peptides-release upon *Salmonella* infection was mostly but not exclusively hemichannel-dependent. From previous studies it is known that *Salmonella* infection induces hemichannel overexpression (Saccheri et al. 2010) but how, and why preferentially proteasome-produced tumor antigens are conveyed toward hemichannels for their release requires further investigation. However, it is evident that the treatment of tumor cells with *Salmonella* is a strategy to unravel novel T cell epitopes that are expressed by tumor cells. We validated this approach on three different tumor types, melanoma, osteosarcoma and sarcoma, but it might potentially be applied to other solid tumors. Importantly, the peptides provided by our approach are pre-processed by tumor proteasome and *in vivo*, once taken up by DCs, could not require further trimming by the immune-proteasome of DC-proteasome. This is an advantage considering that antigens presented by tumor cells often do not correspond to the ones presented by DCs due to the diverse proteasomes expressed by the two cell types (Vigneron & Van den Eynde 2014). DCs express constitutively the immunoproteasome and very little of the standard proteasome that is instead expressed by tumor cells. One of the first evidence of this discrepancy was shown in melanoma patients. The immunodominant HLA-A2-resctricted MelanA antigen (Melan-A_{26-35}), highly expressed by tumor cells was not produced by DC's immunoproteasome (Chapatte et al. 2006). Significantly, the inhibition of DCs-immunoproteasome to favor the standard proteasome, enabled DCs to induce a strong anti Melan-A specific T cell response *in vitro* and *in vivo* (Dannull et al. 2009; Chapatte et al. 2006). A way to overcome this DC-proteasome processing is to exogenously provide tumor-processed antigens of the right size and affinity for MHC-I

molecules, as proposed in our strategy. Another advantage of our approach is that several antigens are simultaneously provided to the immune system thus leading to a multi-target and specific tumor-directed T cell response that addresses tumor heterogeneity as well as minimizes the chance of tumor escape by loss of antigens.

In conclusion, we demonstrated that infection of tumor cells with *Salmonella* induced the extracellular release of immunogenic tumor antigens that could be successfully exploited as cancer vaccines for the prevention or treatment of tumors. By a novel MS-based approach we identified the non-mutated tumor antigens and we will soon derive the sequence of neoantigens and likely spliced-tumor antigens. By the implementation of the vaccine in veterinarian clinical practice for the treatment of dogs affected by spontaneous osteosarcoma and high grade sarcoma we assessed the safety, feasibility and efficacy of the protocol.

Neoantigens, non-common antigens (as TEIPP peptides) or spliced peptides released by tumor cells following *Salmonella* infection could be applied in a clinical setting as a prophylactic cancer vaccine in the adjuvant setting for the therapeutic treatment of solid cancer to avoid recurrence. Initially, we envisage an autologous personalized cancer vaccine and cancer biopsies would be necessary in the first phase of clinical development, for the enrichment of patient-specific tumor-antigens. We will then evaluate whether there is a 'signature' of these antigens (including neoantigens) commonly released by patients-derived tumor cells upon *Salmonella* infection and whether this correlates with vaccine efficacy with the aim of identifying a 'universal' vaccine treatment. A 'universal' vaccine formulation would pave the way to a robust mass vaccination schedule treatment as it could be administered to patients soon after tumor resection, boosting rapidly an antitumor response directed against micro-metastases that are often not clinically visible at the moment of primary tumor diagnosis. To enhance cancer vaccine effect it will be pivotal to

monitor the expression of both immunocheckpoint and HLA molecules at tumor level. A personalized combinatorial therapy would be instrumental for patients clinical benefits.

6. Bibliography

Albini, A. et al., 2015. SANIST: A rapid mass spectrometric SACI/ESI data acquisition and elaboration platform for verifying potential candidate biomarkers. *Rapid Communications in Mass Spectrometry*, 29(19), pp.1703–1710.

Andtbacka, R.H.I. et al., 2015. Talimogene laherparepvec improves durable response rate in patients with advanced melanoma. *Journal of Clinical Oncology*, 33(25), pp.2780–2788.

Antwi, K. et al., 2009. Proteomic identification of an MHC-binding peptidome from pancreas and breast cancer cell lines. *Molecular Immunology*, 46(15), pp.2931–2937.

Aucouturier, J. et al., 2002. Montanide ISA 720 and 51: a new generation of water in oil emulsions as adjuvants for human vaccines. *Expert Review of Vaccines*.

Avogadri, F. et al., 2005. Cancer immunotherapy based on killing of Salmonella -infected tumor cells. *Cancer Research*, 10(9), pp.3920–3927.

Avogadri, F. et al., 2008. Intra-tumoral Salmonella typhimurium induces a systemic anti-tumor immune response that is directed by low-dose radiation to treat distal disease. *European Journal of Immunology*, 38(7), pp.1937–1947.

Balch, C.M. et al., 2009. Final version of 2009 AJCC melanoma staging and classification. *Journal of Clinical Oncology*, 27(36), pp.6199–6206.

Bassani-Sternberg, M. et al., 2015. Mass Spectrometry of Human Leukocyte Antigen Class I Peptidomes Reveals Strong Effects of Protein Abundance and Turnover on Antigen Presentation. *Molecular & Cellular Proteomics*, 14(3), pp.658–673.

Bassani-Sternberg, M. & Coukos, G., 2016. Mass spectrometry-based antigen discovery for cancer immunotherapy. *Current Opinion in Immunology*, 41, pp.9–17.

Ben-Shahar, S. et al., 1999. 26 S proteasome-mediated production of an authentic major histocompatibility class I-restricted epitope from an intact protein substrate. *Journal of Biological Chemistry*, 274(31), pp.21963–21972.

Berlin, C. et al., 2015. Mapping the HLA ligandome landscape of acute myeloid leukemia: a targeted approach toward peptide-based immunotherapy. *Leukemia*, 29(3), pp.647–59.

Bijker, M.S. et al., 2007. CD8 + CTL Priming by Exact Peptide Epitopes in Incomplete Freund's Adjuvant Induces a Vanishing CTL Response, whereas Long Peptides Induce Sustained CTL Reactivity. *The Journal of Immunology*, 179(8), pp.5033–5040.

Bray, J.P. et al., 2014. Canine soft tissue sarcoma managed in first opinion practice: Outcome in 350 cases. *Veterinary Surgery*, 43(7), pp.774–782.

Bray, J.P., 2016. Soft tissue sarcoma in the dog – part 1: a current review. *Journal of Small Animal Practice*, 57(10), pp.510–519.

Brennan, P.J., Brigl, M. & Brenner, M.B., 2013. Invariant natural killer T cells: An innate activation scheme linked to diverse effector functions. *Nature Reviews Immunology*, 13(2), pp.101–117.

By Paola Paglia, Claudia Chiodoni, Monica Rodolfo, and M.P.C., 1996. Murine Dendritic Cells Loaded In Vitro with Soluble Protein Prime Cytotoxic T Lymphocytes against Tumor Antigen In Vivo By. *The Journal of Experimental Medicine*, 184(August), pp.0–5.

Caron, E. et al., 2015. Analysis of Major Histocompatibility Complex (MHC) Immunopeptidomes Using Mass Spectrometry. *Molecular & Cellular Proteomics*, 14(12), pp.3105–3117.

Carreno, B., 2015. A dendritic cell vaccine increases the breadth and diversity of melanoma neoantigen-specific T cells. *Science*, 348(6236), p.803.

Castle, J.C. et al., 2012. Exploiting the mutanome for tumor vaccination. *Cancer Research*, 72(5), pp.1081–1091.

Chambers, B. et al., 2007. Induction of protective CTL immunity against peptide transporter TAP-deficient tumors through dendritic cell vaccination. *Cancer Research*, 67(18), pp.8450–8455.

Chapatte, L. et al., 2006. Processing of tumor-associated antigen by the proteasomes of dendritic cells controls in vivo T-cell responses. *Cancer Research*, 66(10), pp.5461–5468.

Chapman, P.B. et al., 2011. Improved Survival with Vemurafenib in Melanoma with BRAF V600E Mutation. *The New England journal of medicine*, 364(26), pp.2507–2516.

Chen, D.S. & Mellman, I., 2013. Oncology meets immunology: The cancer-immunity cycle. *Immunity*, 39(1), pp.1–10.

Chiocca, E. & Rabkin, S., 2015. Oncolytic Viruses and Their Application to Cancer Immunotherapy. *Cancer Immunol Res*, 2(4), pp.295–300.

Christian Bode, 2011. CpG DNA as a vaccine adjuvant. *Expert Rev Vaccines*, 10(4), pp.499–511.

Coley, W.B., 1891. Contribution to the knowledge of sarcoma. *Annals of Surgery*, 14(199), pp.199–200.

Coulie, P.G. et al., 2014. Tumour antigens recognized by T lymphocytes: At the core of cancer immunotherapy. *Nature Reviews Cancer*, 14(2), pp.135–146.

Dancsok, A.R., Asleh-Aburaya, K. & Nielsen, T.O., 2017. Advances in sarcoma diagnostics and treatment. *Oncotarget*, 8(4), pp.7068–7093.

Dannull, J. et al., 2009. Immunoproteasome down-modulation enhances the ability of dendritic cells to stimulate antitumor immunity. *Bibliothek*, 110(13), pp.4341–4350.

Dennis, M.M. et al., 2011. Prognostic Factors for Cutaneous and Subcutaneous Soft Tissue Sarcomas in Dogs. *Veterinary Pathology*, 48(1), pp.73–84.

Dranoff, G. et al., 1993. Vaccination with irradiated tumor cells engineered to secrete murine granulocyte-macrophage colony-stimulating factor stimulates potent, specific, and long-lasting anti-tumor immunity. *Proceedings of the National Academy of Sciences*, 90(8), pp.3539–3543.

Van Duin, D., Medzhitov, R. & Shaw, A.C., 2006. Triggering TLR signaling in vaccination. *Trends in Immunology*, 27(1), pp.49–55.

Dummer, R. et al., 2015. Cutaneous melanoma: ESMO Clinical Practice Guidelines for diagnosis, treatment and follow-up. *Annals of Oncology*, 26(November), pp.v126–v132.

Dunn, G.P., Old, L.J. & Schreiber, R.D., 2004a. The immunobiology of cancer immunosurveillance and immunoediting. *Immunity*, 21(2), pp.137–148.

Dunn, G.P., Old, L.J. & Schreiber, R.D., 2004b. The Three Es of Cancer Immunoediting. *Annual Review of Immunology*, 22(1), pp.329–360.

Durgeau, A. et al., 2011. Different Expression Levels of the TAP Peptide Transporter Lead to Recognition of Different Antigenic Peptides by Tumor-Specific CTL. *The Journal of Immunology*, 187(11), pp.5532–5539.

Ebstein, F. et al., 2016. Proteasomes generate spliced epitopes by two different mechanisms and as efficiently as non-spliced epitopes. *Scientific Reports*, 6(January), pp.1–12.

Elgueta, R. et al., 2009. Gap Junctions at the Dendritic Cell-T Cell Interface Are Key Elements for Antigen-Dependent T Cell Activation. *The Journal of Immunology*, 183(1), pp.277–284.

Ferrone, S. & Marincola, F.M., 1995. Loss of HLA class I antigens by melanoma cells: molecular mechanisms, functional significance and clinical relevance. *Immunology Today*, 16(10), pp.487–494.

Fong, L. et al., 2001. Dendritic Cell-Based Xenoantigen Vaccination for Prostate Cancer Immunotherapy. *The Journal of Immunology*, 167(12), pp.7150–7156.

Frezza, A.M., Stacchiotti, S. & Gronchi, A., 2017. Systemic treatment in advanced soft tissue sarcoma: what is standard, what is new. *BMC Medicine*, 15(1), p.109.

Garbe, C. et al., 2016. Diagnosis and treatment of melanoma. European consensus-based interdisciplinary guideline - Update 2016. *European Journal of Cancer*, 63, pp.201–217.

Gloger, A. et al., 2016. Mass spectrometric analysis of the HLA class I peptidome of melanoma cell lines as a promising tool for the identification of putative tumor-associated HLA epitopes. *Cancer Immunology, Immunotherapy*, 65(11), pp.1377–1393.

Goldinger, S.M. et al., 2012. Nano-particle vaccination combined with TLR-7 and -9 ligands triggers memory and effector CD8+ T-cell responses in melanoma patients. *European Journal of Immunology*, 42(11), pp.3049–3061.

Greenman, C. et al., 2007. Patterns of somatic mutation in human cancer genomes. *Nature*, 446(7132), pp.153–158.

Gros, A. et al., 2014. PD-1 identifies the patient-specific in filtrating human tumors. *The Journal of Clinical Investigation*, 124(5), pp.2246–59.

Gros, A. et al., 2016. Prospective identification of neoantigen-specific lymphocytes in the peripheral blood of melanoma patients. *Nature medicine*, 22(4), pp.433–8.

Gross, L., 1943. Intradermal Immunization of C3H Mice against a Sarcoma That Originated in an Animal of the Same Line. *Cancer Research*, 3(5), pp.326–333.

Gross, S. et al., 2017. Twelve-year survival and immune correlates in dendritic cell–vaccinated melanoma patients. *JCI Insight*, 2(8), pp.1–19.

Hailemichael, Y.M. et al., 2013. Persistent antigen at vaccination sites induces tumor-specific CD8+ T cell sequestration, dysfunction and deletion. *Nature Medicine*, 19(4), pp.465–472.

van Hall, T. et al., 2006. Selective cytotoxic T-lymphocyte targeting of tumor immune escape variants. *Nature medicine*, 12(4), pp.417–424.

Hanada, K., Yewdell, J.W. & Yang, J.C., 2004. Immune recognition of a human renal cancer antigen through post-translational protein splicing. *Nature*, 427(6971), pp.252–256.

Hanahan, D. & Weinberg, R.A., 2011. Hallmarks of cancer: The next generation. *Cell*, 144(5), pp.646–674.

Heemskerk, B., Kvistborg, P. & Schumacher, T.N.M., 2012. The cancer antigenome. *The EMBO Journal*, 32(2),

pp.194–203.

Hendriks, J. et al., 2000. CD27 is required for generation and long-term maintenance of T cell immunity. *Nature immunology*, 1(5), pp.433–40.

Hong, E.H. et al., 2013. Intratumoral injection of attenuated Salmonella vaccine can induce tumor microenvironmental shift from immune suppressive to immunogenic. *Vaccine*, 31(10), pp.1377–1384.

Hosken, N.A. & Bevan, M.J., 1990. Defective presentation of endogenous antigen by a cell line expressing class I molecules. *Science (New York, N.Y.)*, 248(4953), pp.367–70.

Hugo, W. et al., 2017. Erratum: Genomic and Transcriptomic Features of Response to Anti-PD-1 Therapy in Metastatic Melanoma. *Cell* 168(3), p.542.

Jeong, K., Kim, S. & Bandeira, N., 2012. False discovery rates in spectral identification. *BMC Bioinformatics*, 13(Suppl 16), p.S2.

Joffre, O.P. et al., 2012. Cross-presentation by dendritic cells. *Nature Reviews Immunology*, 12(8), pp.557–569..

Kalaora, S. et al., 2016. Use of HLA peptidomics and whole exome sequencing to identify human immunogenic neo-antigens. *Oncotarget*, 7(5), pp.5110–7.

Kang, J. et al., 2008. Connexin 43 Hemichannels Are Permeable to ATP. *Journal of Neuroscience*, 28(18), pp.4702–4711.

Kaufman, H.L., Kohlhapp, F.J. & Zloza, A., 2015. Oncolytic viruses: a new class of immunotherapy drugs. *Nature Reviews Drug Discovery*, 14(9), pp.642–662.

Kawakami, B.Y. et al., 1994. Identification of the Immunodominant Peptides of the MART-1 Human Melanoma Antigen Recognized by the Majority of HLA-A2-restricted Tumor Infiltrating Lymphocytes. *The Journal of Experimental Medicine*, 180(July), pp.1–6.

Kenter, G.G. et al., 2009. Vaccination against HPV-16 Oncoproteins for Vulvar Intraepithelial Neoplasia. *New England Journal of Medicine*, 361(19), pp.1838–1847.

Khan, A.N.H., Gregorie, C.J. & Tomasi, T.B., 2008. Histone deacetylase inhibitors induce TAP, LMP, Tapasin genes and MHC class I antigen presentation by melanoma cells. *Cancer Immunology, Immunotherapy*, 57(5), pp.647–654.

Kincaid, E.Z. et al., 2012. Alterations in Antigen Presentation. *Nature immunology*, 13(2), pp.129–135.

Kleffel, S. et al., 2015. Melanoma cell-intrinsic PD-1 receptor functions promote tumor growth. *Cell*, 162(6), pp.1242–1256.

Kreiter, S. et al., 2015. Mutant MHC class II epitopes drive therapeutic immune responses to cancer. *Nature*, 520(7549), pp.692–696.

Krenacs T, van Dartel M, Lindhout E, and R.M., 1997. Direct celllcell communication in the Iymphoid germinal center: connexin43 gap junctions functionally couple follicular dendritic cells to each other and to B Iymphocytes. *Eur J Immunol*, 27, pp.1489–1497.

Kumari, S. et al., 2014. Alloreactive cytotoxic T cells provide means to decipher the immunopeptidome and reveal a plethora of tumor-associated self-epitopes. *Proceedings of the National Academy of Sciences*, 111(1), pp.403–408.

Lampen, M.H. et al., 2010. CD8+ T Cell Responses against TAP-Inhibited Cells Are Readily Detected in the Human Population. *The Journal of Immunology*, 185(11), pp.6508–6517.

Larkin, J. et al., 2015. Combined Nivolumab and Ipilimumab or Monotherapy in Untreated Melanoma. *The New England journal of medicine*, 373(1), pp.23–34.

Le, D.T. et al., 2015. PD-1 Blockade in Tumors with Mismatch-Repair Deficiency. *The New England journal of medicine*, 372(26), pp.2509–2520.

Leone, P. et al., 2013. MHC class i antigen processing and presenting machinery: Organization, function, and defects in tumor cells. *Journal of the National Cancer Institute*, 105(16), pp.1172–1187.

Liepe, J. et al., 2016. A large fraction of HLA class I ligands are proteasome-generated spliced peptides. *Science*, 354(6310), pp.605–610.

London, C.A. et al., 2015. Impact of toceranib/piroxicam/cyclophosphamide maintenance therapy on outcome of dogs with appendicular osteosarcoma following amputation and carboplatin chemotherapy: A multi-institutional study. *PLoS ONE*, 10(4), pp.1–17.

Lu, Y.C. et al., 2014. Efficient identification of mutated cancer antigens recognized by T cells associated with durable tumor regressions. *Clinical Cancer Research*, 20(13), pp.3401–3410.

Matsue, H. et al., 2005. Gap Junction-Mediated Intercellular Communication between Dendritic Cells (DCs) Is Required for Effective Activation of DCs. *The Journal of Immunology*, 176(1), pp.181–190.

Maude, S.L. et al., 2014. Chimeric Antigen Receptor T Cells for Sustained Remissions in Leukemia. *New England Journal of Medicine*, 371(16), pp.1507–1517.

Mazzini, E. et al., 2014. Oral Tolerance Can Be Established via Gap Junction Transfer of Fed Antigens from CX3CR1+ Macrophages to CD103+ Dendritic Cells. *Immunity*, 40(2), pp.248–261.

McGranahan, N. et al., 2016. Clonal neoantigens elicit T cell immunoreactivity and sensitivity to immune checkpoint blockade. *Science*, 351(6280), pp.1463–1469.

Mellman, I., Coukos, G. & Dranoff, G., 2011. Cancer immunotherapy comes of age. *Nature*, 480(7378), pp.480–9.

Menard, S. et al., 2000. Role of HER2 gene overexpression in breast carcinoma. *Journal of Cellular Physiology*, 182(2), pp.150–162.

Mendoza-Naranjo, A. et al., 2011. Functional gap junctions accumulate at the immunological synapse and contribute to T cell activation. *Journal of immunology (Baltimore, Md. : 1950)*, 187(6), pp.3121–3132.

Mendoza-Naranjo, A. et al., 2007. Functional Gap Junctions Facilitate Melanoma Antigen Transfer and Cross-Presentation between Human Dendritic Cells. *The Journal of Immunology*, 178(11), pp.6949–6957.

Mesnil, M. et al., 2005. Defective gap junctional intercellular communication in the carcinogenic process. *Biochimica et Biophysica Acta - Biomembranes*, 1719(1–2), pp.125–145.

Mirabello, L., Troisi, R.J. & Savage, S.A., 2009. Osteosarcoma incidence and survival rates from 1973 to 2004: Data from the surveillance, epidemiology, and end results program. *Cancer*, 115(7), pp.1531–1543.

Mishto, M. & Liepe, J., 2017. Post-Translational Peptide Splicing and T Cell Responses. *Trends in Immunology*, xx, pp.1–12.

Morel, S. et al., 2000. Processing of some antigens by the standard proteasome but not by the immunoproteasome results in poor presentation by dendritic cells. *Immunity*, 12(1), pp.107–117.

Nair, S.K. et al., 1997. Antigen-presenting cells pulsed with unfractionated tumor-derived peptides are potent tumor vaccines. *European Journal of Immunology*, 27(3), pp.589–597.

Neijssen, J. et al., 2005. Cross-presentation by intercellular peptide transfer through gap junctions. *Nature*, 434(7029), pp.83–88.

Oliveira, C.C. et al., 2011. Peptide transporter TAP mediates between competing antigen sources generating distinct surface MHC class I peptide repertoires. European Journal of Immunology, 41(11), pp.3114–3124.

Ott, P.A. et al., 2017. An immunogenic personal neoantigen vaccine for patients with melanoma. *Nature*, 547(7662), pp.217–221.

Overwijk, W.W. & Restifo, N.P., 2001. *B16 as a Mouse Model for Human Melanoma*,

Oyamada, M., Oyamada, Y. & Takamatsu, T., 2005. Regulation of connexin expression. *Biochimica et Biophysica Acta - Biomembranes*, 1719(1–2), pp.6–23.

Paterson, Y., Guirnalda, P.D. & Wood, L.M., 2015. Listeria and Salmonella Bacterial Vectors of Tumor-associated antigens for Cancer Immunotherapy. *Semin Immunology*, 22(3), pp.183–189.

Pearson, H. et al., 2016. MHC class I – associated peptides derive from selective regions of the human genome. *The Journal of Clinical Investigation*, 126(12), pp.1–12.

Pittet, M.J. et al., 1999. High frequencies of naive Melan-A/MART-1-specific CD8(+) T cells in a large proportion of human histocompatibility leukocyte antigen (HLA)-A2 individuals. *The Journal of experimental medicine*, 190(5), pp.705–15.

De Plaen, E. et al., 1988. Immunogenic (tum-) variants of mouse tumor P815: Cloning of the gene of tum-antigen P91A and identification of the tum-mutation*. *Immunology*, 85(April), pp.2274–2278.

Platteel, A.C.M. et al., 2017. Multi-level Strategy for Identifying Proteasome-Catalyzed Spliced Epitopes Targeted by CD8+T Cells during Bacterial Infection. *Cell Reports*, 20(5), pp.1242–1253.

Posey, A.D. et al., 2016. Engineered CAR T Cells Targeting the Cancer-Associated Tn-Glycoform of the Membrane Mucin MUC1 Control Adenocarcinoma. *Immunity*, 44(6), pp.1444–1454.

Postow, M. a. et al., 2015. Nivolumab and Ipilimumab versus Ipilimumab in Untreated Melanoma. *The New England journal of medicine*, p.150420053025009.

Redmond, W.L. & Sherman, L.A., 2005. Peripheral tolerance of CD8 T lymphocytes. *Immunity*, 22(3), pp.275–284.

Restifo, N.P. et al., 1993. Identification of human cancers deficient in antigen processing. *J Exp Med*, 177(2), p.265–72.

Rizvi, N.A. et al., 2015. Mutational landscape determines sensitivity to PD-1 blockade in non-small cell lung cancer. *Science*, 348(6230), pp.124–128.

Rosalia, R.A. et al., 2013. Dendritic cells process synthetic long peptides better than whole protein, improving antigen presentation and T-cell activation. *European Journal of Immunology*, 43(10), pp.2554–2565.

Rosenberg, B.Y.S.A. et al., 1985. Regression of established pulmonary metastases and subcutaneous tumor mediated by the systemic administration of high-dose recombinant interleukin 2. *New England Journal of Medicine*, 161(May).

Rosenberg, S.A. et al., 1998. Immunologic and therapeutic evaluation of a synthetic peptide vaccine for the treatment of patients with metastatic melanoma. *Nature medicine*, 4(3), pp.321–7.

Rowell, J.L., McCarthy, D.O. & Alvarez, C.E., 2011. Dog models of naturally occurring cancer. *Trends in Molecular*

Medicine, 17(7), pp.380–388.

Sabbatini, P. et al., 2012. Phase I trial of overlapping long peptides from a tumor self-antigen and poly-ICLC shows rapid induction of integrated immune response in ovarian cancer patients. *Clinical Cancer Research*, 18(23), pp.6497–6508.

Saccheri, F. et al., 2010. Bacteria Induced Gap Junctions in Tumor Favor Ag cross presentation and Antitumor Immunity. *Science Translational Medicine*, 57.

Salem, M.L., Rubinstein, M.P. & Cole, D.J., 2007. Tumours: Immunotherapy. *eLS*.

Schadendorf, D., Paschen, a & Sun, Y., 2000. Autologous, allogeneic tumor cells or genetically engineered cells as cancer vaccine against melanoma. *Immunology letters*, 74(1), pp.67–74.

Schmitt, M., 2017. Chimeric antigen receptor transduced T cells-Turning up for the next generation. *International Journal of Cancer*, 2.

Schreurs, M.W.J. et al., 2000. Dendritic cells break tolerance and induce protective immunity against a melanocyte differentiation antigen in an autologous melanoma model. *Cancer Research*, 60(24), pp.6995–7001.

Schümann, J. et al., 2007. Differential alteration of lipid antigen presentation to NKT cells due to imbalances in lipid metabolism. *European Journal of Immunology*, 37(6), pp.1431–1441.

Seidel, U.J.E. et al., 2012. A novel category of antigens enabling CTL immunity to tumor escape variants: Cinderella antigens. *Cancer Immunology, Immunotherapy*, 61(1), pp.119–125.

Seliger, B. et al., 2001. Characterization of the major histocompatibility complex class I deficiencies in B16 melanoma cells. *Cancer Research*, 61(3), pp.1095–1099.

Selmic, L.E. et al., 2014. Comparison of carboplatin and doxorubicin-based chemotherapy protocols in 470 dogs after amputation for treatment of appendicular osteosarcoma. *Journal of Veterinary Internal Medicine*, 28(2), pp.554–563.

Selvaraj, P., 2014. Allogeneic tumor cell vaccines: the promise and limitations in clinical trials. *Human vaccines & immunotherapeutics*, 10(1), pp.52–63.

Shimizu, J., Yamazaki, S. & Sakaguchi, S., 1999. Induction of tumor immunity by removing CD25+CD4+ T cells: a common basis between tumor immunity and autoimmunity. *Journal of immunology (Baltimore, Md. : 1950)*, 163(10), pp.5211–8.

Singh, M. et al., 2014. Direct incorporation of the NKT-cell activator α-galactosylceramide into a recombinant Listeria monocytogenes improves breast cancer vaccine efficacy. *British Journal of Cancer*, 111(10), pp.1945–1954.

Smith, C.R. et al., 2011. Improved Survival with Ipilimumab in Patients with Metastatic Melanoma. *The New England journal of medicine*, pp.2187–2198.

Speiser, D.E. et al., 2005. Rapid and strong human CD8+ T cell responses to vaccination with peptide, IFA, and CpG oligodeoxynucleotide 7909. *Journal of Clinical Investigation*, 115(3), pp.739–746.

Spodnick GJ, 1992. Prognosis for dogs with appendicular osteosarcoma treated by amputation alone. *Journal of Small Animal Practice*.

Steinman, R.M. & Banchereau, J., 2007. Taking dendritic cells into medicine. *Nature*, 449(7161), pp.419–426.

Stronen, E. et al., 2016. Targeting of cancer neoantigens with donor-derived T cell receptor repertoires. *Science*, 352(6291), pp.1337–1341.

Sukhan, A. et al., 2001. Genetic Analysis of Assembly of the. *Society*, 183(4), pp.1159–1167.

Sun, H.K. et al., 2009. High efficacy of a Listeria-based vaccine against metastatic breast cancer reveals a dual mode of action. *Cancer Research*, 69(14), pp.5860–5866.

Taube, J.M. et al., 2012. Colocalization of Inflammatory Response with B7-H1 Expression in Human Melanocytic Lesions Supports an Adaptive Resistance Mechanism of Immune Escape. *Science Translational Medicine*, 4(127), p.127ra37-127ra37.

Tautenhahn, R. et al., 2012. XCMS online: A web-based platform to process untargeted metabolomic data. *Analytical Chemistry*, 84(11), pp.5035–5039.

Terabe, M. et al., 2000. NKT cell-mediated repression of tumor immunosurveillance by IL-13 and the IL-4R-STAT6 pathway. *Nature immunology*, 1(6), pp.515–520.

Toes, R.E.M. et al., 2001. Discrete cleavage motifs of constitutive and immunoproteasomes revealed by quantitative analysis of cleavage products. *J Exp Med*, 194(1), p.1–12.

Träger, U. et al., 2012. The immune response to melanoma is limited by thymic selection of self-antigens. *PLoS ONE*, 7(4).

Twyman-Saint Victor, C. et al., 2015. Radiation and dual checkpoint blockade activate non-redundant immune mechanisms in cancer. *Nature*, 520(7547), pp.373–377.

Unger, V.M. et al., 1999. Expression, two-dimensional crystallization, and electron cryo-crystallography of recombinant gap junction membrane channels. *Journal of structural biology*, 128(1), pp.98–105.

VanderBruggen, P. et al., 1991. A gene encoding an antigen recognized by cytolytic T- lymphocytes on a human

melanoma. *Science*, 254(5038), pp.1643–1647.

Vendrell, A. et al., 2011. A novel Salmonella Typhi-based immunotherapy promotes tumor killing via an antitumor Th1-type cellular immune response and neutrophil activation in a mouse model of breast cancer. *Vaccine*, 29(4), pp.728–736.

Vigneron, N., 2004. An Antigenic Peptide Produced by Peptide Splicing in the Proteasome. *Science*, 587(April).

Vigneron, N. & Van den Eynde, B.J., 2014. Proteasome subtypes and regulators in the processing of antigenic peptides presented by class I molecules of the major histocompatibility complex. *Biomolecules*, 4(4), pp.994–1025.

Voedisch, S. et al., 2009. Mesenteric lymph nodes confine dendritic cell-mediated dissemination of Salmonella enterica serovar typhimurium and limit systemic disease in mice. *Infection and Immunity*, 77(8), pp.3170–3180.

Walter, S. et al., 2012. Multipeptide immune response to cancer vaccine IMA901 after single-dose cyclophosphamide associates with longer patient survival. *Nature Medicine*, 18(8), pp.1254–1261.

Warren, E.H. et al., 2006. An Antigen Produced by Splicing of Noncontiguous Peptides in the Reverse Order. *Science*, 313(5792), pp.1444–1447.

Weber, P.A. et al., 2004. The Permeability of Gap Junction Channels to Probes of Different Size Is Dependent on Connexin Composition and Permeant-Pore Affinities. *Biophysical Journal*, 87(2), pp.958–973.

Winzler, C. et al., 1997. Maturation stages of mouse dendritic cells in growth factor-dependent long-term cultures. *The Journal of experimental medicine*, 185(2), pp.317–28.

Wolchok, J.D. et al., 2013. Nivolumab plus ipilimumab in advanced melanoma. *The New England journal of medicine*, 369(2), pp.122–33.

Wycislo, K.L. & Fan, T.M., 2015. The Immunotherapy of Canine Osteosarcoma: A Historical and Systematic Review. *Journal of Veterinary Internal Medicine*, 29(3), pp.759–769.

Yadav, M. et al., 2014. Predicting immunogenic tumour mutations by combining mass spectrometry and exome sequencing. *Nature*, 515(7528), pp.572–6.

Yoon, W. et al., 2017. Application of genetically engineered Salmonella typhimurium for interferon-gamma–induced therapy against melanoma. *European Journal of Cancer*, 70, pp.48–61.

Young, R.J. et al., 2014. First-line anthracycline-based chemotherapy for angiosarcoma and other soft tissue sarcoma subtypes: Pooled analysis of eleven European Organisation for Research and Treatment of Cancer Soft Tissue and Bone Sarcoma Group trials. *European Journal of Cancer*, 50(18), pp.3178–3186.

Zaretsky, J.M. et al., 2016. Mutations Associated with Acquired Resistance to PD-1 Blockade in Melanoma. *New England Journal of Medicine*, 375(9), pp.819–829.

Zheng, J.H. et al., 2017. Two-step enhanced cancer immunotherapy with engineered *Salmonella typhimurium* secreting heterologous flagellin. *Science Translational Medicine*, 9(376), p.eaak9537.

7. Appendix

7.1 Peptides released by *Salmonella* infected tumor cells.

In this study, MS analysis have been conducted to identify peptides specifically released from tumor cells upon Salmonella infection (described in Chapter 4.4). The results are additionally shown below in descriptive tables.

7.1.1 Peptides specifically released by B16 murine melanoma cell line treated with *Salmonella*

Sequence	Proteins	Gene names	Protein names	id	Charges
ADKVPKTAENFR	Q5SVY2	Ppia	Peptidyl-prolyl cis-trans isomerase	85	3
APEEKASVGP	Q9Z1W5	Serp1	Stress-associated endoplasmic reticulum protein 1	238	2
AQASAPAQAPK	Q5M8M8	Rpl29	60S ribosomal protein L29	283	2
AQASAPAQAPKGAQAPK	Q5M8M8	Rpl29	60S ribosomal protein L29	285	3
DVSKPDITA	Q5FWJ3	Vim	Vimentin	523	2
EIEGGSASEGAARP	Q3U4F9	Csf1	Macrophage colony-stimulating factor 1	609	2
GGGGGGGRYYGGGNEG	Q3UMT7	Hnrnpl	Heterogeneous nuclear ribonucleoprotein L	899	2
GQTPKVAKQEK	Q642K5	Fau	40S ribosomal protein S30	1148	2;3
GVIKAVDK	Q58E64	Eef1a1	Elongation factor 1-alpha	1255	2
HIDKAQQNNVE	F6SVV1	Gm9493	40S ribosomal protein S7	1284	2;3
KKEKVIATVTK	Q3UFI4	Rpl6	60S ribosomal protein L6	1751	3
KVPAVPETIKK	Q5M9N8	Rpl7	60S ribosomal protein L7	1852	3
NETNEIANANS	A2A547	Rpl19	Ribosomal protein L19	1960	2
NQGGYGGSSSSSSYGSGR	Q3TIK8	Hnrnpa1	Heterogeneous nuclear ribonucleoprotein A1	2053	2
PGVTVKDVN	Q5M9P3	Rps19	40S ribosomal protein S19	2205	2
PTPQDAGKPSGPG	Q3TQF7	Adamts1	A disintegrin and metalloproteinase with thrombospondin motifs 1	2321	2
PVVQPSVVDRVA	Q2XSQ4	Plin3	Perilipin	2334	2
SGGGGGGGGSWGGRSNS	Q9CX86	Hnrnpa0	Heterogeneous nuclear ribonucleoprotein A0	2863	2
TEEEKNFK	P47963	Rpl13	60S ribosomal protein L13	3231	2
TVTKTVGGDKNGGTR	Q3UFI4	Rpl6	60S ribosomal protein L6	3378	2;3
VDKKAAGAGKVT	Q58E64	Eef1a1	Elongation factor 1-alpha	3410	2;3
YDATYETKESKKEDI	Q544Y7	Cfl1	Cofilin-1	3627	3

YQSHADTATKSGSTTK	A0A0G2JFB4	Eif4e	Eukaryotic translation initiation factor 4E	3713	2;3

Table 7-1. Peptides released by B16 cells upon *Salmonella* infection. Supernatants of murine melanoma B16 cells were analyzed through nLC-MS both control supernatants and the ones derived from Salmonella treated melanoma cells (Chapter 4.4.2.2). 23 identified peptides were significantly more abundant in *Salmonella*-derived supernatants; analysis was performed with MaxQuant software on the identified peptides. *P <0.05.

7.1.2 Peptides specifically released by 624.38 human melanoma cell line treated with *Salmonella*

Sequence	Proteins	Gene names	Protein names	id	Charges
AAGKGPIATGGIKKSGKK	A0A024R306	TMA7	Translation machinery-associated protein 7	3	3;4
AQGPKGGSGSGPTIEE	B4E1T6	HEL-S-103		23	2
DDWDIITR	H0YLV1	MORF4L1	Mortality factor 4-like protein 1	41	2
DYPSSRDTRD	B3KRG5	RBMX	RNA binding motif protein, X-linked-like-1	65	2
EAPRPYSK	C9J6H5	ADAM9	Disintegrin and metalloproteinase domain-containing protein 9	67	2
ESKTAVEMIQNQI	P49454	CENPF	Centromere protein F	88	2
FGGPGTASRPS	V9HWE1	HEL113	Vimentin	107	2
GGGNYGPGGSGGSGGYGGR	A0A024RA28	HNRPA2B1	Heterogeneous nuclear ribonucleoproteins A2/B1	123	2
IRPAVSSSDQQS	C9JVB2	KIAA0319L	Dyslexia-associated protein KIAA0319-like protein	186	2
ISHEIDSASSE	F2YQ21	SPP1	Osteopontin	187	2
KANDESNEHSDVIDSQEISK	F2YQ21	SPP1	Osteopontin	209	3
KIEKEEEEGISQESSEEEQ	P17096	HMGA1	High mobility group protein HMG-I/HMG-Y	214	2;3
MGESDDSIIR	Q6FGH5	RPS21	40S ribosomal protein S21	227	2
RKSPENTEGKDGSKVTKQEPTR	A0A087WZE9	HMGN3	High mobility group nucleosome-binding domain-containing protein	295	4

			3		
RSAPGGGSKVPQK	Q9NX34	NPM1	Nucleophosmin	304	3
RSGPTDDGEEEMEEDTVTNGS	Q53G61	SNRPA1	U2 small nuclear ribonucleoprotein A	306	2
SPEEATPSSRPNR	H3BMM8	HN1L	Hematological and neurological expressed 1-like protein	322	2
TVAGGAWTYNTTSAVTVK	C9J4Z3	RPL37A	60S ribosomal protein L37a	357	2
VGGEGGAGGRSP	Q6UW78	C11orf83	UPF0723 protein C11orf83	372	2
VIYTRNTKGGDAPAAGEDA	P62851	RPS25	40S ribosomal protein S25	378	2;3
VPDRDPASP	B4DZS5	GPNMB	Transmembrane glycoprotein NMB	380	2
YGGGNYGPGGSGGSGGYG	A0A024RA28	HNRPA2B1	Heterogeneous nuclear ribonucleoproteins A2/B1	406	2
YGGGNYGPGGSGGSGGYGGR	A0A024RA28	HNRPA2B1	Heterogeneous nuclear ribonucleoproteins A2/B1	407	2
YGGGSEGGRAPK	B2R959	HNRNPL	Heterogeneous nuclear ribonucleoprotein L	410	2

Table 7-2. Peptides released by human melanoma 62438 cell line upon *Salmonella* infection. Supernatants of human melanoma 624.38 cells were analyzed through nLC-MS both control supernatants and the ones derived from *Salmonella*-treated melanoma cells (Chapter 4.4.2.3). 24 identified peptides were significantly more abundant in *Salmonella*-derived supernatants; analysis was performed with MaxQuant software on the identified peptides. *P <0.05.

7.1.3 Peptides specifically released by patients-derived melanoma cells treated with *Salmonella*

Sequence	Proteins	Gene names	Protein names	id	Charges
AAGKGPIATGGIKKSGKK	A0A024R306	CCDC72	Translation machinery-associated protein 7	27	3;4

ADGYNQPDSKR	B4DMD1	HNRNPR	Heterogeneous nuclear ribonucleoprotein R	105	2
ADKVPKTAENFR	V9HWF5	HEL-S-69p	Peptidyl-prolyl cis-trans isomerase	112	2;3
AEINANRADAEEEAATRIPA	Q9H5W7	DYNC1I2	Cytoplasmic dynein 1 intermediate chain 2	135	2;3
AKDQTKAQAAAPASVPAQAPK	A0A024R326	RPL29	60S ribosomal protein L29	229	2;3
ANPNSAIFGGARPREEVVQKEQE	Q75MT8	WBSCR1	Eukaryotic translation initiation factor 4H	268	3;4
APVPPVNEPETIKQQNQ	G3V153	CAPRIN1	Caprin-1	329	2
AQASSTPISPTR	P02545	LMNA	Prelamin-A/C	336	2
AQVIYTRNTKGGDAPAAGEDA	P62851	RPS25	40S ribosomal protein S25	351	2;3
ASSPGGVYATRSSA	V9HWE1	HEL113	Vimentin	370	2
ATGGNRTKTPGPGAQ	P62263	RPS14	40S ribosomal protein S14	378	2;3
ATSAKKVVVSPTK	A0A024R4A0	NCL	Nucleolin	390	2;3
AVDKKAAGAGKVT	Q6IPT9	EEF1A1	Elongation factor 1-alpha	402	2
AVDKKAAGAGKVTKSAQKAQ	Q6IPT9	EEF1A1	Elongation factor 1-alpha	409	3;4;5
AVRAIKNNSNDIVN	H0YHX9	NACA	Nascent polypeptide-associated complex subunit alpha	432	2
DDVKEQIYKIAK	J3KMX5	RPS13	40S ribosomal protein S13	526	2;3
DESGPSIVHR	P63261	ACTG1	Actin, cytoplasmic 2	551	2;3
DKVPKTAENFR	V9HWF5	HEL-S-69p	Peptidyl-prolyl cis-trans isomerase	640	2;3
DMRQTVAVGVIK	Q6IPT9	EEF1A1	Elongation factor 1-alpha	642	2
DSIIRIAKADGIVSKNF	Q6FGH5	RPS21	40S ribosomal protein S21	692	2;3
DSVKPGAHITVK	P51991	HNRNPA3	Heterogeneous nuclear ribonucleoprotein A3	706	2;3
DVTPIPSDSTRR	P62263	RPS14	40S ribosomal protein S14	734	2;3
EADRDTYR	P46783	RPS10	40S ribosomal protein S10	759	2
EEEMREIR	V9HWE1	HEL113	Vimentin	851	2
EGHDPKEPEQIR	P51991	HNRNPA3	Heterogeneous nuclear ribonucleoprotein A3	918	2;3;4
EIFADKVPKTAEN	V9HWF5	HEL-S-69p	Peptidyl-prolyl cis-trans isomerase	954	2
ESDDSIIRIAKADGIVSKNF	Q6FGH5	RPS21	40S ribosomal protein S21	1076	2;3
EVDKVTGRFNGQ	Q6FGH5	RPS21	40S ribosomal protein S21	1109	2
FEEYGKIDTIEIITDRQSGKK	P22626	HNRNPA2B1	Heterogeneous nuclear ribonucleoproteins A2/B1	1199	3;4;5

FEIFADKVPK	V9HWF5	HEL-S-69p	Peptidyl-prolyl cis-trans isomerase	1202	2
GAIAPIAIPSAAAAAAAAGR	A6NLN1	PTBP1	Polypyrimidine tract-binding protein 1	1277	2
GDSRGGGGNFGPGPGSNF	P22626	HNRNPA2B1	Heterogeneous nuclear ribonucleoproteins A2/B1	1309	2
GGDQQSGYGKVSR	A0A024RDF4	HNRPD		1344	2;3
GGPGTASRPSSSRSYVTT	V9HWE1	HEL113	Vimentin	1397	2;3
GGPGTASRPSSSRSYVTTST	V9HWE1	HEL113	Vimentin	1399	2;3
GHDPKEPEQIR	P51991	HNRNPA3	Heterogeneous nuclear ribonucleoprotein A3	1422	2;3
GSAIRPSTSR	V9HWE1	HEL113	Vimentin	1566	2
HGIQPDGQMPSDK	A8JZY9	TUBA1A	Tubulin alpha-1A chain	1661	2
HKEVDPGTKTA	J3QL69	LIMD2	LIM domain-containing protein 2	1673	2
IDAEPPAKR	Q9NUW4	BRIX	Ribosome biogenesis protein BRX1 homolog	1728	2
IDEVRTGTYR	A8JZY9	TUBA1A	Tubulin alpha-1A chain	1736	2;3
IDPNETNEIANANSR	J3QR09	RPL19	Ribosomal protein L19	1748	2
IEEQFQQGK	Q5JR95	RPS8	40S ribosomal protein S8	1790	2
IGGIGTVPVGRVETGVIKPGMVVT	Q6IPT9	EEF1A1	Elongation factor 1-alpha	1836	2;3
IGGISFETTDDSIR	P51991	HNRNPA3	Heterogeneous nuclear ribonucleoprotein A3	1838	2
IIEEQKIVVK	A0A024RDH8	RPL34	60S ribosomal protein L34	1863	2;3
IIKTISKEEETKK	J3QR09	RPL19	Ribosomal protein L19	1876	2;3
IISKIENHEGVR	V9HWB8	HEL-S-30	Pyruvate kinase	1889	2;3
IKEQISDIDDAVRKI	Q6IBA2	PC4	Activated RNA polymerase II transcriptional coactivator p15	1897	2;3;4
IREAGEQGDIEPR	B7Z8K4	G3BP	Ras GTPase-activating protein-binding protein 1	1970	2;3
IVSKGTIVQTKGTGASG	B2R984	HIST1H1E	Histone H1.4	2062	2
IYTRNTKGGDAPAAGEDA	P62851	RPS25	40S ribosomal protein S25	2079	2;3
KAAATPAKKTVTPAK	A0A024R4A0	NCL	Nucleolin	2081	2;3;4
KAAVTPGKKAAATPAK	A0A024R4A0	NCL	Nucleolin	2090	2;3
KAEGDAKGDKAKVKDEPQR	P05204	HMGN2	Non-histone chromosomal protein HMG-17	2095	3;4
KAPRGDVTAEEAAGASPA	P49006	MARCKSL1	MARCKS-related protein	2111	2
KASGPPVSEIITK	B2R984	HIST1H1E	Histone H1.4	2113	2;3
KDSYVGDEAQSK	P63261	ACTG1	Actin, cytoplasmic 2	2124	2

KGPIATGGIKKSGKK	A0A024R306	CCDC72	Translation machinery-associated protein 7	2165	2;3;4
KIEKEEEEGISQESSEEEQ	P17096	HMGA1	High mobility group protein HMG-I/HMG-Y	2174	2;3
KKAPAQKVPAQKATGQK	Q6IPH7	RPL14	60S ribosomal protein L14	2193	3;4
KKIEKEEEEGISQESSEEEQ	P17096	HMGA1	High mobility group protein HMG-I/HMG-Y	2197	2;3
KQPPVSPGTA	P17096	HMGA1	High mobility group protein HMG-I/HMG-Y	2224	2
KSPENTEGKDGSKVTKQEPTR	Q15651	HMGN3	High mobility group nucleosome-binding domain-containing protein 3	2243	3;4
KTETQEKNTIPTKETIEQEKRSEIS	D6W5K2	TMSB10	Thymosin beta-10	2253	3;4;5
KTGGADQSIQQGEGSKKGKG	A0A087WYR0	SRP19	Signal recognition particle 19 kDa protein	2254	3;4
KVAPAPAVVKKQEAK	P62424	RPL7A	60S ribosomal protein L7a	2269	2;3;4
KVSSAEGAAKEEPKR	P05114	HMGN1	Non-histone chromosomal protein HMG-14	2292	2;3
KVSSAEGAAKEEPKRR	P05114	HMGN1	Non-histone chromosomal protein HMG-14	2293	3;4
MKETIMNQEKIAKIQAQVR	P20290	BTF3	Transcription factor BTF3	2335	3
NQQPSNYGPMKSGNFGGSR	P22626	HNRNPA2B1	Heterogeneous nuclear ribonucleoproteins A2/B1	2444	2;3
NVAEVDKVTGR	Q6FGH5	RPS21	40S ribosomal protein S21	2475	2
PEPVKSAPVPK	I6L9F7	HIST1H2BM	Histone H2B	2531	2;3
PGPTPSGTNVGSSGRSPSK	Q53FA5	SEC61B	Protein transport protein Sec61 subunit beta	2552	2;3
PGPTPSGTNVGSSGRSPSKAVAAR	Q53FA5	SEC61B	Protein transport protein Sec61 subunit beta	2556	3;4
PKRKAEGDAKGDKAKVKDEPQR	P05204	HMGN2	Non-histone chromosomal protein HMG-17	2589	3;4;5;6
PKRKAEGDAKGDKAKVKDEPQRR	P05204	HMGN2	Non-histone chromosomal protein HMG-17	2590	5;6
PKRKVSSAEGAAKEEPKRR	P05114	HMGN1	Non-histone chromosomal protein	2594	5
RARPPSGSSKATDIGGTSQAGTSQ	A8K9U6	ZC3HAV1	Zinc finger CCCH-type antiviral protein 1	2687	3
RATRSGAQASSTPISPTR	P02545	LMNA	Prelamin-A/C	2688	3;4

RDSYGGPPRREPIPSR	B4E352	RBMX	RNA-binding motif protein, X chromosome	2699	4
REPTEEERAQRPR	Q75MT8	WBSCR1	Eukaryotic translation initiation factor 4H	2711	3;4
RGPAETEATTD	Q12792	TWF1	Twinfilin-1	2733	2
RIAPITSDPTEATAVGAVE	V9HWB8	HEL-S-30	Pyruvate kinase	2738	2
RQTVAVGVIKAVDK	Q6IPT9	EEF1A1	Elongation factor 1-alpha	2800	2;3
RSAPGGGSKVPQK	Q9NX34	NPM1	Nucleophosmin	2813	2;3
RSAVPPGADKKAEAGAGSATE	P46783	RPS10	40S ribosomal protein S10	2820	2;3
RVIQAIEGIKMVE	B0ZBD0	RPS19	40S ribosomal protein S19	2858	2
RVPPPPPIAR	G3V2D6	HNRNPC	Heterogeneous nuclear ribonucleoproteins C1/C2	2860	2
SAAEMYGSVTEHPSPSPIIS	G3V555	HNRNPC	Heterogeneous nuclear ribonucleoproteins C1/C2	2869	2
SAAPSTIDSSSTAPAQIGK	H7C4H2	SRPRB	Signal recognition particle receptor subunit beta	2870	2
SAPGGGSKVPQK	Q9NX34	NPM1	Nucleophosmin	2903	2
SAPSGPVRSSSGMGGRAP	B4E352	RBMX	RNA-binding motif protein, X chromosome	2911	3
SDIDDAVRKI	Q6IBA2	PC4	Activated RNA polymerase II transcriptional coactivator p15	2932	2
SEEVTASQVAATK	Q15149	PLEC	Plectin	2945	2
SGGTTMYPGIADR	P63261	ACTG1	Actin, cytoplasmic 2	2990	2
SGKGKVQFQGK	Q14730	SSB	Lupus La protein	2991	2;3
SGRPVTPPRTANPPKKR	B4DJ75	HEL-S-80p	Serine/threonine-protein phosphatase	3010	4
SIPIVDTHSKR	V9HWE1	HEL113	Vimentin	3043	2;3
SRPETGRPRPKGIEGERPA	P46783	RPS10	40S ribosomal protein S10	3138	4;5
STTPGGTIFSTTPGGTR	Q13541	EIF4EBP1	Eukaryotic translation initiation factor 4E-binding protein 1	3217	2
SVIISIKQAPIVH	C9J8P9	CLTA	Clathrin light chain A	3231	2
SYVTTSTR	V9HWE1	HEL113	Vimentin	3271	1;2
TAGPIASAQKQPAGKVQIVSK	E7EVA0	MAP4	Microtubule-associated protein	3287	2;3
TGPPVSEIITK	P16401	HIST1H1B	Histone H1.5	3386	2
TGSPGSPGAGGVQSTAK	J3KRI4	DYNC1LI2	Cytoplasmic dynein 1 light intermediate chain 2	3388	2
TIVTRTQGTK	H0Y9Y4	RPS3A	40S ribosomal protein S3a	3427	2
TQEKNTIPTKETIEQEKRSEIS	D6W5K2	TMSB10	Thymosin beta-10	3467	3;4

VAVGVIKAVDK	Q6IPT9	EEF1A1	Elongation factor 1-alpha	3606	2
VFKEDGQEYAQVIK	A6NJH9	EIF1AY	Eukaryotic translation initiation factor 1A, X-chromosomal	3705	2;3
VGVIKAVDK	Q6IPT9	EEF1A1	Elongation factor 1-alpha	3744	2
VKIAKAGKNQGDPK	A0A024R4A0	NCL	Nucleolin	3798	2
VMVGMGQKDSYVGDEAQSK	P63261	ACTG1	Actin, cytoplasmic 2	3804	2;3
VNEPETIKQQNQYQA	G3V153	CAPRIN1	Caprin-1	3810	2
YGGGNYGPGGSGGSGGYGGR	P22626	HNRNPA2B1	Heterogeneous nuclear ribonucleoproteins A2/B1	4012	2

Table 7-3. Peptides released by patient-derived melanoma cells upon *Salmonella* infection. Supernatants of human patient-derived melanoma cells were analyzed through nLC-MS both control supernatants and the ones derived from *Salmonella*-treated melanoma cells (Chapter 4.4.2.4). 115 identified peptides were significantly more abundant in *Salmonella*-derived supernatants; analysis was performed with MaxQuant software on the identified peptides. *P <0.05.

7.1.4 Peptides specifically released by dog melanoma cells treated with *Salmonella*

Sequence	Proteins	Gene names	Protein names	id	Charges
FPEPRPGGAPAP	A0A140T8E2	ADM	ADM	174	2
FTDKDKDGVAPRS	A0A140T8E2	ADM	ADM	179	2;3
IAEVKAGPAQT	A0A140T8E2	ADM	ADM	228	2
IRTQDVKGASRNPQTSGPDAA	A0A140T8E2	ADM	ADM	271	3
PEPRPGGAPAPR	A0A140T8E2	ADM	ADM	358	3
RQSMNNFQ	A0A140T8E2	ADM	ADM	391	2
RQSMNNFQGPR	A0A140T8E2	ADM	ADM	392	2
VKGASRNPQTSGPDAA	A0A140T8E2	ADM	ADM	554	2;3
VSSSYPTGIAEVKAGPAQT	A0A140T8E2	ADM	ADM	565	2
YRQSMNNFQ	A0A140T8E2	ADM	ADM	596	2
YRQSMNNFQGPR	A0A140T8E2	ADM	ADM	597	3
TPEPGEDPR	B8ZXI2	gnas1	Guanine nucleotide binding protein alpha subunit (Fragment)	502	2
ANAESASNRQPR	D5IGF6	Smoc2	SPARC-like modular calcium binding 2 protein (Fragment)	40	2
SVYYNEATGGKYVPR	E2QSF4	TUBB	Tubulin beta chain	476	2;3
YNEATGGKYVPR	E2QSF4	TUBB	Tubulin beta chain	593	2
SQPVAVRGGGGKQV	E2QTN0	KIF5B	Kinesin-like protein	438	2
VSGQIDDATR	E2QW82	MMP19	Matrix metallopeptidase 19	561	2
APVNVTTEVKS	E2QW85		Elongation factor 1-alpha	57	2
AVDKKAAGAGKVT	E2QW85		Elongation factor 1-alpha	79	2
AVDKKAAGAGKVTK	E2QW85		Elongation factor 1-alpha	80	2
KAAGAGKVTKSAQKAQKA	E2QW85		Elongation factor 1-alpha	302	2;4;5
KAAGAGKVTKSAQKAQKAK	E2QW85		Elongation factor 1-alpha	303	2;3;4;5
VGVIKAVDK	E2QW85		Elongation factor 1-alpha	536	2
VIKAVDKKAAGAGKVT	E2QW85		Elongation factor 1-alpha	543	2
DEQKNDVAGSQPQVETEA	E2QWF5	FKBP4	Peptidylprolyl isomerase (EC 5.2.1.8)	97	2
GPGPGSNF	E2QXH4	HNRNPA2B1	Heterogeneous nuclear ribonucleoprotein A2/B1	201	1
TINGHNAEVRKA	E2QXH4	HNRNPA2B1	Heterogeneous nuclear ribonucleoprotein A2/B1	498	2;3
IVYDQEIIGPSDKSQA	E2QZA1	C19orf70	MICOS complex subunit MIC13	295	2
AAAGYDVEKNN	E2R494	HIST1H1T	Histone cluster 1 H1 family	0	2

			member t		
TKGTGASGSFK	E2R494	HIST1H1T	Histone cluster 1 H1 family member t	499	2
AYSDMREANYK	E2RBD0	LOC476879	Serum amyloid A protein	84	2
FIKEAGQGTRD	E2RBD0	LOC476879	Serum amyloid A protein	171	2
IKEAGQGTRD	E2RBD0	LOC476879	Serum amyloid A protein	255	2
RIKNWKKQS	E2RBF0	LOC476879	Serum amyloid A protein	384	2
GEEGHDPKEPEQIR	E2RFV7	HNRNPA3	Heterogeneous nuclear ribonucleoprotein A3	188	3
TETKTITYESSQVD	E2RHR2	EPB41L3	Erythrocyte membrane protein band 4.1 like 3	489	2
ARPVKEPRG	E2RIQ3	PCSK1N	Proprotein convertase subtilisin/kexin type 1 inhibitor	65	2;3
SVGTSIATDKS	E2RK67	TMX1	Thioredoxin related transmembrane protein 1	471	2
RTPREVEAT	E2RK68	SEMA3G	Semaphorin 3G	396	2
APQQEAIPDETEVVEETVAE	E2RMA3	SPARC	Secreted protein acidic and cysteine rich	55	2
VITVINQTQKE	E2RPE5	RPL35	Ribosomal protein L35	550	2
VITVINQTQKEN	E2RPE5	RPL35	Ribosomal protein L35	551	2
VITVINQTQKENIR	E2RPE5	RPL35	Ribosomal protein L35	552	2;3
EAPAPAKTNVAVGESKAKE	E2RPY8	C2orf40	Chromosome 2 open reading frame 40	128	2;3
EIADAIKKQSMSE	E2RQU1		Uncharacterized protein	133	2
AAIQEIISK	E2RS49	RPS25	Uncharacterized protein	5	2
IYTRNTKGGDAPAAGEDA	E2RS49	RPS25	Uncharacterized protein	301	2;3
NTKGGDAPAAGEDA	E2RS49	RPS25	Uncharacterized protein	347	2
RNTKGGDAPAAGEDA	E2RS49	RPS25	Uncharacterized protein	389	2
VIYTRNTKGGDAPAAGEDA	E2RS49	RPS25	Uncharacterized protein	553	2;3
AEQNDSVSPR	E2RST6	STC1	Stanniocalcin 1	19	2
NIRGEAASPSHIK	E2RST6	RPL5	Ribosomal protein L5	341	2
RTSEPQKIK	E2RST6	RPL5	Ribosomal protein L5	398	2;3
THEAEQNDSVSPR	E2RST6	RPL5	Ribosomal protein L5	493	2;3
IRAQERAAES	F1P7B0	RPL5	Ribosomal protein L5	270	2

ISDRDYEKNG	F1P7G8	GFRA1	GDNF family receptor alpha 1	273	2
SPAQPEGGQASEGAAGAI	F1P7H1	CSF1	Colony stimulating factor 1	428	2
SPAQPEGGQASEGAAGAIAHSNAIP	F1P7H1	CSF1	Colony stimulating factor 1	430	2
FGDSIVTRSY	F1PBJ3	LMNA	Uncharacterized protein	159	2
GGSGGGSFGDSIVTRSY	F1PBJ3	LMNA	Uncharacterized protein	197	2
GSISSGSSASSVTVTR	F1PBJ3	LMNA	Uncharacterized protein	211	2
ISVQQQATQPTR	F1PCG5	YTHDF2	YTH N6-methyladenosine RNA binding protein 2	277	2
FVGGAENTAHPR	F1PEQ5	IGFBP5	Insulin like growth factor binding protein 5	182	2;3
AITGASIADIMAK	F1PGD7	RPL24	Uncharacterized protein	35	2
AATESFASDPIIYR	F1PHR2	PKM	Pyruvate kinase (EC 2.7.1.40)	10	2
APVPASEI	F1PHS5	PLEC	Plectin	59	1
RYASGPVSSIGGPESAAA	F1PHS5	PLEC	Plectin	399	2
SSSSYSSSGYGR	F1PHS5	PLEC	Plectin	451	2
DEIAPAGTGVSREAVSG	F1PKW5	APLP1	Amyloid beta precursor like protein 1	96	2
AINTEFKNTRTN	F1PLS4	VIM	Uncharacterized protein	32	2
AINTEFKNTRTNEK	F1PLS4	VIM	Uncharacterized protein	33	4
AIRPSTSRS	F1PLS4	VIM	Uncharacterized protein	34	2
AQIQDQHVQ	F1PLS4	VIM	Uncharacterized protein	61	2
ASSPGGAYATR	F1PLS4	VIM	Uncharacterized protein	71	2
ASSPGGAYATRSS	F1PLS4	VIM	Uncharacterized protein	72	2
ASSPGGAYATRSSA	F1PLS4	VIM	Uncharacterized protein	73	2
ASSPGGAYATRSSAVR	F1PLS4	VIM	Uncharacterized protein	74	3
ASSPGGAYATRSSAVRIR	F1PLS4	VIM	Uncharacterized protein	75	3
DAIRQAKQESNE	F1PLS4	VIM	Uncharacterized protein	87	2
EAANRNNDAIRQ	F1PLS4	VIM	Uncharacterized protein	125	2
ETRDGQVINETSQ	F1PLS4	VIM	Uncharacterized protein	143	2
FGGPGTGSRP	F1PLS4	VIM	Uncharacterized protein	160	2
FGGPGTGSRPS	F1PLS4	VIM	Uncharacterized protein	161	2
FGGPGTGSRPSS	F1PLS4	VIM	Uncharacterized protein	162	2
FGGPGTGSRPSST	F1PLS4	VIM	Uncharacterized protein	163	2
FGGPGTGSRPSSTR	F1PLS4	VIM	Uncharacterized protein	164	3
FGGPGTGSRPSSTRS	F1PLS4	VIM	Uncharacterized protein	165	3
GAYATRSSAVR	F1PLS4	VIM	Uncharacterized protein	185	2
GGPGTGSRPS	F1PLS4	VIM	Uncharacterized protein	191	2

GGPGTGSRPSS	F1PLS4	VIM	Uncharacterized protein	192	2
GGPGTGSRPSST	F1PLS4	VIM	Uncharacterized protein	193	2
GGPGTGSRPSSTR	F1PLS4	VIM	Uncharacterized protein	194	2;3
GGPGTGSRPSSTRS	F1PLS4	VIM	Uncharacterized protein	195	2;3
GGPGTGSRPSSTRSY	F1PLS4	VIM	Uncharacterized protein	196	2
GQVINETSQHHDDIE	F1PLS4	VIM	Uncharacterized protein	208	2;3
GSAIRPSTSR	F1PLS4	VIM	Uncharacterized protein	209	2
GSAIRPSTSRS	F1PLS4	VIM	Uncharacterized protein	210	2
IGSAIRPSTS	F1PLS4	VIM	Uncharacterized protein	241	2
IGSAIRPSTSR	F1PLS4	VIM	Uncharacterized protein	242	2
IIKTVETRDGQ	F1PLS4	VIM	Uncharacterized protein	246	2
IIKTVETRDGQVINETSQHHDDIE	F1PLS4	VIM	Uncharacterized protein	249	2;3;4
INETSQHHDDIE	F1PLS4	VIM	Uncharacterized protein	262	2
IQDSVDFSIA	F1PLS4	VIM	Uncharacterized protein	267	2
IQEAEEWYKSK	F1PLS4	VIM	Uncharacterized protein	268	2
IVDTHSKRTI	F1PLS4	VIM	Uncharacterized protein	285	2;3
IYASSPGGAYATR	F1PLS4	VIM	Uncharacterized protein	296	2
IYASSPGGAYATRS	F1PLS4	VIM	Uncharacterized protein	297	2
KTVETRDGQVINETSQ	F1PLS4	VIM	Uncharacterized protein	316	2
MFGGPGTG	F1PLS4	VIM	Uncharacterized protein	320	1
MFGGPGTGSRP	F1PLS4	VIM	Uncharacterized protein	322	2
MFGGPGTGSRPS	F1PLS4	VIM	Uncharacterized protein	323	2
MFGGPGTGSRPSS	F1PLS4	VIM	Uncharacterized protein	324	2
MFGGPGTGSRPSST	F1PLS4	VIM	Uncharacterized protein	325	2
MFGGPGTGSRPSSTR	F1PLS4	VIM	Uncharacterized protein	326	2;3
MFGGPGTGSRPSSTRS	F1PLS4	VIM	Uncharacterized protein	327	3
NDAIRQAKQESNE	F1PLS4	VIM	Uncharacterized protein	333	2
NDKARVEVERDN	F1PLS4	VIM	Uncharacterized protein	334	3
NIQEAEEWYKSK	F1PLS4	VIM	Uncharacterized protein	339	2
RDGQVINETSQ	F1PLS4	VIM	Uncharacterized protein	379	2
RDVRQQYES	F1PLS4	VIM	Uncharacterized protein	381	2
RMFGGPGTGSRPSSTR	F1PLS4	VIM	Uncharacterized protein	387	4
RMFGGPGTGSRPSSTRS	F1PLS4	VIM	Uncharacterized protein	388	3
RSYVTTSTR	F1PLS4	VIM	Uncharacterized protein	395	2
SAIRPSTSR	F1PLS4	VIM	Uncharacterized protein	404	2;3
SAIRPSTSRSI	F1PLS4	VIM	Uncharacterized protein	406	2
SIGSAIRPSTS	F1PLS4	VIM	Uncharacterized protein	417	2

SIYASSPGGAYATRS	F1PLS4	VIM	Uncharacterized protein	422	2
SIYASSPGGAYATRSS	F1PLS4	VIM	Uncharacterized protein	423	2
SIYASSPGGAYATRSSAVR	F1PLS4	VIM	Uncharacterized protein	425	2;3
SPGGAYATR	F1PLS4	VIM	Uncharacterized protein	431	2
SPGGAYATRSSA	F1PLS4	VIM	Uncharacterized protein	434	2
SPGGAYATRSSAV	F1PLS4	VIM	Uncharacterized protein	435	2
SSINIRETN	F1PLS4	VIM	Uncharacterized protein	442	2
SSPGGAYATRSS	F1PLS4	VIM	Uncharacterized protein	446	2
SSPGGAYATRSSA	F1PLS4	VIM	Uncharacterized protein	447	2
SSPGGAYATRSSAVR	F1PLS4	VIM	Uncharacterized protein	448	3
SSVPGVRIIQ	F1PLS4	VIM	Uncharacterized protein	455	2
SVAAKNIQEAEE	F1PLS4	VIM	Uncharacterized protein	464	2
SVSSSSYRR	F1PLS4	VIM	Uncharacterized protein	474	2
SYVTTSTRT	F1PLS4	VIM	Uncharacterized protein	477	2
TEFKNTRTNEK	F1PLS4	VIM	Uncharacterized protein	488	2;3
TRDGQVINETSQ	F1PLS4	VIM	Uncharacterized protein	503	2
TVETRDGQVINET	F1PLS4	VIM	Uncharacterized protein	510	2
TVETRDGQVINETS	F1PLS4	VIM	Uncharacterized protein	511	2
TVETRDGQVINETSQ	F1PLS4	VIM	Uncharacterized protein	512	2
TVETRDGQVINETSQHHDD	F1PLS4	VIM	Uncharacterized protein	513	3
TVETRDGQVINETSQHHDDIE	F1PLS4	VIM	Uncharacterized protein	514	2;3;4
TYSIGSAIRPST	F1PLS4	VIM	Uncharacterized protein	518	2
TYSIGSAIRPSTS	F1PLS4	VIM	Uncharacterized protein	519	2
VETRDGQVINE	F1PLS4	VIM	Uncharacterized protein	528	2
VETRDGQVINETSQ	F1PLS4	VIM	Uncharacterized protein	530	2
YASSPGGAY	F1PLS4	VIM	Uncharacterized protein	581	1
YASSPGGAYATR	F1PLS4	VIM	Uncharacterized protein	582	2
YASSPGGAYATRS	F1PLS4	VIM	Uncharacterized protein	583	2
YASSPGGAYATRSS	F1PLS4	VIM	Uncharacterized protein	584	2
YASSPGGAYATRSSAVR	F1PLS4	VIM	Uncharacterized protein	586	3
YESVAAKNIQ	F1PLS4	VIM	Uncharacterized protein	588	2
YSIGSAIRPSTS	F1PLS4	VIM	Uncharacterized protein	598	2
YVTTSTRTY	F1PLS4	VIM	Uncharacterized protein	600	2
YVTTSTRTYS	F1PLS4	VIM	Uncharacterized protein	601	2
YVTTSTRTYSIG	F1PLS4	VIM	Uncharacterized protein	602	2
FIAEKNIPRNPSE	F1PLT8	QSOX1	Sulfhydryl oxidase (EC 1.8.3.2)	169	2;3
FPQEPPSQPSSTYSIVN	F1PNV7	SCIMP	Uncharacterized protein	176	2
APITSRGSQQ	F1PQ68	TUBB2A	Tubulin beta chain	48	2

ISDEHGIDPT	F1PQ68	TUBB2A	Tubulin beta chain	272	2
NEAAGNKYVPR	F1PQ68	TUBB2A	Tubulin beta chain	335	2
THSIGGGTGSGMGT	F1PQ68	TUBB2A	Tubulin beta chain	495	2
TSRGSQQYR	F1PQ68	TUBB2A	Tubulin beta chain	506	2
APAAAAAPAKVE	F1PUX4	RPLP0	60S acidic ribosomal protein P0	41	2
APAAAAAPAKVEA	F1PUX4	RPLP0	60S acidic ribosomal protein P0	42	2
TAAPAAAAAPAKVE	F1PUX4	RPLP0	60S acidic ribosomal protein P0	479	2
AVNPDASSSQDPQTNSPR	F1PVS7	PVR	Poliovirus receptor	81	2
SQDPQTNSPR	F1PVS7	PVR	Poliovirus receptor	437	2
SSQDPQTNSPR	F1PVS7	PVR	Poliovirus receptor	449	2
PATEKDIAE	F1PWW0	FLNA	Filamin A	351	2
HGRPGIGATHS	F1Q1T5	RPS15	Ribosomal protein S15	216	2
DEAQSKRGIIT	F2Z4N8	ACTG2	Actin, gamma 2, smooth muscle, enteric	91	2
GDEAQSKRGIIT	F2Z4N8	ACTG2	Actin, gamma 2, smooth muscle, enteric	186	2
GMGQKDSYVGDEA	F2Z4N8	ACTG2	Actin, gamma 2, smooth muscle, enteric	199	2
TEAPINPKANR	F2Z4N8	ACTG2	Actin, gamma 2, smooth muscle, enteric	487	2;3
VGDEAQSKRGIIT	F2Z4N8	ACTG2	Actin, gamma 2, smooth muscle, enteric	532	2
VGMGQKDSYVG	F2Z4N8	ACTG2	Actin, gamma 2, smooth muscle, enteric	535	2
VMVGMGQKDS	F2Z4N8	ACTG2	Actin, gamma 2, smooth muscle, enteric	555	2
RTPSASNDDQQE	F6XMP7	SGTA	Small glutamine rich tetratricopeptide repeat containing alpha	397	2
PEPAKSAPAPKK	H9GWB1	HIST1H2BG	Histone H2B	355	2
PEPAKSAPAPKKGSK	H9GWB1	HIST1H2BG	Histone H2B	356	4
PEPAKSAPAPKKGSKKA	H9GWB1	HIST1H2BG	Histone H2B	357	3
ISSWVSSSS	J9JHY2	TBX20	T-box 20	276	2
KIEISQHAK	J9NUU3		Uncharacterized protein	309	2
YNTTSAVTVK	J9NVE6	LOC10655	Uncharacterized protein	594	2

		9486			
RSAVPPGADKKAEAGAGSATE	J9NVU2	RPS10	Ribosomal protein S10	393	3
IVTADRAATGN	J9NVZ6	QKI	Protein quaking	292	2
FATPSFAAGTA	J9NX04	AAK1	AP2 associated kinase 1	154	2
PVTVTRTTITTTT	J9NYK7	LOC10085 5913	Uncharacterized protein	369	2
PVTVTRTTITTTTSSSSG	J9NYK7	LOC10085 5913	Uncharacterized protein	371	2
HGKYVKEQEQ	J9NYN5	MINOS1	MICOS complex subunit MIC10	215	2
FKNIQTVNVDEN	J9NZ04		Uncharacterized protein	172	2
KNIQTVNVDEN	J9NZ04		Uncharacterized protein	311	2
NIQTVNVDEN	J9NZ04		Uncharacterized protein	340	2
SAINEVVTREY	J9NZ04		Uncharacterized protein	403	2
FEGDEDVSNKVS	J9NZ79	SDC4	Syndecan 4	157	2
SSTAQGGNIFERTEVIAA	J9NZ79	SDC4	Syndecan 4	454	2
STAQGGNIFERTEVIAA	J9NZ79	SDC4	Syndecan 4	460	2
TSPQGMPQHPPAPQGQ	J9P014	FUBP1	Far upstream element binding protein 1	505	2
PIPSKETIEQEKQAGES	J9P127	TMSB4X	Thymosin beta 4, X-linked	365	2;3
AEQENEKDPFH	J9P1V9	FXYD6	FXYD domain containing ion transport regulator 6	18	2
SAAEQENEKDPFH	J9P1V9	FXYD6	FXYD domain containing ion transport regulator 6	401	2;3
SAAEQENEKDPFHYD	J9P1V9	FXYD6	FXYD domain containing ion transport regulator 6	402	2;3
DTPENIRIKQQSEIQ	J9P3M1	LASP1	LIM and SH3 protein 1	116	2
IAGQVAAANKKH	J9P425	RPS19	Uncharacterized protein	230	2
PGVTVKDVNQQE	J9P425	RPS19	Uncharacterized protein	363	2
PGPPPPPPP	J9P7U7		Uncharacterized protein	359	1
QESQAQAIIQQAR	J9P8F7	COL5A1	Collagen type V alpha 1 chain	372	2
RPPPPPPPP	J9P8I5		XK-related protein	390	2
DETQGQQPPQR	J9P9A0		Uncharacterized protein	98	2
IHSDSGISVDSQS	J9PAM0	NGFR	Nerve growth factor receptor	243	2
VVTRGTADN	J9PAM0	NGFR	Nerve growth factor receptor	578	2
STGGKAPRKQIA	J9PB22	LOC10655 8266	Histone H3	462	2
DIEPTVIDEVRTGTYR	L7N0B2	TUBA1B	Tubulin alpha chain	107	2
ETGAGKHVPR	L7N0B2	TUBA1B	Tubulin alpha chain	140	2

FHSFGGGTGSG	L7N0B2	TUBA1B	Tubulin alpha chain	167	2
FSETGAGKHVPR	L7N0B2	TUBA1B	Tubulin alpha chain	177	2
NAAIATIKTK	L7N0B2	TUBA1B	Tubulin alpha chain	330	2
SVDYGKKSKIE	L7N0B2	TUBA1B	Tubulin alpha chain	466	2
TYAPVISAEKA	L7N0B2	TUBA1B	Tubulin alpha chain	517	2
VDIEPTVIDEVR	L7N0B2	TUBA1B	Tubulin alpha chain	524	2
VSSITASIR	L7N0B2	TUBA1B	Tubulin alpha chain	563	2
VVEPYNSIITTHT	L7N0B2	TUBA1B	Tubulin alpha chain	575	2
ISKQEYDESGPS	O18840	ACTB	Actin, cytoplasmic 1	274	2
IVMDSGDGV	O18840	ACTB	Actin, cytoplasmic 1	290	1
NPGPAGPAGPRG	O46392	COL1A2	Collagen alpha-2(I) chain	343	2
IDVMQDSFNRA	P25473	CLU	Clusterin (Glycoprotein 80)	233	2
GPIASQVRR	P34962	NMU	Neuromedin-U-25 (NmU-25) [Cleaved into: Neuromedin-U-8 (NmU-8)]	204	2
IDEEFQGPIASQVR	P34962	NMU	Neuromedin-U-25 (NmU-25) [Cleaved into: Neuromedin-U-8 (NmU-8)]	232	2
PGPTPSGTNVGSSGRSPS	P60467	SEC61B	Protein transport protein Sec61 subunit beta	360	2
PGPTPSGTNVGSSGRSPSK	P60467	SEC61B	Protein transport protein Sec61 subunit beta	361	3
IIEPSIRQIAQK	P63050	UBA52	Ubiquitin-60S ribosomal protein L40	244	2
FAEDVGSNKG	Q28280	APP	Amyloid-beta A4 protein	146	2
IVFFAEDVGSNK	Q28280	APP	Amyloid-beta A4 protein	286	2
IVNKEPSETPDQ	Q28284	CD44	CD44 antigen	291	2
VQPSTFSSYSRR	Q30DN6	KDM5D	Lysine-specific demethylase 5D	558	3
RAGEITEDEVER	Q5TJE9	RPS18	40S ribosomal protein S18	377	2
VINTNIDGRRK	Q5TJE9	RPS18	40S ribosomal protein S18	547	2
NEEQEYIETVK	Q6JDN3	ANXA1	Annexin I (Fragment)	336	2
KIEKEEEEGISQESSEEEQ	Q6URC2-2	HMGA1	High mobility group protein HMG-I/HMG-Y (HMG-I(Y))	310	2;3
ITGSPGSPGPDGKTGPPGPAG	Q9XSJ7	COL1A1	Collagen alpha-1(I) chain (Alpha-1 type I collagen)	282	2
SIADIQNDEVAFR	Q9XST7	rpS3A	Ribosomal protein (Fragment)	414	2
ATGGNRTKTPGPGAQSAIR	Q9XSU9	rpS14	Ribosomal protein S14	77	3

Table 7-4. Peptides released by dog patient-derived melanoma cells upon *Salmonella* infection. Supernatants of dog patient-derived melanoma cells were analyzed through nLC-MS both control supernatants and the ones derived from *Salmonella*-treated melanoma cells (Chapter 4.4.2.4). 243 identified peptides were significantly more abundant in *Salmonella*-derived supernatants; analysis was performed with MaxQuant software on the identified peptides. *P <0.05.